1966

The plastic behavior of reinforced concrete beams with varying percentages of reinforcing steel symmetrically placed

J. Leroy Hulsey

THE PLASTIC BEHAVIOR OF REINFORCED CONCRETE BEAMS WITH VARYING PERCENTAGES OF REINFORCING STEEL SYMMETRICALLY PLACED

BY

Johnny LEROY HULSEY

A

THESIS

submitted to the faculty of the

UNIVERSITY OF MISSOURI AT ROLLA

in partial fulfillment of the requirements for the

Degree of

MASTER OF SCIENCE IN CIVIL ENGINEERING

Rolla, Missouri

1966

Approved by

Jerry R Bayless (Advisor) W. G. Andrews

Bill L Atchley Billy C Gillett

ABSTRACT

The purpose of this study is to determine the limitations of the plastic behavior of reinforced concrete beams with varying percentages of high strength steel (ASTM-A-432) cutoff in the compression region d distance beyond the point of inflection. Comparison was made with the derived equations.

Steel was placed symmetrically in order to obtain like action at critical sections. The members tested were of a propped beam nature having a total clear span of 5'6" with a 6" overhang on one end and 1'6" overhang on the other. Concentrated loads were applied so as to obtain midspan loading and fixed end conditions at only one end. Beam sections were 3" X 6" with a 5¼" depth to steel. Reinforcing cover requirements were not met (American Concrete Institute) due to the limited size of sections. Shear reinforcing consisted of closed loop stirrups made from no. 9 gage wire. Electric Sr-4 strain gages were applied to the steel and concrete at all critical sections in order to obtain moment-curvature relationships. Dial gages were used to obtain the deflection at midspan.

Of the eight speciments tested, three had shear-bond failures at or near the point of inflection, thus limiting the plastic design theory for reinforcing that is symmetrically placed in beams of this kind. The moment and load deflection curves compared favorably with theory except for the high percentages of steel.

ACKNOWLEDGEMENT

The author is especially grateful to Professor Jerry R. Bayless, Assistant Professor of Civil Engineering, for his advice and guidance throughout this investigation.

The author would also like to thank Dr. Joesph H. Senne for his interest and advice, and Mr. A. Carl Weber, Vice President, Laclede Steel Company, St. Louis, Missouri, for providing the valuable reinforcing bars which made this thesis possible.

In addition, the author would like to thank Alan Kamp, Richard Rintoul, and Graham Sutherland, Graduate Assistants in Civil Engineering, for their willing assistance in preparing and testing the specimens.

The author is deeply indebted to Velma, his beloved wife, who contributed encouragement and self sacrifice to the completion of this thesis.

TABLE OF CONTENTS

TABLE OF CONTENTS

LIST OF FIGURES

LIST OF FIGURES (Cont.)

LIST OF FIGURES (Cont.)

LIST OF TABLES

LIST OF SYMBOLS

This list of symbols is presented for convenience and all symbols will be defined as they first appear in the text.

a = Depth of compression block for ultimate strength

A_s = Area of reinforcing bars

A_s' = Area of reinforcing bars in compression

b = Width of cross-section

c = Depth to neutral axis

d = Depth to center of steel

d' = Depth to center of compression steel

E_c = Secant modulus of elasticity of concrete

$E_c' = w^{1.5}(33)\sqrt{f_c'}$ = ACI modulus of elasticity

E_s = Modulus of elasticity of steel

E_{sp} = Modulus of elasticity of steel in elasto-plastic region

f_c' = Concrete cylinder strength on day of test

f_s' = Compression stress of steel

f_{su} = Steel stress at failure of section for high strength steels

f_y = Yield stress of steel

H_l = Hinge length

I = Moment of inertia based on transformed net section

k = Ratio indicating relative depth to neutral axis

k_1 = 0.85 for f_c' = 4000 psi and .05 less for every 1000 psi greater than 4000 psi

K = Ratio indicating relative depth to neutral axis for beams reinforced in compression

L = Span length

M = Moment

M_1 = Elastic moment at section 1

M_2 = Elastic moment at section 2

M_{ep1} = Elastic-plastic moment at section 1

M_{ep2} = Elastic-plastic moment at section 2

M_u = Yield moment for high strength steels

M_{ult} = Ultimate resisting moment

M_{ult1} = Ultimate resisting moment at section 1

M_{ult2} = Ultimate resisting moment at section 2

M_y = Yield moment for low strength steels

M_{y1} = Yield moment at section 1

M_{y2} = Yield moment at section 2

$n = E_s/E_c$ = Modular ratio

$p = A_s/bd$ = Tension steel ratio

$p' = A_s'/bd$ = Compression steel ratio

P = Load acting on beam

P_{y1} = Load causing section 1 to yield

P_{y2} = Load causing section 2 to yield

P_{ult} = Ultimate load the structure can support

ϵ_u = Maximum concrete strain

ϵ_s = Maximum steel strain

ϕ_{ep} = Curvature in elastic-plastic range

ϕ_{ep2} = Curvature in elastic-plastic range at section 2

$\phi_i = 2\theta_2/H_1$ = Incremental curvature at section 2 over that at first yield

ϕ_{mech} = Total curvature at section 2 once section 1 begins yielding

ϕ_{mech}/ϕ_{y2} = Required rotation at section 2

ϕ_{y2} = Curvature at first yield

ϕ_{ult} = Ultimate curvature at a section

ϕ_{ult}/ϕ_{y2} = Rotation capacity at section 2 (the critical section)

θ_o = Angle occuring at simple support when mechanism forms

θ_1 = Angle formed at section 1 as a result of mechanism formation

θ_2 = Angle occuring at section 2 when section 1 begins yielding

Δ_1 = Deflection at section 1

Δ_i = Incremental deflection

Δ_{mech} = Deflection at section 1 at formation of mechanism

I. INTRODUCTION

1.1 General Remarks

Unlike the strict elastic theory used for many years or the more recent ultimate strength theory, which recognizes the post-yield behavior of concrete, the author feels that a more realistic theory for indeterminate structures would be the plastic theory of behavior. Most concrete research in the past few years in America has been involved with the ultimate strength theory (defined internal stress block), a very important step toward the plastic theory in reinforced concrete. Plastic analysis of reinforced concrete would not only be a much easier and simpler solution of indeterminate structures but more realistic.

The plastic theory is a theory that recognizes both the inelastic stress behavior at a critical section and moment redistribution in an indeterminate system. After a section begins to yield (yield of the reinforcing steel), strain or rotation will increase more rapidly with little or no increase in stress or resisting moment. If the section was considered to form a rusty or plastic hinge at yield, the hinge would rotate at a relatively constant moment, unlike the simple hinge which rotates with zero moment. After a critical section yields and more load is applied to the structure, the section rotates at a relatively constant moment and less critical sections begin taking additional moment. At collapse load a sufficient number of critical sections have yielded to form a collapse mechanism or an unstable structure.

Because of steel's ductility and rotation ability, under normal circumstances, the actual strain of any one section for steel structures need not be considered since the ultimate strain is greater than 15% and it far exceeds the strains needed to develop moment redistribution (23).*

Concrete, unlike steel, is very brittle in tension and must develop its ductility from the reinforcing steel applied. It has been found by Charles S. Whitney and others that ultimate strain in flexural compression is between 0.3 and 0.7 percent while the ultimate strains in the tension steel can be 0.5% to over 2% depending on the amount of reinforcement used (22). Since the ductility of concrete sections is limited, rotation capacity must be considered in any derived theory. Knowing the rotation capacity (based on a reasonable assumption) and the required rotation to cause plastic development the structure may be designed provided bond, shear, and compression failures do not develop.

It is the author's belief that ductility may be changed by changing the percent of reinforcing steel and/or the amount and type of web reinforcing. In order to develop an economical structure it is desirable to have the critical sections to yield simultaneously.

The following investigation involved cutting off all

---

*Numbers in parenthesis refer to entries in the bibliography.

reinforcing bars past the point of inflection as determined by plastic analysis and studying its effect on the plastic theory developed herein. Theoretically cutting off the bars should have no effect, however the Amercian Concrete Institute (ACI) does not allow cutting off all bars. ACI requires a designer to extend $\frac{1}{4}$ of the positive moment steel into the support of a continuous beam.

It is the author's belief that cutoff limitations can be reduced thus allowing more flexibility in steel placement.

The following study involved propped cantilever beams simulating a single span continuous beam with one fixed end and one free end. The primary variable was the percentage of reinforcing steel. Reinforcing steel was symmetrically placed (critical sections equally reinforced) with an ASTM-A-432 grade high strength steel and was cutoff in the compression region in all cases. A preliminary beam was studied having a low strength steel (ASTM-A-15) and cutoff in the compression region. Web reinforcing consisted of closed loop stirrups (no. 9 gage wire) placed in an upright position. Moment-curvature and load-deflection relationships were established at each critical section for all beams tested. Moments, loads, curvatures, and deflections were compared with the developed theory at yield in all cases.

II. REVIEW OF LITERATURE

The development of design methods based on inelastic behavior for redundant steel structures preceded that for concrete. A great deal can be learned from the methods used in steel, however one must recognize that concrete rotation capacity must be studied unlike that of steel. Lynn S. Beedle in his book, Plastic Design of Steel Frames, shows the rotation and deflection ability of steel structures (3).

In the past decade the inelastic stress behavior of structural concrete has been a major concern of investigators in the United States. It appears that Charles S. Whitney's empirically simplified stress block initiated the ultimate strength idea in the United States (22). Until 1956, the ACI code recognized only the straight line theory for proportioning members. At the recommendation of the Joint ACI-ASCE Committee, the ultimate strength theory became an alternate approach and later in 1963 it became the accepted approach for proportioning. As shown in their report, "Ultimate Strength Theory", the ACI-ASCE Committee made recommendations as to the best approach to take (1).

In his report "Comparison of Measured and Calculated Stiffnesses for Beams Reinforced in Tension Only" Bill G. Eppes subjected simply supported underreinforced beams to pure moment (6). He showed that the measured stiffness decreased with increasing measured moment and that larger measured values of stiffness compared reasonably well with the calculated values of stiffness of the gross section of a reinforced concrete beam while the lower values compared fairly well with the values of the stiffness of the net section of the reinforced beam with the transformed area of steel included. The same general conclusions were drawn by Carl Berwanger in his thesis, "Application of Plastic Design Theory to Reinforced Concrete Beams". Mr. Berawanger's tests were concerned with two-span beams having concentrated loads at varying locations. The plastic theory developed by Mr. Berwanger was shown to be valid for the beams tested (4).

Moment distribution methods, comparisons of plastic rotations, and deflections for certain specific cases were given by G.C. Ernest in his report, "Ultimate Loads and Deflections from Limit Design of Continuous Structural Concrete" (7). In order to have a complete picture of research done to date, a review of limit design for concrete structures must be made, as C.W. Yu and Eivind Hognestad have done in their report, "Review of Limit Design for Structural Concrete" (23).

In their report, "Concrete stress Distribution in Ultimate Strength Design", Eivind Hognestad, N.W. Hanson, and Douglas McHenery verified from their series of tests that stress-strain relationships of concrete obtained from concentric cylinder tests can be made applicable to flexure (13). A. Mattock verified that limit design can be applied to structural concrete by a series of tests on structural concrete frames (15).

In his report, "Plastic Hinging at the Intersection of

Beams and Columns", G.C. Ernest concluded that concentrated plastic rotations at concrete crushing and at maximum moment are markedly reduced when the steel ratio exceeds .001, and are also decreased by increasing the loading rate. At concrete crushing for .05 steel ratios under fast loading, concentrated plastic rotations were virtually negligible (8). Herbert A. Sawyer presented an elastic-plastic theory for the development of limit design and applied it to tests run at the University of Connecticut (17).

The summary of investigations regarding the unpublished material (20,21) shows that confining action of ties can be very profitable in limit design thus giving added ductility. It was also felt that bond could be a problem if the stirrups were put in a vertical position.

III. THEORY

A propped cantilever beam with a single concentrated load at midspan was considered in this investigation. The elastic theory for critical moments applies until yielding occurs (Fig. 1). The so called critical elastic moments are:

$$M_1 = \frac{5PL}{32} \qquad M_2 = \frac{3PL}{16} \qquad \text{Eqs. 1-2}$$

Where M = Moment
P = Load
L = Span Length

In the following derivation, section 2 is assumed to be the critical section in all cases. Rearranging the above expressions in terms of moments and yield loads results in the following equations:

$$P_{y2} = \frac{16M_{y2}}{3L} \qquad P_{y2} = \frac{32M_1}{5L} \qquad \text{Eqs. 3-4}$$

First yield moment (M_y) means that the moment at a critical section has reached a value where initial yielding of the tension reinforcement has occurred. P_{y2} is the load causing yielding at section 2. The tension reinforcement continues to yield under increased load. The neutral axis rises, and there is a slight increase in moment resistance. The moment reached when the concrete crushes at the compression face of the cross section is called the ultimate resisting moment (M_{ult}). For beams reinforced in compression, it is assumed that compression steel buckles as the concrete crushes. This is a reasonable assumption since most web reinforcing or ties are not spaced close enough to give the lateral support needed to prevent buckling.

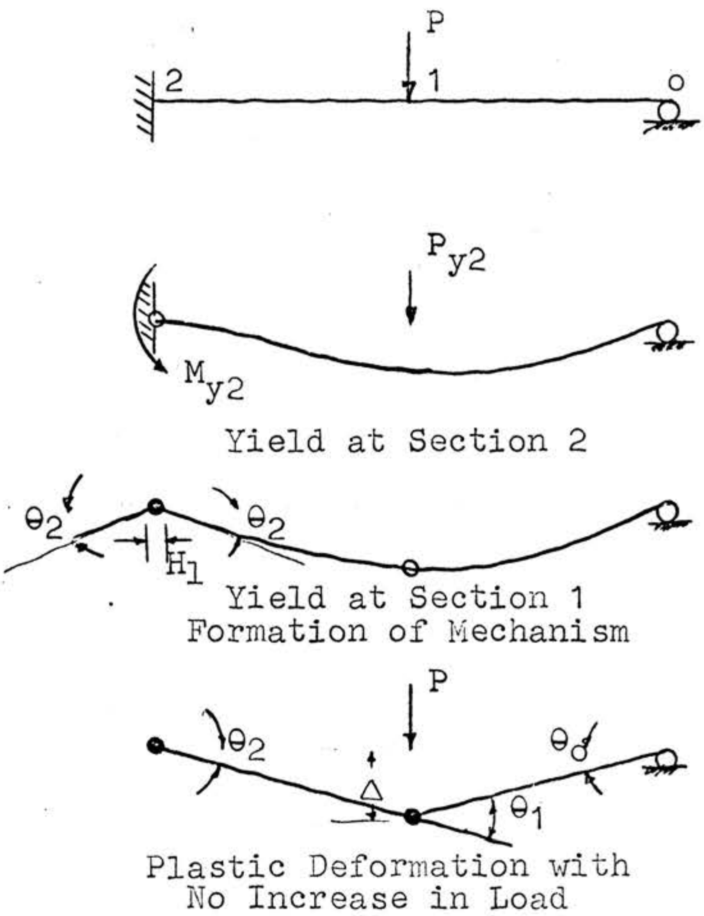

FIG. 1 LOAD-MOMENT RELATIONSHIPS

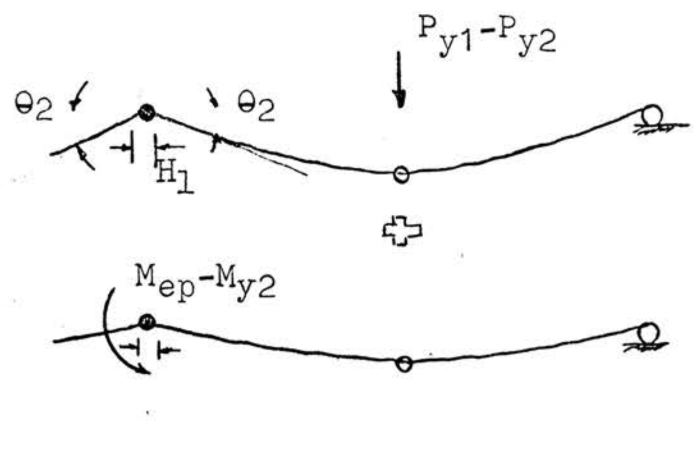

FIG. 2 CURVATURE FORMATION AT CRITICAL SECTION

In order for beams to have the ductility needed, they must be limited to underreinforced sections. Shear, bond, and compression failures (over-reinforced) are considered as undesirable modes of failure due to the sudden failures which may occur.

3.1 Low Strength Steels

The following assumptions are valid until the section being studied yields (straight line theory).

1. Plane sections before bending remain plane after bending.

2. The stress-strain relation for concrete is considered linear up to yield. Stresses vary linearly as the distance from the neutral axis.

3. The steel takes all of the tension due to flexure.

4. The tension reinforcement is replaced in design computations with a concrete tension area equal to n times that of the reinforcing steel.

Based on the above assumptions, singly reinforced beam section properties is found by the following equations (Figs. 4 and 5):

$$k = \sqrt{2pn + (pn)^2} - pn \qquad \text{Eq. 5}$$

$$M_y = A_s f_y (1-\frac{k}{3}) d \qquad \text{Eq. 6}$$

Where k = ratio indicating relative depth to neutral axis.
d = depth to center of steel
A_s = area of reinforcing steel
E_s = modulus of elasticity of steel
E_c = modulus of elasticity of concrete
$n = E_s/E_c$ = modular ratio
$p = A_s/bd$ = tension steel ratio
f_y = yield point stress of the steel

Based on the above assumptions, the stress distribution shown in Fig. 4 for the doubly reinforced section was used to develop the following equations.

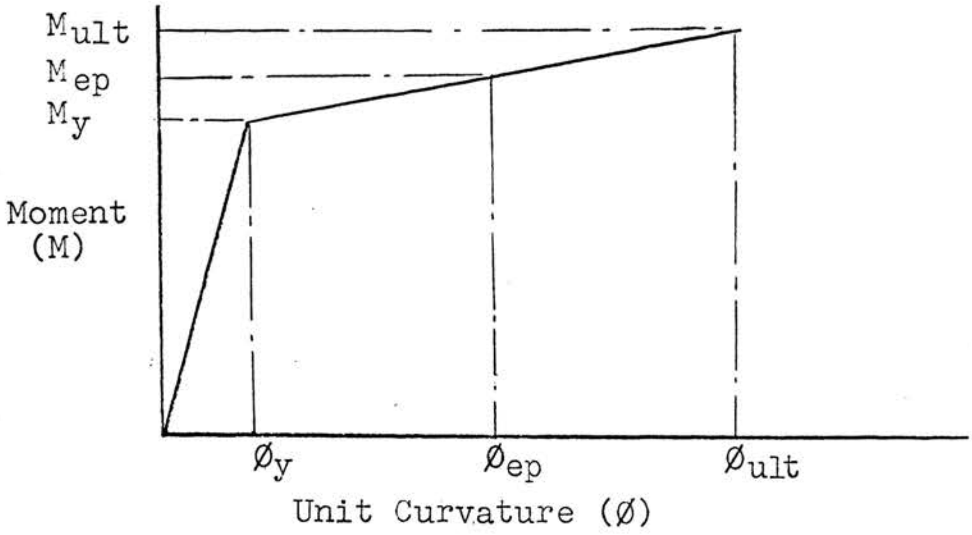

FIG. 3 THEORETICAL MOMENT-CURVATURE (M-Ø) RELATIONSHIP FOR LOW STRENGTH STEELS

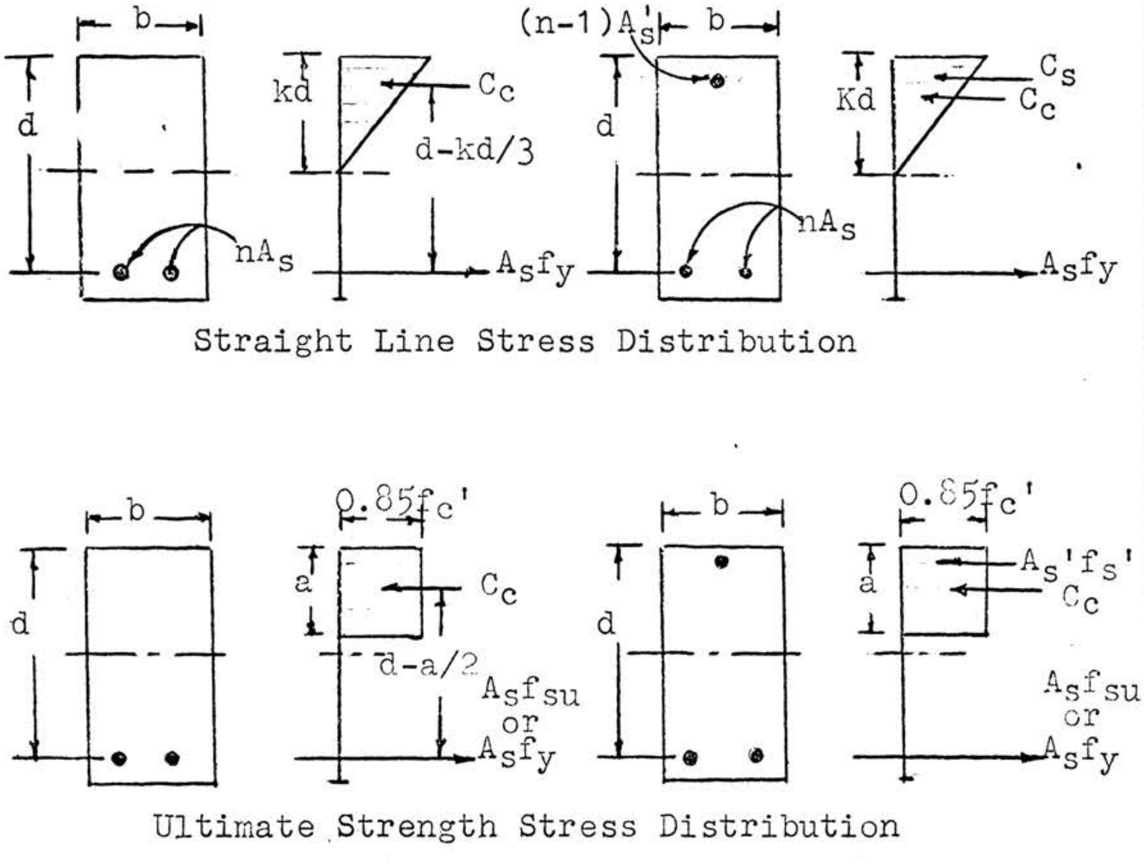

FIG. 4 STRESS DISTRIBUTION AT CRITICAL SECTIONS

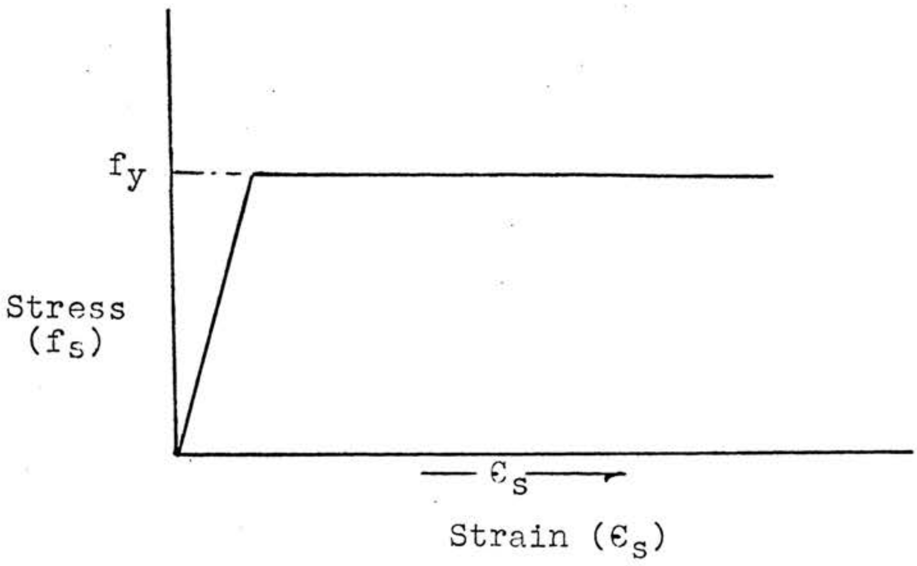

FIG. 5 ASSUMED STRESS-STRAIN BEHAVIOR FOR LOW STRENGTH STEELS

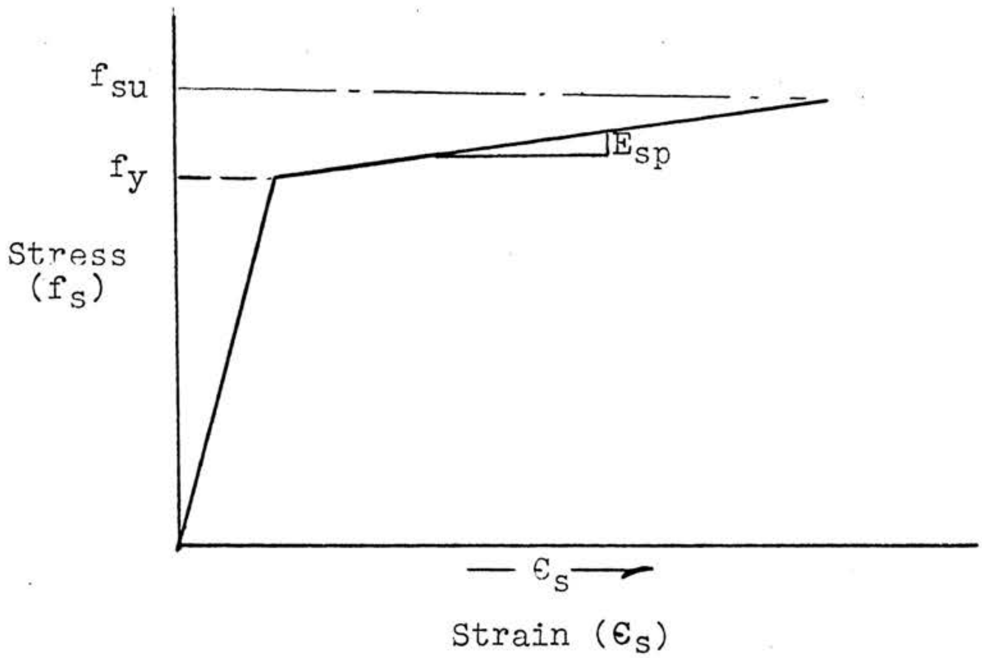

FIG. 6 ASSUMED STRESS-STRAIN BEHAVIOR FOR HIGH STRENGTH STEELS

$$K = \sqrt{2\left[pn+p'(n-1)\frac{d'}{d}\right] + \left[pn+p'(n-1)\right]^2} - pn+p'(n-1) \qquad \text{Eq. 7}$$

$$M_y = f_c b\overline{Kd}^2(1-\frac{K}{3}) + A_s'f_s'(d-d') \qquad \text{Eq. 8}$$

$$f_c = \frac{Kf_y}{n(1-K)} \qquad \text{Eq. 9}$$

Where A_s' = area of compression steel
d' = depth to compression steel
f_c = concrete stress at outermost fiber
f_s' = compression steel stress
K = ratio indicating relative depth to neutral axis for beams reinforced in compression.
p' = A_s'/bd = compression steel ratio

The ultimate resisting moment occurs when the concrete begins crushing at the critical section. The assumed and accepted rectangular stress block (ACI) will be used for both singly and doubly reinforced sections (Fig. 4) as shown below by the following expressions:

Singly Reinforced

$$M_{ult} = A_sf_y(d-\frac{a}{2}) \qquad \text{Eq. 10}$$

$$a = \frac{A_sf_y}{0.85f_c'b} \qquad \text{Eq. 11}$$

Where a = depth of compression stress block
f_c' = concrete strength on day of test
M_{ult} = ultimate resisting moment

Doubly Reinforced

$$M_{ult} = (A_s-A_s'\frac{f_s'}{f_y})f_y(d-\frac{a}{2}) + A_s'f_s'(d-d') \qquad \text{Eq. 12}$$

$$a = (A_s-A_s'\frac{f_s'}{f_y})f_y/0.85f_c'b \qquad \text{Eq. 13}$$

The true factor of safety in an indeterminate system is the ratio of the ultimate load the structure can withstand to the working load that the structure will have to support. The expressions for loading conditions beyond first yield are largely dependent on what assumptions are made for the moment-curvature relationship used in the derivation. The idealized curve shown in Fig. 3 is used.

In order to determine the load the structure will support beyond first yielding, the principal of virtual work, which gives an upper bound solution, is used. Depending on the rotation capacity of the critical section, the moment at formation of a collapse mechanism may be either M_{ep} (Moment in elastic-plastic range) or M_{ult}. Expressions for the ultimate load in terms of the above moments (Fig. 1) developed by equating the energy absorbed at the hinges and external work are as follows:

Case I

$$\text{Work in} = \text{Work out}$$
$$P_{y1}(\Delta) = M_{ep2}(\theta_2) + M_{y1}(\theta_1)$$
$$P_{y1}(\Delta) = M_{ep2}\left(\frac{2\Delta}{L}\right) + M_{y1}\left(\frac{4\Delta}{L}\right)$$
$$P_{y1} = \frac{1}{L}(2M_{ep2} + 4M_{y1}) \qquad \text{Eq. 14}$$

Case II

$$\text{Work in} = \text{Work out}$$
$$P_{y1}(\Delta) = M_{ult2}(\theta_2) + M_{y1}(\theta_1)$$
$$P_{y1} = \frac{1}{L}(2M_{ult2} + 4M_{y1}) \qquad \text{Eq. 15}$$

In all cases the ultimate moment depends upon the stress-strain characteristics of the steel. In the derivation presented here it is assumed that the steel has a definite yield stress (f_y).

In order for a structure to attain the computed ultimate load, it is necessary for redistribution of moment to occur. As pointed out earlier, the necessary transfer of moment is possible only if the rotation capacity of the critical section is sufficient. Since sections were assumed to act elastically up to yield of the section, curvature may be expressed as follows:

$$\phi_{y2} = \frac{M_y}{E_c I} \qquad \text{Eq. 16}$$

Where ϕ_{y2} = Curvature
E_c = Secant modulus of elasticity for concrete
I = Moment of inertia based on transformed net section

As can be seen from the above expression, the curvature is definitely a function of the flexural rigidity of the section. Thus the limitations of these curvature relationships are subject to the assumptions used for flexural rigidity. Upon formation of the collapse mechanism which occurs when section 1 yields, the beam deflection increases much more rapidly and therefore increases the curvature at section 2 markedly. Beam sections between hinges will behave elastically. Thus the beam will act as a simply supported beam with an incremental load ($P_{y1} - P_{y2}$) acting and an incremental moment ($M_{ep2} - M_{y2}$) acting at section 2. In order to predict the curvature at section 2, it must be realized that concrete, unlike steel, must have a definite hinge length (H_l). Assuming H_l = d (2,5,13), the incremental curvature at section 2 (Fig. 2) is:

$$\phi_i = \frac{2\theta_2}{H} \qquad \text{Eq. 17}$$

Realizing that any incremental moment tends to reduce the deflection at section 1 and the rotation at section 2, the incremental load ($P_{y1} - P_{y2}$) superimposed on the beam with the incremental moment ($M_{ep2} - M_{y2}$) develops an angle of discontinuity at section 2 which can be expressed as follows (4):

$$\theta_2 = \frac{(P_{y1}-P_{y2})L^2}{16E_cI} - \frac{(M_{ep2}-M_{y2})L}{3E_cI} \qquad \text{Eq. 18}$$

Combining equations 17 and 18 results in the following expression for incremental curvature:

$$\phi_i = \frac{3(P_{y1}-P_{y2})L^2 - 16(M_{ep2}-M_{y2})L}{24H_1E_cI} \qquad \text{Eq. 19}$$

The following expression (total curvature at mechanism formation) is the result of the curvature at first yield plus any incremental curvature:

$$\phi_{mech} = \phi_{y2} + \frac{3(P_{y1}-P_{y2})L^2 - 16(M_{ep2}-M_{y2})L}{24H_1E_cI} \qquad \text{Eq. 20}$$

The curvature may also be expressed by combining equations (3,14,&20) giving the following expression:

$$\phi_{mech} = \phi_{y2} + \frac{(-10M_{ep2} + 12M_{y1})L}{24H_1E_cI} \qquad \text{Eq. 21}$$

The curvature beyond first yield may be obtained by proportions from the assumed moment-curvature diagram (Fig. 3):

$$\phi_{ep} = \frac{\phi_y(M_{ult}-M_y) + (\phi_{ult}-\phi_y)(M_{ep}-M_y)}{M_{ult}-M_y} \qquad \text{Eq. 22}$$

It may be convenient to express the curvature at a section as ϕ_{mech}/ϕ_{y2} which is the required rotation ratio (eliminating the flexural rigidity-relationship) for the mechanism to form (3,4). The required rotation at a section is expressed by the following equation:

$$\phi_{mech}/\phi_{y2} = 1 + \frac{3(P_{y1}-P_{y2})L^2 - 16(M_{ep2}-M_{y2})L}{24H_1M_{y2}} \qquad \text{Eq. 23}$$

Four cases of failure may occur when a structure reaches ultimate load. Depending on the rotation capacity of the critical sections, one or all of the sections will reach ultimate moment as expressed below:

Case I $$P_{ult}(\Delta) = M_{ult2}\frac{(2\Delta)}{L} + M_{y1}\frac{(4\Delta)}{L}$$ Eq. 24

Case II $$P_{ult}(\Delta) = M_{ult2}\frac{(2\Delta)}{L} + M_{ep1}\frac{(4\Delta)}{L}$$ Eq. 25

Case III $$P_{ult}(\Delta) = M_{ult2}\frac{(2\Delta)}{L} + M_{ult1}\frac{(4\Delta)}{L}$$ Eq. 26

Case IV $$P_{ult}(\Delta) = M_{ep2}\frac{(2\Delta)}{L} + M_{ult1}\frac{(4\Delta)}{L}$$ Eq. 27

Case four failure will occur only if there is additional rotation capacity, or where the ductility at section 2 is greater than that at section 1. The ultimate curvature that the concrete can withstand at any one section is expressed by the following relation, shown by Fig. 7:

$$\phi_{ult} = \frac{\epsilon_s + \epsilon_u}{d}$$ Eq. 28

Where ϵ_s = maximum strain in steel
ϵ_u = maximum concrete strain

$$\epsilon_s = \frac{(d-c)\epsilon_u}{c}$$ Eq. 29

Where $c = a/k_1$
$k_1 = 0.85$ for $f_c' = 4000$ psi and .05 less for every 1000 psi greater than 4000 psi.

Combining equations 28 and 29 results in the following ultimate curvature relationship:

$$\phi_{ult} = \frac{\epsilon_u}{c}$$ Eq. 30

Since the beam behaves elastically up to the first yield, the deflection at section 1 may be found by elastic methods as shown by the following expression:

$$\Delta_1 = \frac{7P_{y2}L^3}{768E_cI}$$ Eq. 31

When the mechanism forms, the beam will act as a simply supported beam undergoing continued deformation. The incre-

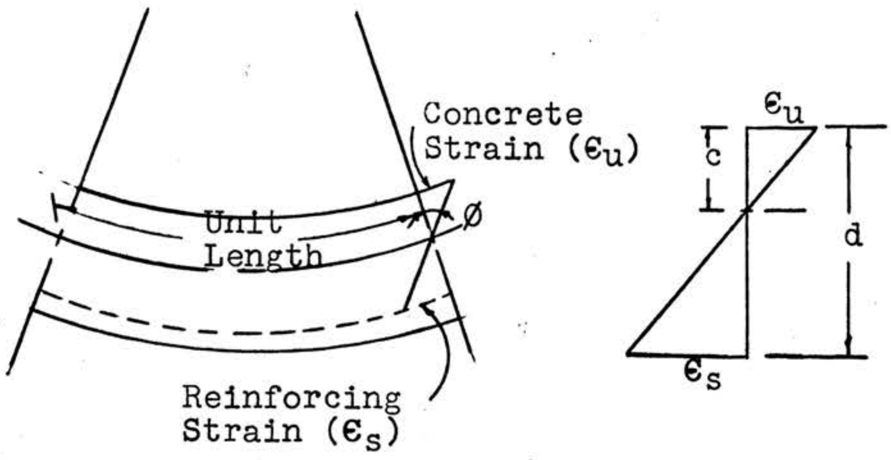

FIG. 7 ULTIMATE CURVATURE RELATIONSHIP

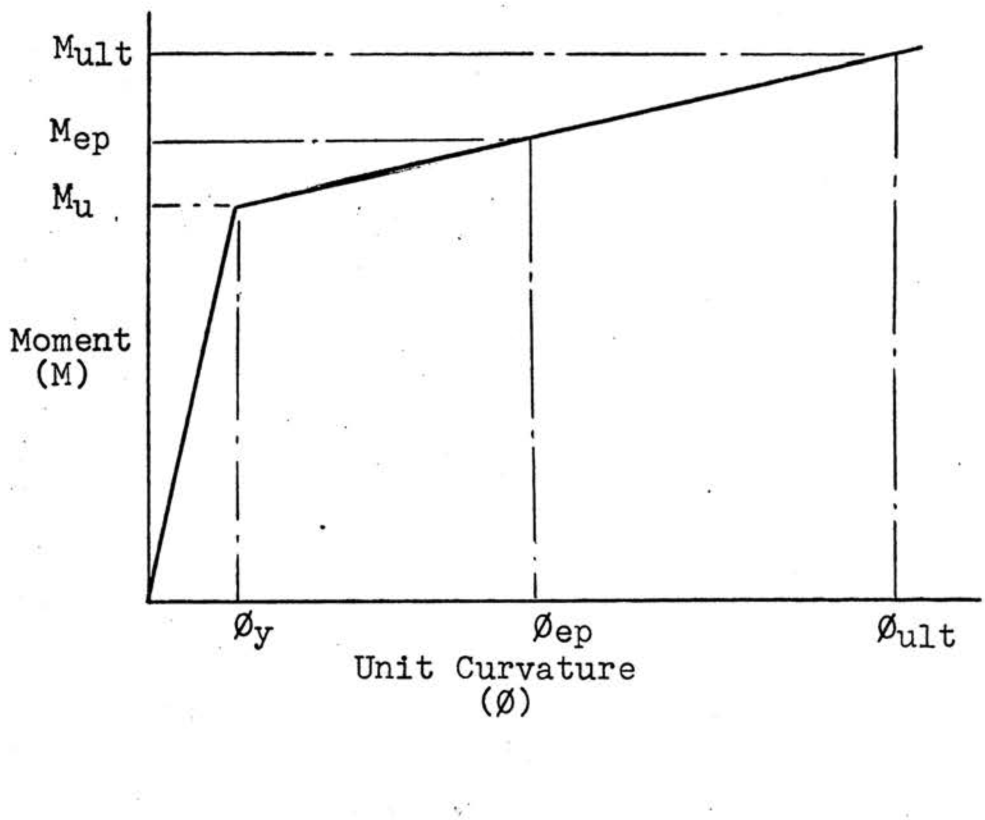

FIG. 8 THEORETICAL MOMENT-CURVATURE (M-ϕ) RELATIONSHIP FOR HIGH STRENGTH STEELS

mental deflection caused by $(P_{y1} - P_{y2})$ results in the following expression:

$$\Delta_i = \frac{(P_{y1} - P_{y2})L^3}{48E_cI} \qquad \text{Eq. 32}$$

The following expression for total deflection is a result of the combination of equations 31 and 32 and the superimposed incremental moment:

$$\Delta_{mech} = \frac{7P_{y2}L^3}{768E_cI} + \frac{(P_{y1} - P_{y2})L^3}{48E_cI} - \frac{(M_{ep2} - M_{y2})L^2}{16E_cI} \qquad \text{Eq. 33}$$

Internally ϕ_{ult} can be expressed by combining equations 11 and 30:

$$\phi_{ult} = \frac{\epsilon_u(0.85k_1 f_c')}{pf_yd} \qquad \text{Eq. 34}$$

Combining equations 16 and 34 results in the following expression for the rotation capacity of a section:

$$\phi_{ult}/\phi_{y2} = \frac{\epsilon_u(0.85k_1 f_c')E_cI}{pf_ydM_{y2}} \qquad \text{Eq. 35}$$

By combining equation 6 with equation 35, the rotation capacity can be expressed in terms of the sectional properties of the beam as shown by equation 36.

$$\phi_{ult}/\phi_{y2} = \frac{\epsilon_u(0.85k_1 f_c')E_cI}{p^2f_y^2d^3(1-\frac{k}{3})} \qquad \text{Eq. 36}$$

3.2 High Strength Steels

The primary difference concerning these steels is the assumption made regarding the internal resisting moment at yield. In the following derivation, the internal yield moment was assumed to be M_u developed by the ultimate strength approach (equations 10 and 13) rather than M_y (straight line theory). The straight line theory is unrealistic at yield since f_c must be very high to balance the tension force ($A_s f_y$) therefore the ultimate moment development would more closely approximate the second case. The ultimate resisting moment is found by the same approach as that for the low strength steels except recognition is made of the stress-strain behavior of the reinforcement beyond yield as shown in Fig. 6. With the aid of Fig. 6 an equation for the steel strain beyond yield is expressed as shown by equation 37.

$$\epsilon_s = \frac{f_{su}(E_s) - f_y(E_s - E_{sp})}{E_s E_{sp}} \qquad \text{Eq. 37}$$

Combining equations 11,29, and 37 with f_{su} in place of f_y in equation 11, results in equation 38 for the reinforcement steel stress at failure of the section.

$$f_{su} = \sqrt{\frac{E_{sp}\epsilon_u(0.85k_1 f_c')}{p} + \left[\frac{1}{2}\left\{E_{sp}\epsilon_u - f_y\left(1 - \frac{E_{sp}}{E_s}\right)\right\}\right]^2} - \frac{1}{2}\left\{E_{sp}(\epsilon_u) - f_y\left(1 - \frac{E_{sp}}{E_s}\right)\right\} \qquad \text{Eq. 38}$$

The ultimate resisting moment can then be expressed by replacing f_y with f_{su} in equation 10. These same principles are followed for doubly reinforced sections.

See Fig. 8 for the moment-curvature relationships used. Again the beam loads are elastically determined up to first yield and are expressed as follows:

$$P_{y2} = \frac{16M_{u2}}{3L} \qquad P_{y2} = \frac{32M_1}{5L} \qquad \text{Eqs. 39-40}$$

The relationships for load at mechanism formation depend upon the assumptions made regarding the moment-curvature relationship (Fig. 8). The moment-curvature relation beyond first yield depends upon the stress-strain characteristics of the reinforcement and the percent steel. Most high strength steels such as those used in the following investigation have little or no yield plateau, therefore the moment-curvature relation beyond yield can be expressed by defining a necessary elastic-plastic modulus (E_{sp}) which recognizes the yield stress is increasing (Figs. 6 and 8) and recognizing the beam sectional behavior beyond yield.

The load the structure will support at mechanism formation can be obtained in a manner similar to the derivations for low strength steels, shown by equations 14 and 15. The equations shown below were developed by these principals:

Case I $$P_{y1} = \frac{(2M_{ep2} + 4M_{u1})}{L} \qquad \text{Eq. 41}$$

Case II $$P_{y1} = \frac{(2M_{ult2} + 4M_{ep1})}{L} \qquad \text{Eq. 42}$$

The curvature at first yield is expressed (similar to Eq. 16) elastically by the following expression:

$$\phi_{y2} = \frac{M_u}{E_c I} \qquad \text{Eq. 43}$$

The equation for the curvature at section 2 beyond first yield at mechanism formation is:

$$\phi_{mech} = \phi_{y2} + \frac{3(P_{y1} - P_{y2})L^2 - 16(M_{ep2} - M_{u2})L}{24 H_1 E_c I} \qquad \text{Eq. 44}$$

The expression for curvature obtained from the moment-curvature relationship (Fig. 8) is expressed as follows:

$$\phi_{ep} = \frac{(M_{ult} - M_{ep})\phi_y + (M_{ep} - M_u)\phi_{ult}}{M_{ult} - M_u} \qquad \text{Eq. 45}$$

The required rotation for a mechanism to develop can be expressed by the following equation (similar to Eq. 23):

$$\phi_{mech}/\phi_{y2} = 1 + \frac{3(P_{y1}-P_{y2})L^2 - 16(M_{ep2}-M_{u2})L}{24H_1M_{u2}} \qquad \text{Eq. 46}$$

The mechanism that forms depends on the rotation capacity and the required rotation at the critical section. Four cases of failure may occur, the case depending on the rotation capacity. The cases that may occur are given below:

Case I $$P_{ult}(\Delta) = M_{ult2}\frac{(2\Delta)}{L} + M_{u1}\frac{(4\Delta)}{L} \qquad \text{Eq. 47}$$

Case II $$P_{ult}(\Delta) = M_{ult2}\frac{(2\Delta)}{L} + M_{ep1}\frac{(4\Delta)}{L} \qquad \text{Eq. 48}$$

Case III $$P_{ult}(\Delta) = M_{ult2}\frac{(2\Delta)}{L} + M_{ult1}\frac{(4\Delta)}{L} \qquad \text{Eq. 49}$$

Case IV $$P_{ult}(\Delta) = M_{ep2}\frac{(2\Delta)}{L} + M_{ult1}\frac{(4\Delta)}{L} \qquad \text{Eq. 50}$$

The ultimate rotation for a section is expressed by equation 34 with f_y replaced by f_{su} similar to the expression for the low strength steels. The rotation capacity for individual sections may be determined by combining equations 34 and 43 with f_y again replaced by f_{su}.

The deflection at section can be expressed by equation 33 with M_{y2} replaced by M_{u2} when section 1 occurs. The following expression is a relationship for deflection at the formation of the mechanism:

$$\Delta_{mech} = \frac{7P_{y2}L^3}{768E_cI} + \frac{3(P_{y1}-P_{y2})L^3}{48E_cI} - \frac{(M_{ep2}-M_{u2})L^2}{16E_cI} \qquad \text{Eq. 51}$$

IV. LABORATORY PROCEDURE

4.1 Materials

(a) Cement

A high early strength cement was used for all tests. It was purchased in bags of one lot from a nearby dealer and stored in a dry place.

(b) Aggregate

The fine aggregate used was the normal laboratory supply of sand. In order to maintain the same moisture content from the time trial mixes were made to date of mixing, the sand was placed in metal containers and covered with polyethelene. It was found that this kept the moisture content relatively constant.

A special supply of coarse aggregate had to be obtained because of the small sizes of the beams and small clearances around the reinforcing steel. A local supplier was found with a suitable type of ½" gravel meeting gradation requirements. The gravel was obtained sufficiently ahead of time to permit thorough drying in the laboratory storage bins.

(c) Reinforcing Steel

All reinforcing steel used was ASTM 305-A-432 grade steel with yield points between 60,000 and 70,000 psi. However the bar used for a preliminary beam was ASTM 305-A-15 intermediate grade steel with a yield point just above 40,000 psi. It was the author's original intention to obtain all bars from the same heat but this became virtually impossible. Three bar sizes were used; #3, #4, and #5. Tension tests were run on coupons taken from each bar. Loads and strains were automatically and graphically recorded. Tests were run as slowly as possible at first, to make sure that the stress-strain behavior was a characteristic of the bars tested rather than of the testing apparatus. It was found that the #3 bars, ASTM A-432 had no yield point but yielded at a greatly reduced slope on the stress-strain curve. However bars #4 and #5 had a definite yield plateau for a short distance. Results of these tests are presented in Figs. 9-13 in the appendix. Vertical stirrups of one design were made from a smooth no. 9 gage wire and bent into a closed loop stirrup with the corners spot welded together. The particular stirrup design used is shown in Fig. 14.

4.2 Fabrication

The main longitudinal bars were assembled with the vertical stirrups into a complete unit or cage before being placed in the forms, by spot welding when only one bar was used as reinforcement, and tieing in all other cases as shown in Fig. 15.

A-1 Sr-4 electric strain gages (gage length = 13/16") with a minimum trim width of 1/8" were used for measuring both steel and concrete strains. Since deformed bars leave much to be desired in providing a good surface for strain gages, the longitudinal ribs were filed smooth and widened to fit the gage. Finishing to a smooth surface by the use of emery cloth and cleaning solvent such as acetone completed the bar preparation. A liberal coating of Duco Cement was applied to both bar and gage, the gage was then applied to the prepared area and fastened by means of twisted rubber bands (12).

Waterproofing was accomplished by applying a melted beeswax over the trimmed gage. After ample drying time, leads were soldered on and taped back over the beeswax with an electrical plastic tape to prevent any movement of the leads. The final waterproofing was completed by putting a coat of wax over the tape and previous coat (Fig. 19). After waterproofing, the gages were put in water for a 24 hr. period to insure adequate resistance to moisture. Checking entailed determining the resistance between gage and ground (water) by a vacuum tube voltmeter (18). If no leakage is present a resistance of infinity should be noted. If however there is leakage, a minimum gage to ground resistance of 50 megaohms can be allowed and still have the gage function properly (16). In all cases, leakage no greater than 500 megaohms was allowed in a 24 hr. period.

The mix proportions were selected from a previously determined set of trial mixes established for a 4000 psi strength and a 4½" slump. The laboratory mixer is a small-capacity, vertical shaft, rotating horizontal arm mixer which can be raised from or lowered into the mix which is deposited in a stationary mixing bucket below. The mixing properties of this mixer are good. In order to maintain the same mix throughout the investigation, water was sprayed on the entire batching system, allowing everything to become saturated, and then drained. Before pouring, six 6" X 12" cylinder forms and 2 beam forms were oiled with form oil before each pour. At the time of pouring a special wire was placed vertically in the concrete 18" from one end to act as a pointer for measuring fixed end moment (zero rotation for elastic behavior) as shown in Fig. 16. Both beams and cylinders were removed from their forms the day following the pour and moved to the laboratory curing room.

4.3 Specimens

1 (no. 3-A) preliminary and 7 (nos. 1-7) other simi-continuous beams were designed for testing. The beams were propped cantilever beams having a clear span of 5'6" with a total length of 7'6". Single concentrated loads were applied at midspan in all cases. Beam cross-sections were 3" X 6" deep with reinforcing steel placed symmetrically at all critical sections. Three cylinder tests were run for each beam tested on the day of the tests in order to determine the stress-strain properties of the concrete (13). The results of these tests are shown in Fig. 25-29.

4.4 Test Apparatus

A specially built loading frame made from bolted steel I-sections attached together with the vertical loading arms made from T-sections and a horizontal WF cross beam through which load is applied as shown in Fig. 17-18 was used throughout the investigation. Load was applied to a loading beam, 6WF20, cut to specified length, by means of a hydraulic ram in conjunction with a load cell made from aluminum with a load sensitivity of 10 microinches/inch of strain equal to 100 pounds of load as shown in Figs. 21, 22, and 23. Distribution of load was applied through steel bearing plates 2" wide and a 1" roller. These same bearing plates were used for reaction distribution with a $1\frac{1}{4}$" roller. A transit was used to sight on the metal wire pointer attached for the prupose of establishing fixed end moment.

A-1 Sr-4 strain gages were used throughout the investigation. Concrete gages were attached in pairs of two, $\frac{1}{2}$" from the surface at all critical sections for all beams except the preliminary beam. Only one concrete gage at each critical section at a level of 3/4" from the surface was applied for the preliminary beam with an additional gage placed at d/2 distance from the critical section and at the same level as the previous gage. Steel strain was measured with one gage for each beam.

4.5 <u>Test Procedure</u>

At the end of the 6th day both the beams and cylinders were removed from the curing room and allowed to dry for an eight hour period. At this time, the load, reaction, and gage locations were marked. Gage locations on the concrete were cleaned of any loose material, and any roughness was removed by emery cloth. Acetone (cleaning solvent) was then used to remove any form oil or other contamination. After this cleaning small holes were evident on the concrete surface. These surface cavities were filled with 20% epoxy resin cement (No. EPF-200) having good concrete properties and 80% fine sand (12). After several hours the surface was again sanded with emery and cleaned with acetone. Strain gages were placed on the surface with epoxy resin cement and an electrical plastic tape placed along the trim width was used to hold the gage in place until the cement hardened. Steel bearing plates were placed on the beam at all load and reaction points by a plaster of paris cushion, thus distributing the load evenly. A plaster of paris coat was also applied at the critical sections in the tension region in order to see visible cracking take place. Cylinders were capped with sulfur, a good quality capping material. The cement, plaster of paris, and caps were then allowed to dry overnight. The following morning cylinder load-deflection data was taken as given in Tables V through XIII in the appendix. Upon completion of the cylinder testing, the reaction supports were positioned properly both transversely and longitudinally to the hydraulic ram. The load cell was then placed into position and connected to the strain indicator balancing unit. Leads were then soldered into place on the concrete gages and connected to the balancing unit in conjunction with the proper compensating gage made strictly for this purpose. Steel gages were also hooked into the unit with their proper compensating gage. After everything was in place, the transit was set up and the hairline centered on the pointer as shown in Fig. 16. A small load was then applied to the system while any movement of the pointer was noted. Any movement of the pointer required removing the load and adjusting the loading beam until no movement was noted. At this time a fixed end was developed. Once everything was positioned properly the dial gage for the measurement of deflections was positioned and loads applied to the structure. Strain measurements were taken for the load cell and all respective strain gages. Gages were read cyclicly and always in the same order. A complete set of readings took between one and three hours. All beam strain data is given in the appendix, Tables V through XXIII.

V. PRESENTATION AND DISCUSSION OF RESULTS

In all tests, the loads and moments at first yield and mechanism formation, were determined from a study of the deflections, curvatures, and position of the neutral axis. The first yield load was determined to be the load causing section 2, the critical section, to rotate as a result of the reinforcement yielding. The load causing section 1 to yield, and causing mechanism formation, resulted from yielding of the reinforcing at this section. The ultimate concrete strain at the extreme fibers, at any one section, was determined by extrapolating the measured strain for the steel and concrete.

Theoretically, the moments at critical sections (at yield) were determined by the straight line theory for the preliminary beam using a low strength steel with a final ultimate resisting moment based on the ultimate strength theory, while the sections for the high strength steels were proportioned by the ultimate strength theory and recognizing the elastic-plastic behavior if no yield point occurred. The flexural rigidity must be studied very closely since all curvature and deflection studies must be based on this one quantity. The author chose to use the transformed net section method for determining the moment of inertia throughout. This seems to be in line with conclusions of other investigators (6). The stress-strain properties of the concrete were determined by concentric cylinder tests. Results compared to flexural specimens raises some question, but has been proven to compare closely with tests performed on flexural specimens (13). The secant modulus was determined from these stress-strain curves, Figs. 25-29, and compared with the present ACI code formula for modulus of elasticity, Table II. The results of these tests compared very well with the largest deviation being 2.1%. The primary variable involved in the study was percentage of reinforcement, while secondary variables were spacing of web reinforcement and concrete strength. However, these secondary variables were held as constant as possible.

5.1 Beam 3-A

Beam 3-A was designed to check the test procedure. An intermediate grade steel having a well defined yield point of 45.8 ksi (Fig. 9) was used as reinforcing in conjunction with a concrete strength of 4.6 ksi given in Table II. The beam was symmetrically reinforced having only tension steel (2-#3) at each section with a steel ratio of .0141 at section 2 and .0139 at section 1 (Table I). The bars were cut-off in the compression region d distance beyond the occurrence of the point of inflection (not in accordance with the ACI code). Twenty-three closed loop stirrups were placed at $2\frac{1}{2}$" (d/2) as shown in Fig. 24 throughout each section giving equal confinement. The plaster of paris on the side of the beam at section 2, was noticed to have vertical tension cracks at a load of 1.4 kips while cracks at section 1 did not form until the load was 1.81 kips. The result of these cracks can be clearly seen on the moment-curvature curve shown in Fig. 30. With additional loading, tension yielding began at section 2 at a load of 4.25 kips and a moment of 52.6 in-kips. The values of load and moment compared closely to those by theory, within 8.25% and 8.2% respectively, (Table III). With additional increase in load, section 1 yielded at a load of 4.70 kips and a moment of 48.9 in-kips. The theory again checked closely, within 0.72% and 0.21% respectively. Once section 2 began yielding the beam deflected with no additional increase in load until strain hardening began as shown in Fig. 30. The beam finally failed at a load of 4.78 kips and an ultimate moment at section 1 of 51.4 in-kips, while the moment at section 2 was 61.6 in-kips. The ultimate resisting moment was calculated according to the present ultimate strength theory to be 49.2 in-kips assuming the ultimate strain to be .003 in/in. The failure occurred as a result of crushing of the concrete at the edge of the bearing plate block at section 1, with the concrete strain at the outer fiber being .00520 in/in. The added rotation capacity at section 2 allowed the beam to rotate enough for failure to occur at section 1. The ultimate strain being higher than normal might be explained by considering the confining action of the closed loop stirrups or ties. This seems to be in accordance with findings of other investigators (2,5,14). A careful study was made concerning the stress-strain distribution (stress block) at yield of the concrete as shown in Fig. 25. The resulting study indicated that the straight line theory was a reasonable approach. The moment-curvature relationships, Fig. 30, indicates that section 2 began yielding at a curvature of 5.60×10^{-4} and section 1 at 5.10×10^{-4} as shown in Table IV. These compare within 21.1% and 29.4% respectively of the theoretical curvature. The lack of comparison can be contributed to the assumptions made for the flexural rigidity of the sections. The load deflection behavior, Fig. 31, shows the behavior of the beam at yield by a rapid bending over of the curve. Comparison was made between theory and experimental as shown in Table IV. A steel rule (measuring to the .001") limited the accuracy of measurements.

5.2 Beam 1

This particular beam had steel ratios of .0068 and .0066 at sections 1 and 2 (1-#3), respectively, and was reinforced in tension only (Table I). The percentage of steel used was less than the deflection limitation set by the code $p = 0.18f_c'/fy$. The high strength steel used had no definite yield plateau as shown in Fig. 10 and had a yield stress of 70.0 ksi. Twenty-three stirrups were used having a spacing of $2\frac{1}{2}$" as shown in Fig. 24, giving equal tieing or confining action at each section. Upon loading the beam, a characteristic moment crack was noticed at section 2 at a load of 1.0 kip and one at section 1 at a load of 1.25 kips. Additional loading resulted in section 2 yielding at a load of 4.25 kips and a moment of 36.5 in-kips as given in Table III. These compared within 2% and 3.96%, respectively, of the theoretical values. Section 1 yielded later at a load of

3.50 kips and a moment of 37.5 in-kips which are within 0.52% and 4.26% of the theoretical values. The moment-curvature relationship shown in Fig. 32 indicates the characteristic no yield plateau of the reinforcing used. The curvatures found at first yield of sections 2 and 1 were 6.0×10^{-4} and 7.0×10^{-4} comparing within 25% and 4.75% of the theoretical curvatures (Table IV). The rotation capacity of section 2 was seen to be good, allowing section one to yield and rotate until a failure developed at section 2. This specimen had more than ample rotation capacity. failure occurred in an explosive and brittle manner by the breaking of the reinforcing bar at a load of 4.65 kips and a moment of 57.5 in-kips. After failure, a diagonal crack developed at the point of inflection between sections 1 and 2. This particular crack was noticed to begin at the bar cutoff point and develop diagonally as shown in Fig. 20. The load-deflection behavior of section 1 given in Fig. 33 indicates that there was no rapid change in curvature of the load-deflection diagram as was the case in the preliminary beam. This might be due to the nature of the bar used. The deflections measured at section 1 with yielding occurring at section 2 compared within 13.6% of theory and the deflection measured when section 1 yielded compared within 0% of theory as shown in Table IV.

5.3 Beam 2

Sections 1 and 2 had a steel ratio of .0116 and .0119 (1-#4) (Table I). The reinforcing was a high strength steel having a definite but short yield plateau (Fig. 10) with a yield stress of 65.8 ksi shown in Table II. Thirty-five stirrups were used, as shown in Fig. 24, at a spacing of $2\frac{1}{2}$" throughout the beam, thus giving equal confining action at each section. Upon loading of the beam, moment cracks were noticed at sections 1 and 2 at loads of 1.5 and 1.25 kips, respectively. The effects of these cracks can be seen in Fig. 34 on the moment-curvature curve. With additional load, section 2 began yielding at a load of 4.75 kips and a moment of 58.2 in-kips comparing within 2.74% and 1.5%, respectively, with theory. With additional load, section 1 began yielding at a load of 5.50 kips and a moment of 56.5 in-kips comparing within 5.14% and 4.43% of the theoretical values (Table III). The fact that the moment at section 2 at yield was higher than that at section 1 might be due to the limited accuracy of steel placement, as a 0.10" error in placement was found to cause a significant change in moment at a section when yielding occurred. Section 2 rotated with no increase in moment until a region of strain hardening developed, while section 1 increased slightly in moment before development of strain hardening as shown in Fig. 34. The load-deflection behavior had the characteristic semi-elastic action up to development of yield and then the rapid curvature change of the load-deflection curve occurred similar to the one observed for the preliminary beam as shown in Fig. 35. The final failure resulted from a diagonal tension crack developing in the pure shear region near the point of inflection at a load of 6.65 kips. The crack formed at the end of positive moment steel and progressed to the cutoff point of negative moment steel. Thus, the formation of the diagonal tension crack seems to be associated with bar cutoff. At total collapse the bars became visible and pulled out of the concrete for the total embedment length beyond the diagonal crack (compression region) which seems to indicate that high bond stress developed at the crack. This type of failure is not unexpected or unreasonable since it has been found by Ferguson and others in a rigorous series of tests that cutting off bars in "tension zones" reduced the shear strength considerably. It has also been found that bond stress and diagonal tension act together to bring about reduced strengths (9,11). Cover is also a problem if bond stress is critical; this may in itself result in splitting over the bars.

The diagonal crack was found to have no effect on the formation of the mechanism since it developed after the mechanism had formed. By investigating the moment-curvature diagram (Fig. 34) it can be seen that strain hardening had already developed and at formation of the diagonal crack the hardening flattened out. This did however, limit the reserve capacity that would have existed had the beam failed due to flexure.

5.4 Beam 3

The ratios of tension steel used at sections 1 and 2 were .0134 and .0135 (2-#3) respectively as shown in Table I. The reinforcing was high strength having no definite yield plateau as shown in Fig. 11 with a yield stress of 70.0 ksi as given in Table II. The web reinforcing consisted of thirty-five stirrups placed at $2\frac{1}{2}$" throughout the beam giving equal confinement at both sections. With application of load, moment cracks began developing at section 2 at a load of 1.75 kips and later, one occurred at section 1 at a load of 3.435 kips which seemed to be a little high. Additional load caused section 2 to yield at a load of 6.0 kips and a moment of 75.0 in-kips and later, section 1 yielded with a load of 7.20 kips and 73.5 in-kips. The theory is conservatively under these values by 9.1% and 9.08%, respectively, for loads and moments at section 2 and 10.4% and 3.95%, respectively, for loads and moments at section 1 as shown in Table III. Examining the moment-curvature relationship in Fig. 36 shows that curvature at yield for section 2 occurred at 8.5×10^{-4} and for section 1 yield occurred at 8.0×10^{-4} which compared within 12% and 5%, respectively, of the theory. The rotation capacity of section 2 was good. The load-deflection behavior in Fig. 37 showed the characteristic round house (continuous curvature change with moment) curve that would exist for a beam having steel without a yield plateau. The moment-curvature relationship shows a slight increase in moment as curvature increases with a final strain hardening taking place. The deflection at the development of yield at section 2 was within 33.3% of the theory and within 28.0% of theory when section 1 yielded as shown in Table IV. There is no immediate explanation for the large deviation in results for deflection. However, a possible explanation could be what was assumed for flexural rigidity. Failure of the beam resulted in spalling and crushing of the concrete at section 1 and with a small additional load complete collapse occurred as a result of a diagonal tension crack forming at the end of the bar cutoff point and projecting as it did for beam 2. The ultimate concrete fiber strain existing at section 2 on occurrence of spalling was .00834 in/in with a moment of 108.3 in-kips while section 1 had a fiber strain of .00608 in/in. Both were much higher than assumed by theory. Thus, the diagonal crack forming had no resulting influence in this beam.

5.5 Beam 4

The ratios of steel used at section 1 and 2 were .0238 and .0238 (2-#4). The reinforcing was a high strength steel with a definite yield plateau as shown in Fig. 11, having a yield stress of 65.9 ksi as shown in Table II. The web reinforcement consisted of fifty-seven stirrups as shown in Fig. 24 with forty-five placed at $1\frac{1}{4}$" and twelve at $2\frac{1}{2}$" giving equal confinement at each section. As load was applied, moment cracks began to form at sections 1 and 2, at loads of 3.03 kips and 2.54 kips respectively. When additional load was applied, section 2 began yielding at a load of 9.25 kips and a moment of 112.5 in-kips. These compared within 13.5% and 12.2% of theory. Section 1 began yielding at a load of 9.85 kips and moment of 99.0 in-kips comparing within 8.64% and 0% of theoretical values as shown in Table III. After examining the moment-curvature relationship for the beam studied (Fig. 38), the curvature at yield was seen to be 10.75×10^{-4} for section 2 and 8.75×10^{-4} for section 1. These compare within 37.8% and 23.2%, respectively, of the theoretical values. A possible explanation for the large deviation would be that the assumed value for flexural rigidity is too high. The difference between the theoretical and experimental values for deflections is nearly 100%. Again there is no immediate explanation other than the fact that they deviate more than curvature does. Investigation of the load-deflection behavior indicated that the mechanism had formed before failure but only to a limited extent as shown in Fig. 39.

Final failure again resulted in collapse by diagonal cracking at the point of inflection. The crack formed at the bar cutoff point and propagated diagonally up the beam as indicated in beams 2 and 3. Again, this particular failure did not limit the plastic behavior of the beam but did limit the reserve capacity above plasticity. This particular beam was designed to have limited rotation capacity. Based on the ultimate concrete fiber strain of .003 in/in, the rotation capacity was ($\varnothing_{ult}/\varnothing_{y2} = 1.5$) and the required rotation was ($\varnothing_{mech}/\varnothing_{y2} = 2.05$), but as can be seen the mechanism did form and there was ample rotation capacity. The ultimate load at failure was 10.3 kips with ultimate moments at section 1 and 2 of 106.2 and 127.5 in-kips, respectively. The ultimate concrete fiber strains were .00439 in/in at section 1, and .00685 in/in at section 2. These fiber strains may be distorted somewhat due to the action of the diagonal crack.

5.6 Beam 5

Sections 1 and 2 had .0185 and .0186 ratios of steel, and were reinforced in tension only, as shown in Table I. A high strength steel was used, having the yield properties shown in Fig. 12 and tabulated in Table II. The average yield stress was used for all theoretical work done for this beam. Web reinforcing entailed the use of forty-four stirrups with nineteen spaced at 1¼" and twenty-five at 2½" as seen in Fig. 24. As load was applied, tension cracks were observed for section 2 at a load of 3.01 kips and for section 1 at a load of 3.80 kips. With additional load, yielding began at section 2 at a load of 8.25 kips and a moment of 102.0 in-kips. These compare within 15.75% and 15.68% of theoretical values, respectively. Examining the moment-curvature relationship (Fig. 40) it can be seen that curvature at section 2 was 8.5×10^{-4}, comparing within 15.75% of theory (Table IV). The deflection at yield was 0.148 in. as given in Table IV. The theoretical values are very much under the test values. Upon yielding, a diagonal hairline crack appeared in the same loacation as in the other beams. Since failure was not explosive in nature, additional load was added until section 1 yielded. The diagonal crack would seem to have the effect of increasing the rotation of section 2 and decreasing that existing at section 1. The crack would also have the tendency of increasing deflections. Even though the theory no longer holds, the theoretical values compare closely to those obtained experimentally. Examining the moment-curvature relationship indicates that plasticity still developed even though the assumed theory no longer applied.

5.7 Beam 6

This beam had .0310 and .0314 steel ratios in tension at sections 1 and 2 with .0067 used in compression for both sections. The stress-strain properties of the bars used are shown in Fig. 12 with the corresponding yield stress given in Table I. The bars, in order to get the symmetrical reinforcing desired at each section, had a limited splice length of d distance which was not in accordance with the code. The web reinforcement consisted of sixty-two stirrups as shown in Fig. 24 placed at 1, 1¼, and 2½", respectively. Twenty-four were placed at 1", twenty-six at 1¼", and twelve at 2½". The beam at section 2 had 1.25 times the confinement as did section 1. No tension moment cracks were observed to form in the beam. Section 2 began yielding at a load of 11.64 kips and a moment of 144.0 in-kips as shown in Table III. These compared within 9.95% and 8.9% of theory, respectively. Investigating the moment-curvature properties (Fig. 42) indicates that the curvature at yield, given in Table IV, was 10.0×10^{-4} comparing within 25.5% of theory and, as seen from the load-deflection behavior (Fig. 43), there was a sudden jog in the results at a load of 9.78 kips. This is not entirely unexpected as a result of the diagonal tension crack forming. Actually the diagonal tension crack tends to reduce the deflection at section 1 (at formation) and tends to increase it at the location of the crack. Then with additional load the deflection at section 2 begins increasing again. As can be seen from the moment-curvature relationships, the points (shown in Fig. 42) around 120 in-kips for section 1 became very close together at the formation of the crack, thereby decreasing the curvature at section 1 and increasing the rotation at section 2. Splices were observed to cause splitting due to bond (11). This particular type of failure was noticed to occur at final collapse. Theory was not applicable for this beam.

5.8 Beam 7

This beam was designed as an over-reinforced beam, having steel ratios at section 1 and 2 of .0314 each in tension only as shown in Table I. The web reinforcement consisted of sixty-two stirrups spaced at 1, $1\frac{1}{4}$, and $2\frac{1}{2}$", respectively as shown in Fig. 24. Twenty-four were spaced at 1", twenty-six at $1\frac{1}{4}$", and twelve at $2\frac{1}{2}$". The stress-strain curve for the reinforcing steels, shown in Fig. 13, have yield stress values given in Table I.

The rotation capacity was investigated and seen to be $\phi_{ult}/\phi_{y2} = 1.285$ and the required rotation $\phi_{mech}/\phi_{y2} = 2.04$. As the beam was loaded, the typical diagonal tension crack was formed as discussed earlier for the other beams at 9.5 kips. The load at first yield occurred at 10.67 kips and a corresponding moment of 133 in-kips. Even though the theory will no longer hold true as to curvature and deflection, it still was within 10.75% for load and 9.87% for moments. The formation of the diagonal crack tends to give larger rotations at section 2 and smaller ones at section 1. The concrete fiber strains at final loading were observed to be .00281 in/in and .0031 in/in at sections 1 and 2, respectively.

VI. CONCLUSION

This investigation involved testing 8 propped cantilever beams with varying percentages of reinforcement. Seven beams were singly reinforced with equal percentages at each critical section with bars cutoff d distance beyond the occurrence of the point of inflection as determined by the plastic theory. One beam was doubly reinforced with splice lengths of d length.

The preliminary beam tested with intermediate grade steel had ample ductility and compared favorably with theory. Beam no. 1 also compared quite well and had no limitations involving cutoff length. All other beams tested had diagonal cracks form at the bar cutoff point and propagated diagonally up the beam. The beam with double reinforcement had the same characteristic type failure pattern. However cutoff points of the bars limited plastic development of only beams 5 and 7. The splice length of the doubly reinforced beam definitely limited plasticity.

The author can not draw any conclusions as to the cause of the diagonal cracks to form, however cause could possibly have resulted from splitting action over the reinforcing bars as a result of the limited cover. Conclusions can not be drawn regarding how much effect the ties had in delaying the diagonal cracks to form but all indication leads the author to believe that ACI code requirements for cutoff points can be reduced.

The modulus of elasticity determined from the concentric cylinder tests is not completely correct and it is the author's opinion that flexural studies should be made investigating the effect of confinement on the modulus of elasticity. Additional research should be continued investigating cutoff lengths and the percentages of steel. The author believes an investigation should also be made on the effect of confinement on curvature behavior of reinforced concrete beams. Both ties and spirals could be tested with emphasis on ties since they would probably be used more often in engineering practice.

BIBLIOGRAPHY

1. ACI-ASCE Committee 327, "Ultimate Strength Design," ACI Proceedings, Vol. 52, pp. 505-524, (1955).

2. Baker, A.L.L., "The Ultimate-Load Theory Applied to The Design of Reinforced and Prestressed Concrete Frames," Concrete Publications Ltd., London, 1956.

3. Beedle, Lynn S., (1958), Plastic Design of Steel Frames, 2nd Ed., Wiley, New York, pp. 184-204.

4. Berwanger, Carl, "Application of Plastic Design Theory to Reinforced Concrete Continuous Beams," Queen's University, Kingston, Ontario, (thesis), (1957).

5. Chan, W.W.L., "The Ultimate Strength and Deformation of Plastic Hinges in Reinforced Concrete Frameworks," Magazine of Concrete Research 7, pp. 121-132, 1955.

6. Eppes, Bill G., "Comparison of Measured and Calculated Stiffneses for Beams Reinforced in Tension Only," ACI Proceedings, Vol. 56, pp. 313-325, (1959).

7. Ernest, G.C., Riveland, A.R., "Ultimate Loads and Deflections from Limit Design of Continuous Structural Concrete," ACI Proceedings, Vol. 56, pp. 273-286, (1959).

8. Ernest, G.C., "Plastic Hinging at the Intersection of Beams and Columns," ACI Proceedings, Vol. 53, pp. 1119-1144, (1957).

9. Ferguson, Phil M., Matloob, Farid N., "Effect of Bar Cutoff on Bond and Shear Strength of Reinforced Concrete Beams," ACI Proceedings, Vol. 56, pp. 5-23, (1959).

10. Ferguson, Phil M., Breen, John E., "Lapped Splices for High Strength Reinforcing Bars," ACI Proceedings, Vol. 62, pp. 1063-1078, (1965).

11. Ferguson, Phil M., Reinforced Concrete Fundamentals, 2nd Ed., Wiley, New York, pp. 137-159, (1965).

12. Hanson, Norman W., Kurvits, Otto A., "Instrumentation for Structural Testing," Journal of the PCA Research and Development Laboratories, Vol. 7, No. 2, pp. 33-37, (1965).

13. Hognestad, E., Hanson, N.W., Mc Henery, Douglas, "Concrete Stress Distribution in Ultimate Strength Design," ACI Proceedings, Vol. 52, pp. 450-480, (1955).

14. Institution Research Committee, "Ultimate Load Design of Concrete Structures," Proceedings, Institution of Civil Engineers 21, pp. 399-442, (1962).

15. Mattock, Alan H., "Limit Design for Structural Concrete," Journal of the PCA Research and Development Laboratories, Vol. 1, No. 2, pp. 14-23, (1959).

16. Murray, William M., Stein, Peter K., "Strain Gage Techniques," MIT Lectures and Laboratory Excerises, pp. 106, (1956).

17. Sawyer, Herbert A., "Elastic-Plastic Design of Single Span Beams and Frames," ASCE Structural Division Proceedings, Vol. 81, No. 851, pp. 1-29, (1956).

18. Senne, Joesph H., Personal Communication (1965).

19. Sinha, Nripendra C., Ferguson, Phil M., "Ultimate Strength with High Strength Reinforcing Steel with an Indefinite Yield Point," ACI Proceedings, Vol. 61, pp. 399-418, (1964).

20. Untrauer, R.E., Hsieh, Ming-Chih, Special report of Iowa State University Experiment Station, (Part I), "Review of Rotation Characteristics of Concrete Plastic Hinges," pp. 1-61, (1964).

21. Ekber Jr., E.J., Rhomberg, E.J., Special report of Iowa State University Experiment Station, (Part II) "Plastic Rotation in Reinforced Concrete Beams with Combined Moment and Shear," pp. 64-99, (1964).

22. Whitney, Charles S., "Design of Reinforced Concrete Members Under Flexure or Combined Flexure and Direct Compression," ACI Journal, Vol. 33, pp. 483-494, (1937).

23. Yu, C.W., Hognestad, Evind, "Review of Limit Design for Structural Concrete," ASCE Structural Division Proceedings, Vol. 84, No. 1878, pp. 1-24, (1958).

VII. APPENDIX

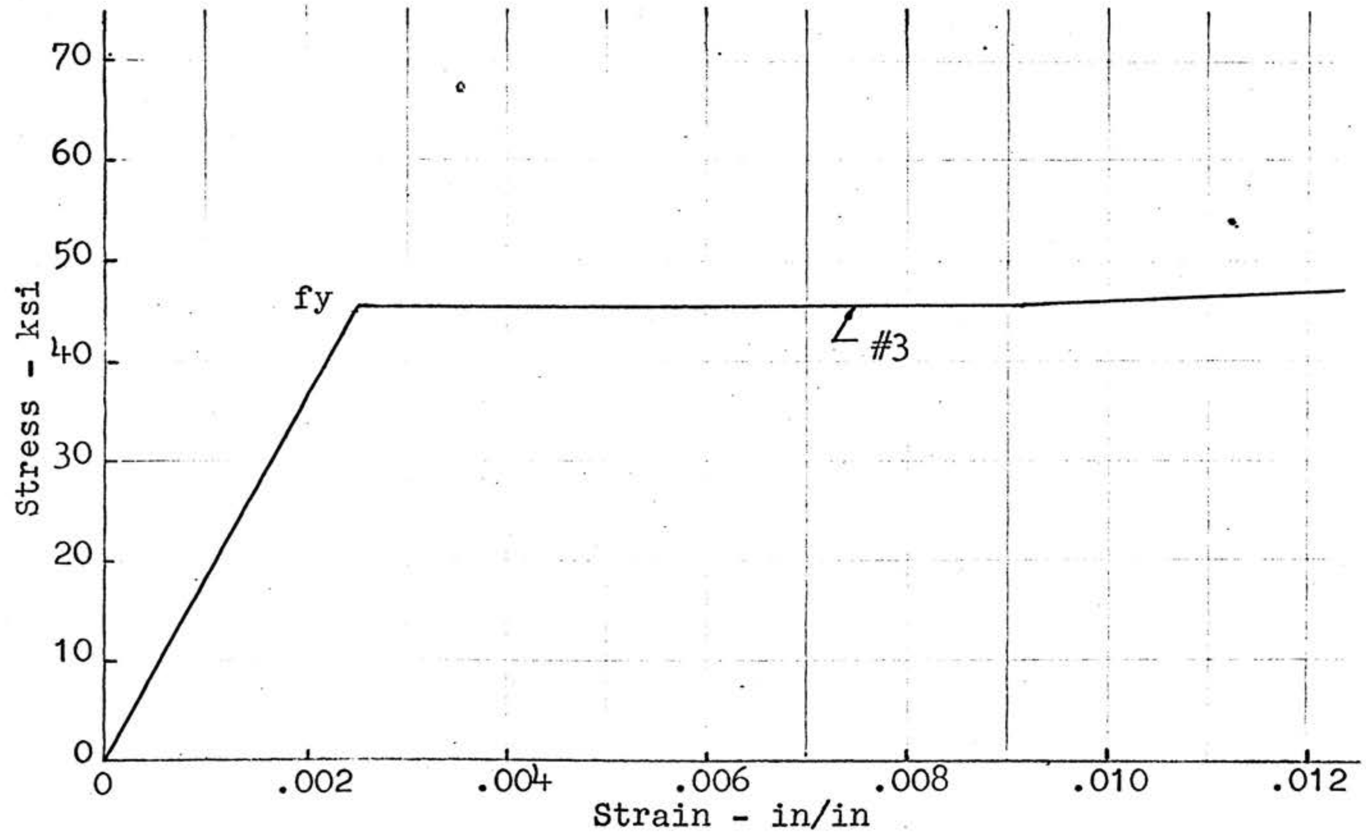

FIG. 9 STRESS VS STRAIN FOR REINFORCEMENT IN BEAM 3-A

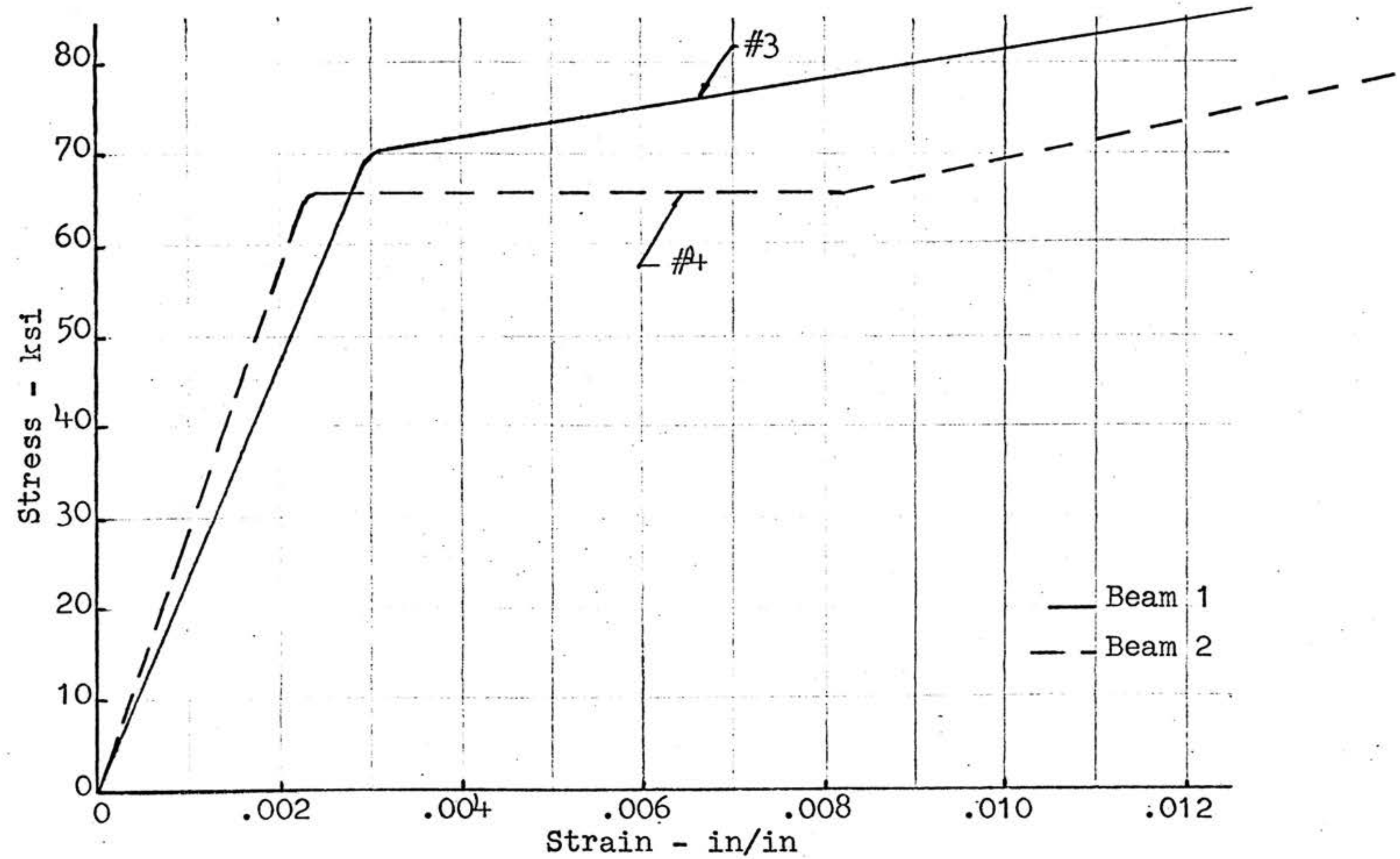

FIG. 10 STRESS VS STRAIN FOR REINFORCEMENT IN BEAMS 1&2

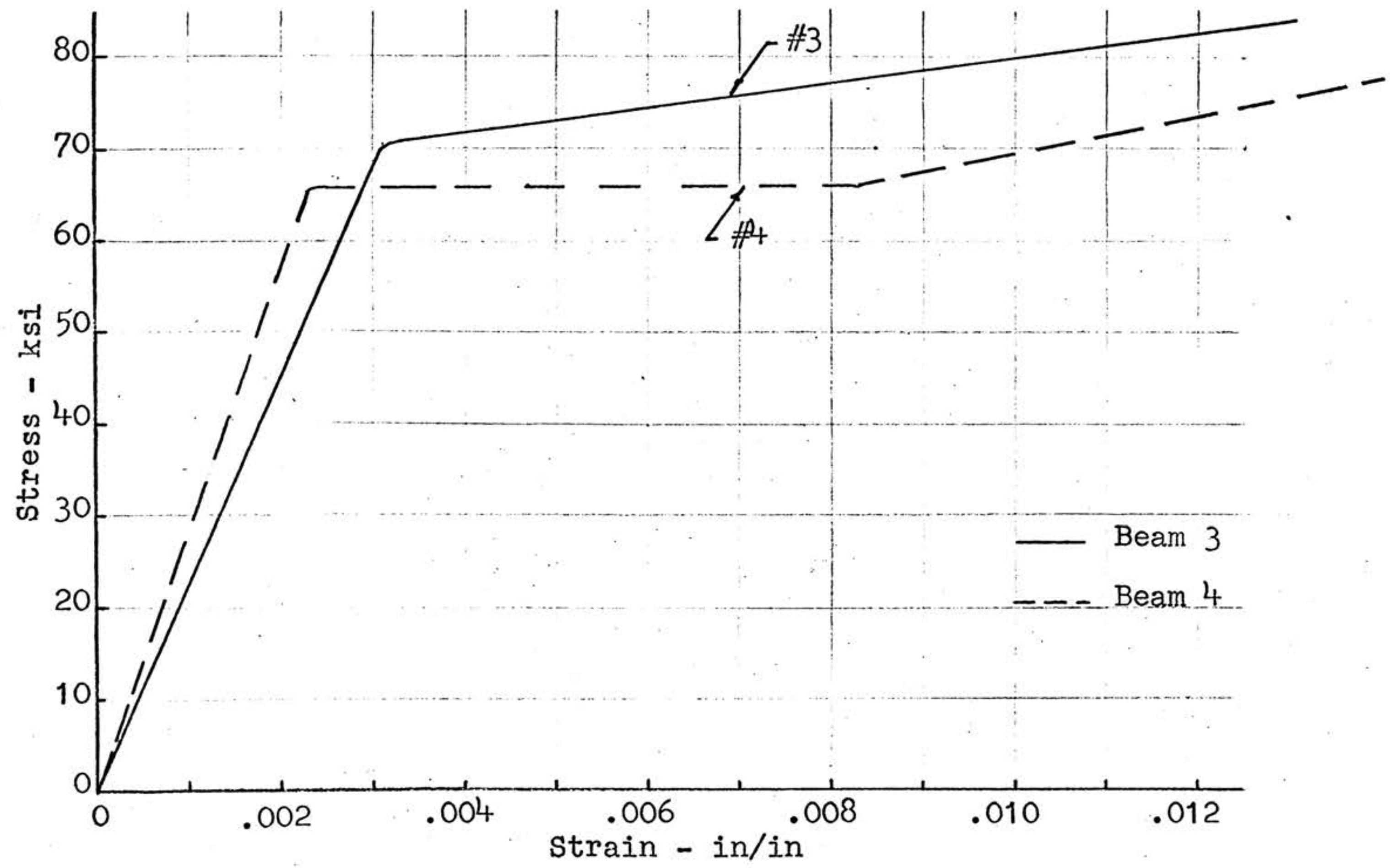

FIG. 11 STRESS VS STRAIN FOR REINFORCEMENT IN BEAMS 3&4

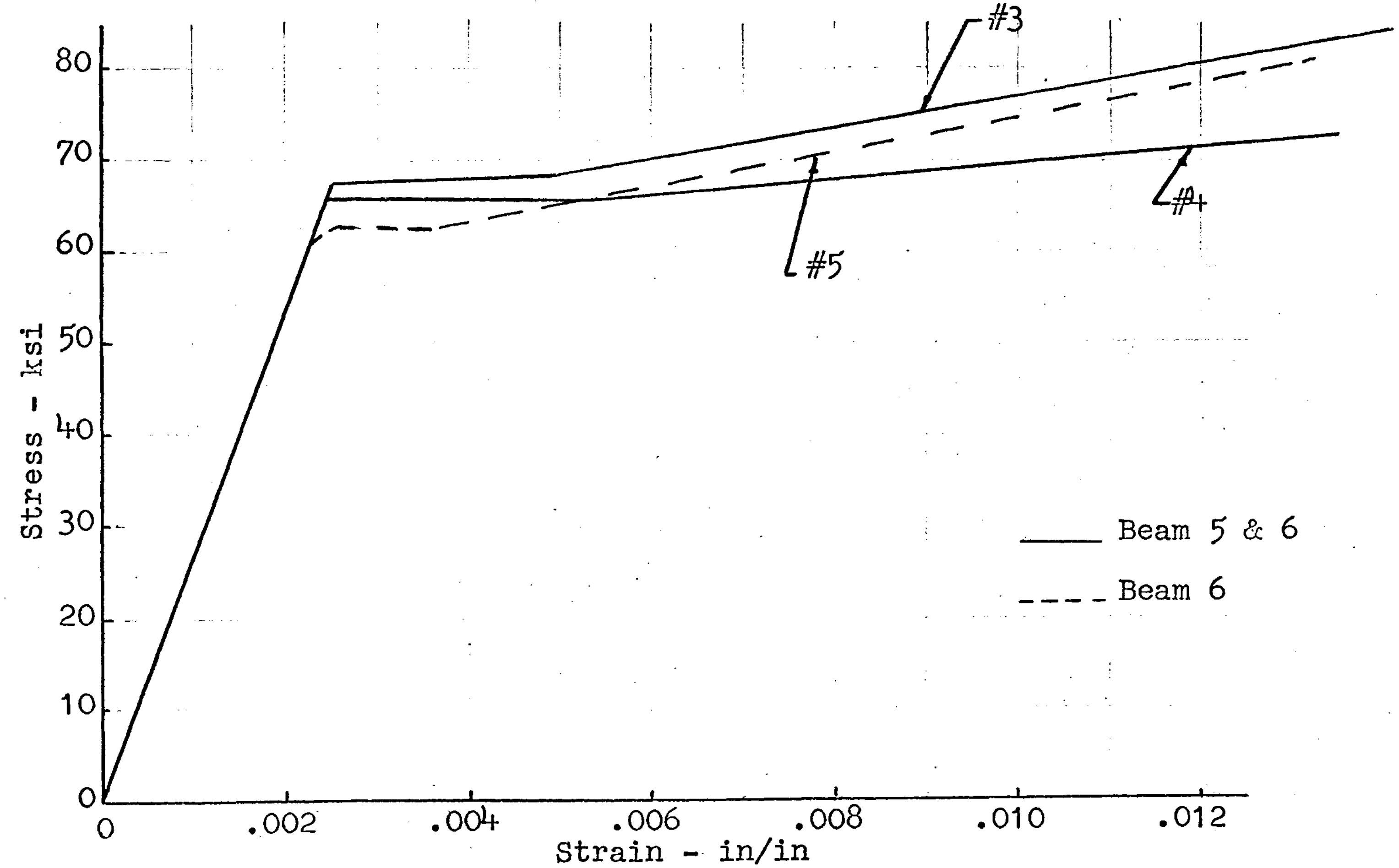

FIG. 12 STRESS VS STRAIN FOR REINFORCEMENT IN BEAMS 5&6

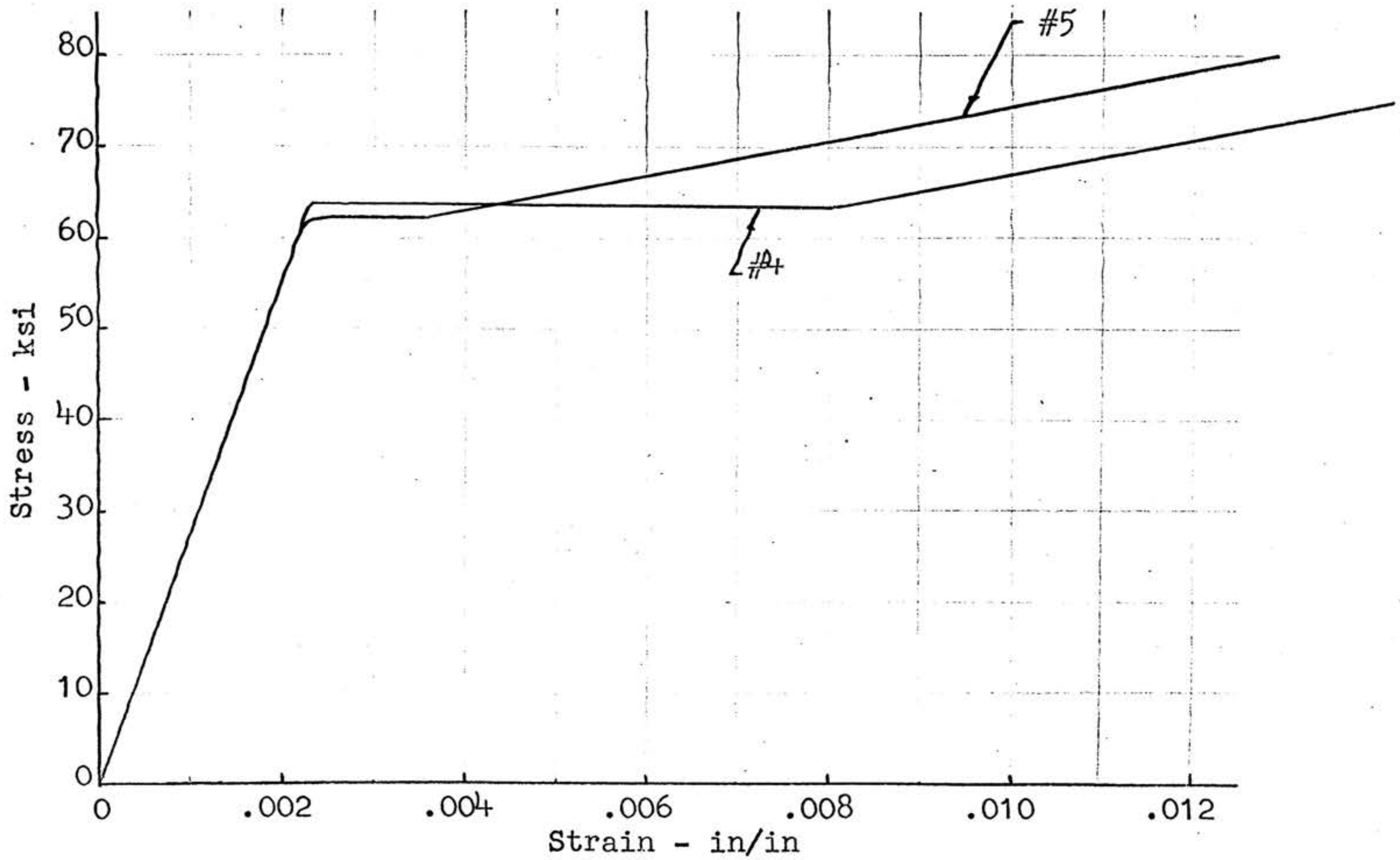

FIG. 13 STRESS VS STRAIN FOR REINFORCEMENT IN BEAM 7

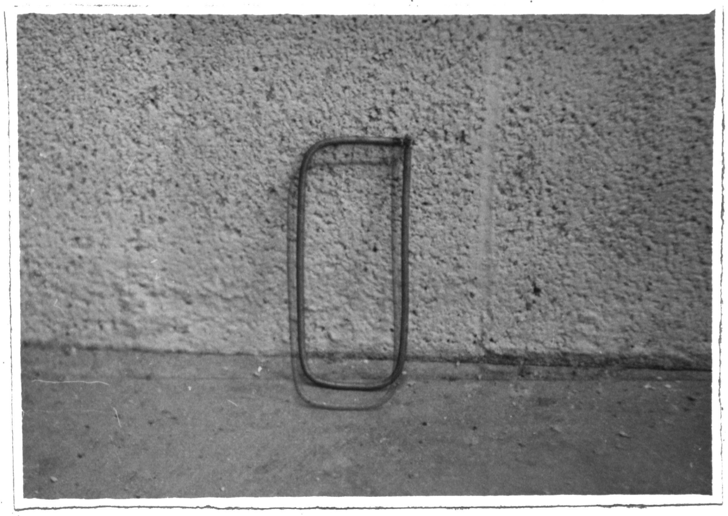

FIG. 14 CLOSED LOOP STIRRUP DETAIL

FIG. 15 REINFORCING CAGE DETAIL

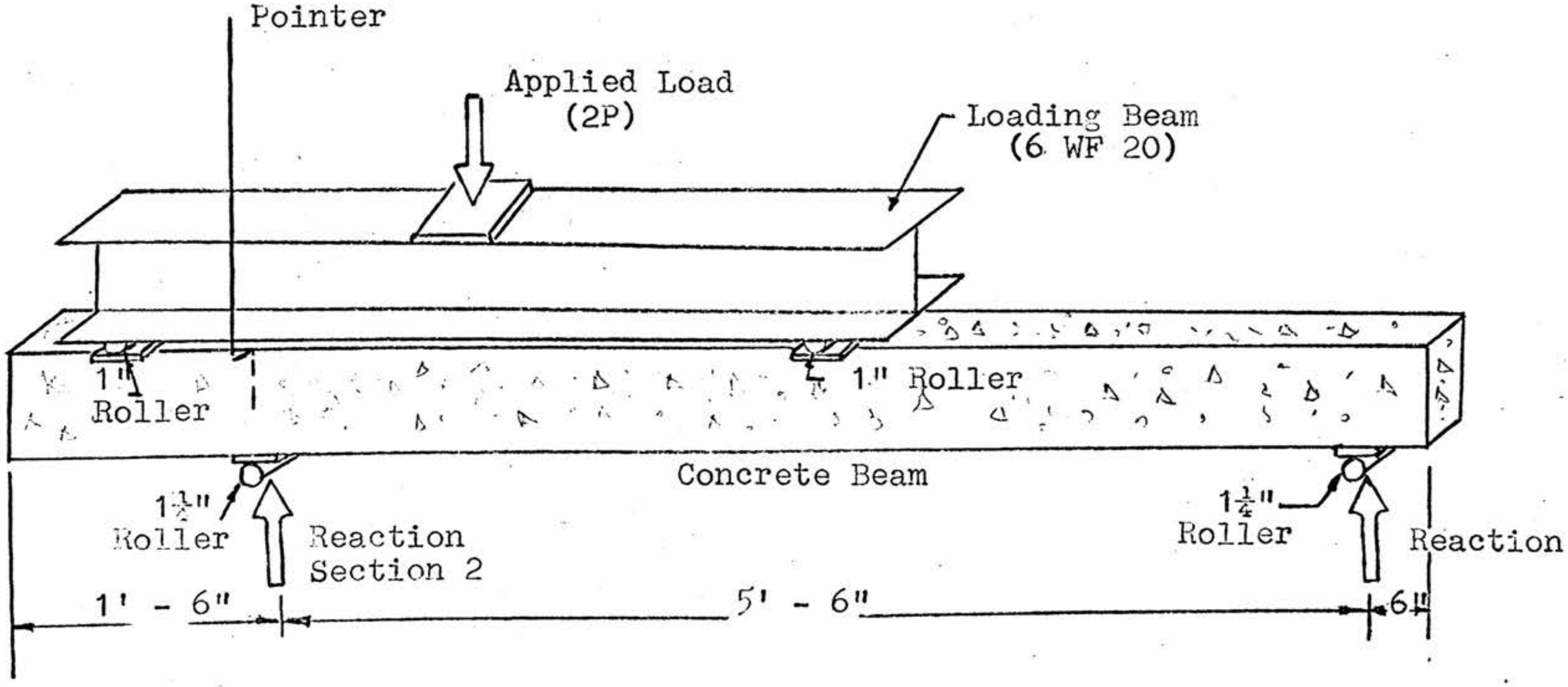

FIG. 16 APPLIED LOADING APPARATUS DETAIL

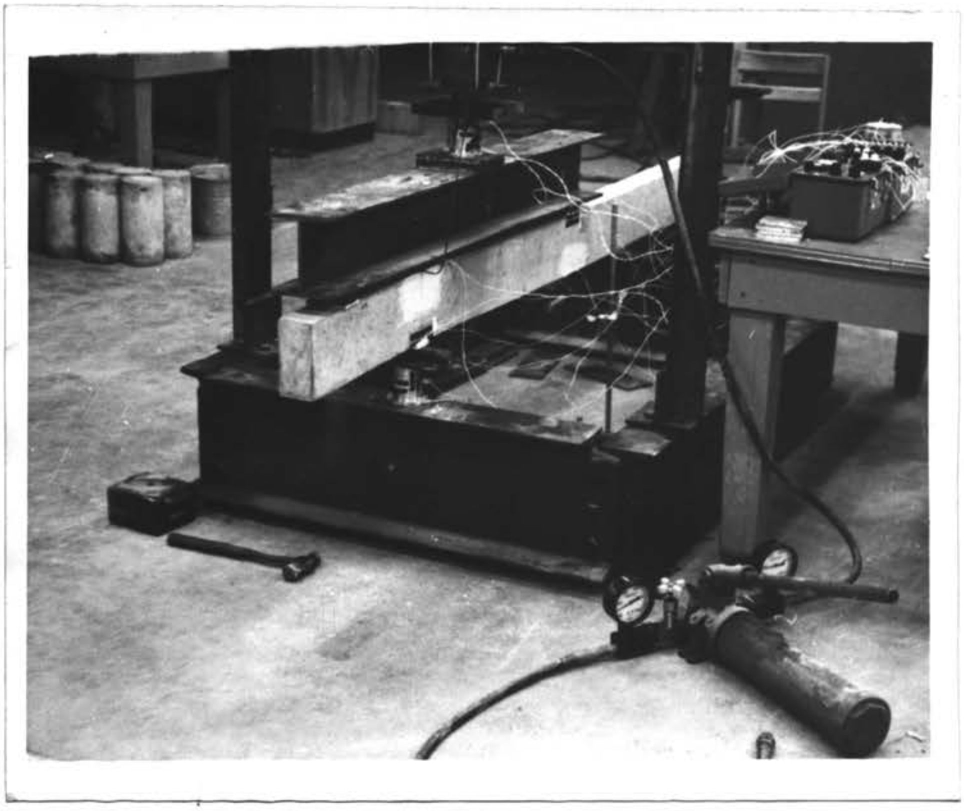

FIG. 17 INSTRUMENTATION OF BEAMS

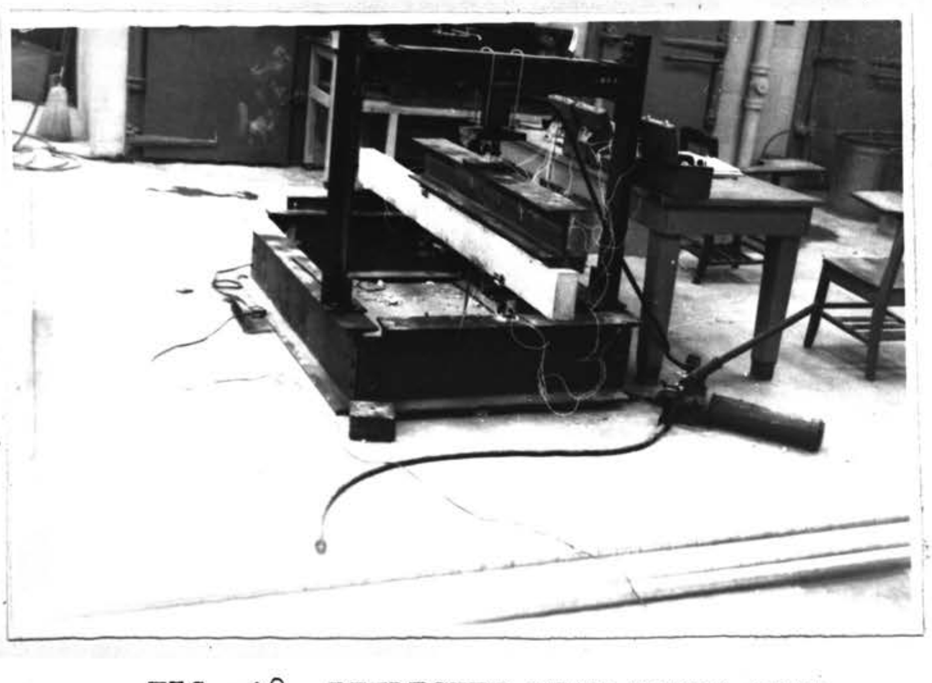

FIG. 18 DEFLECTED BEAM UNDER LOAD

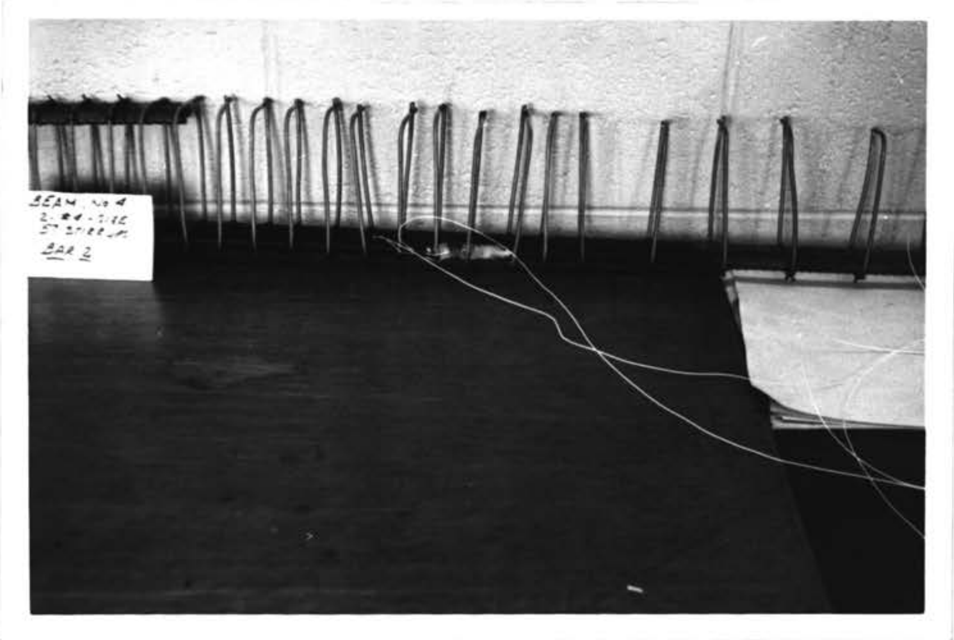

FIG. 19 STRAIN GAGE PREPARATION DETAIL

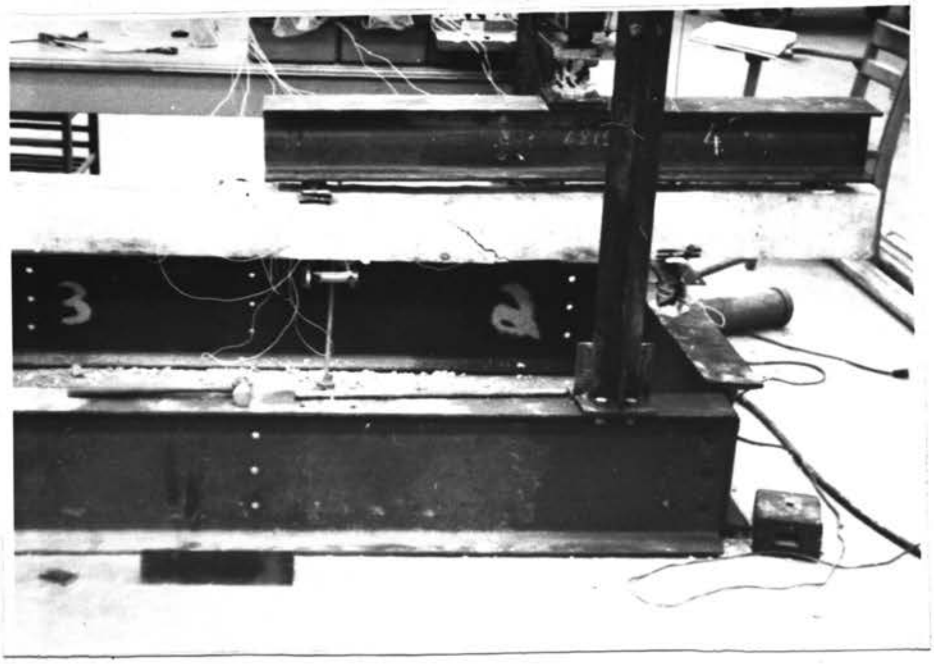

FIG. 20 BEAM UNDER INFLUENCE OF A DIAGONAL TENSION CRACK

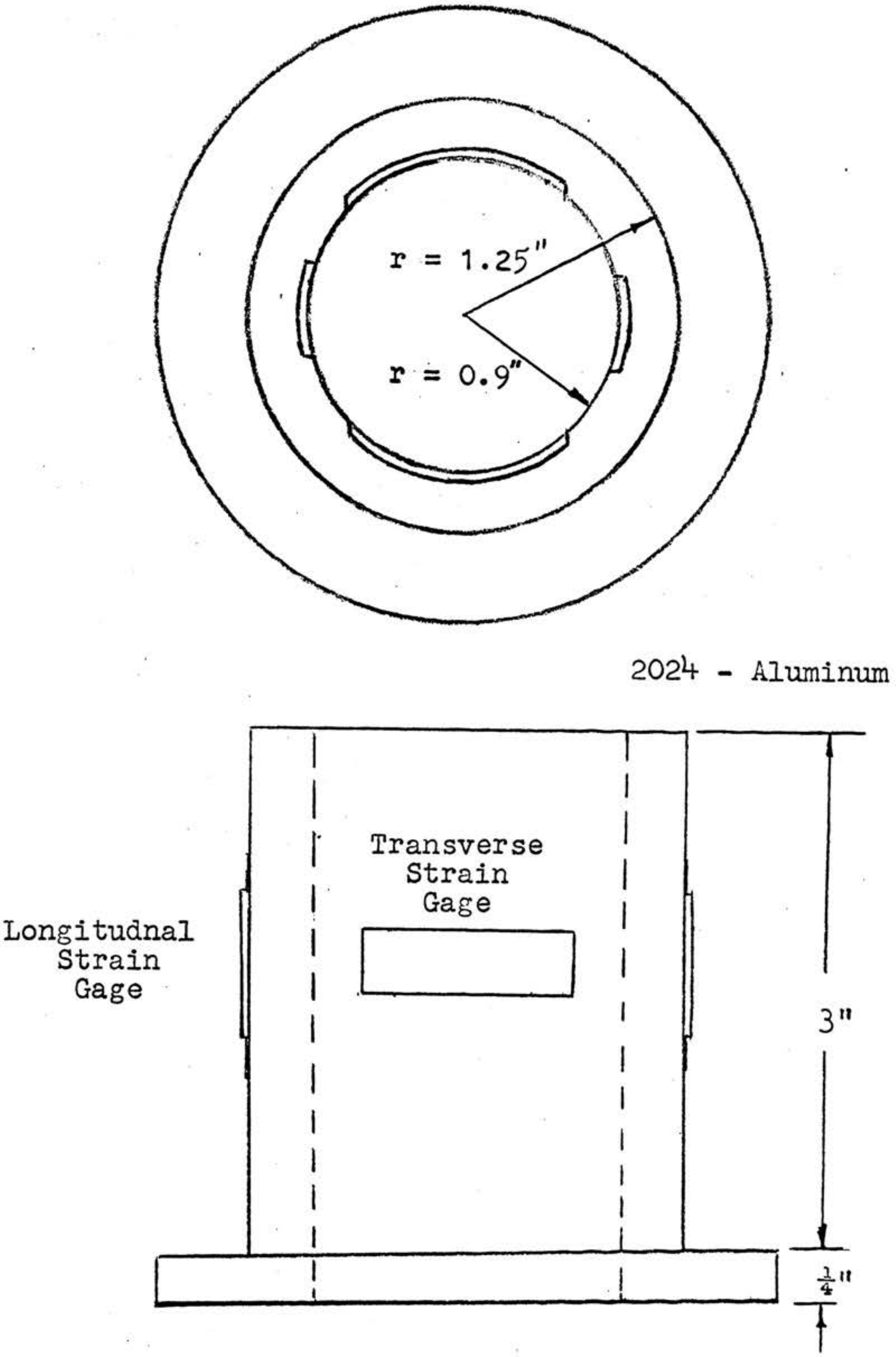

FIG. 21 LOAD CELL MADE FOR TESTING PURPOSES

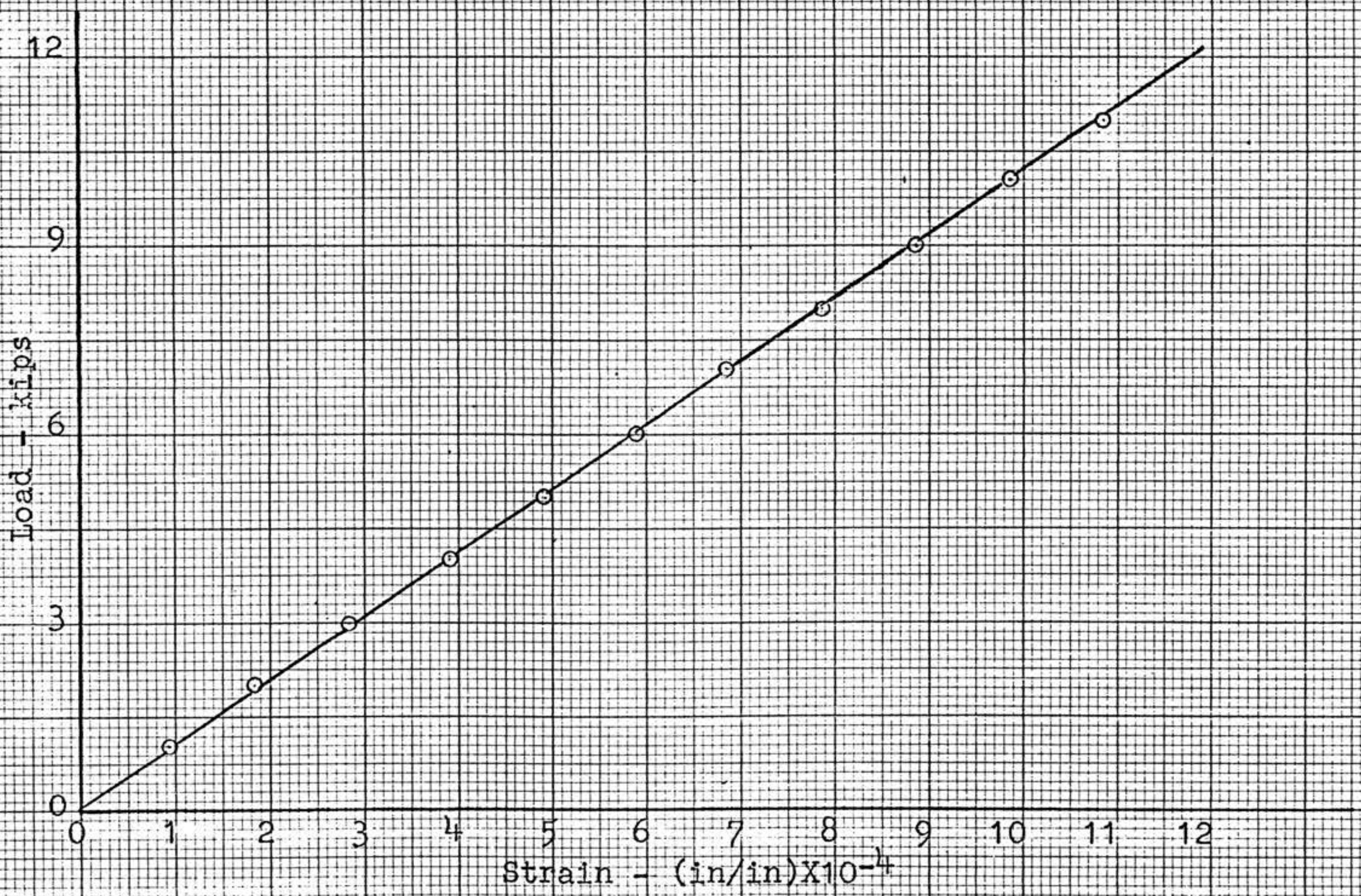

FIG. 22 LOAD CELL CALIBRATION CURVE SENSITIVE TO 12 KIPS

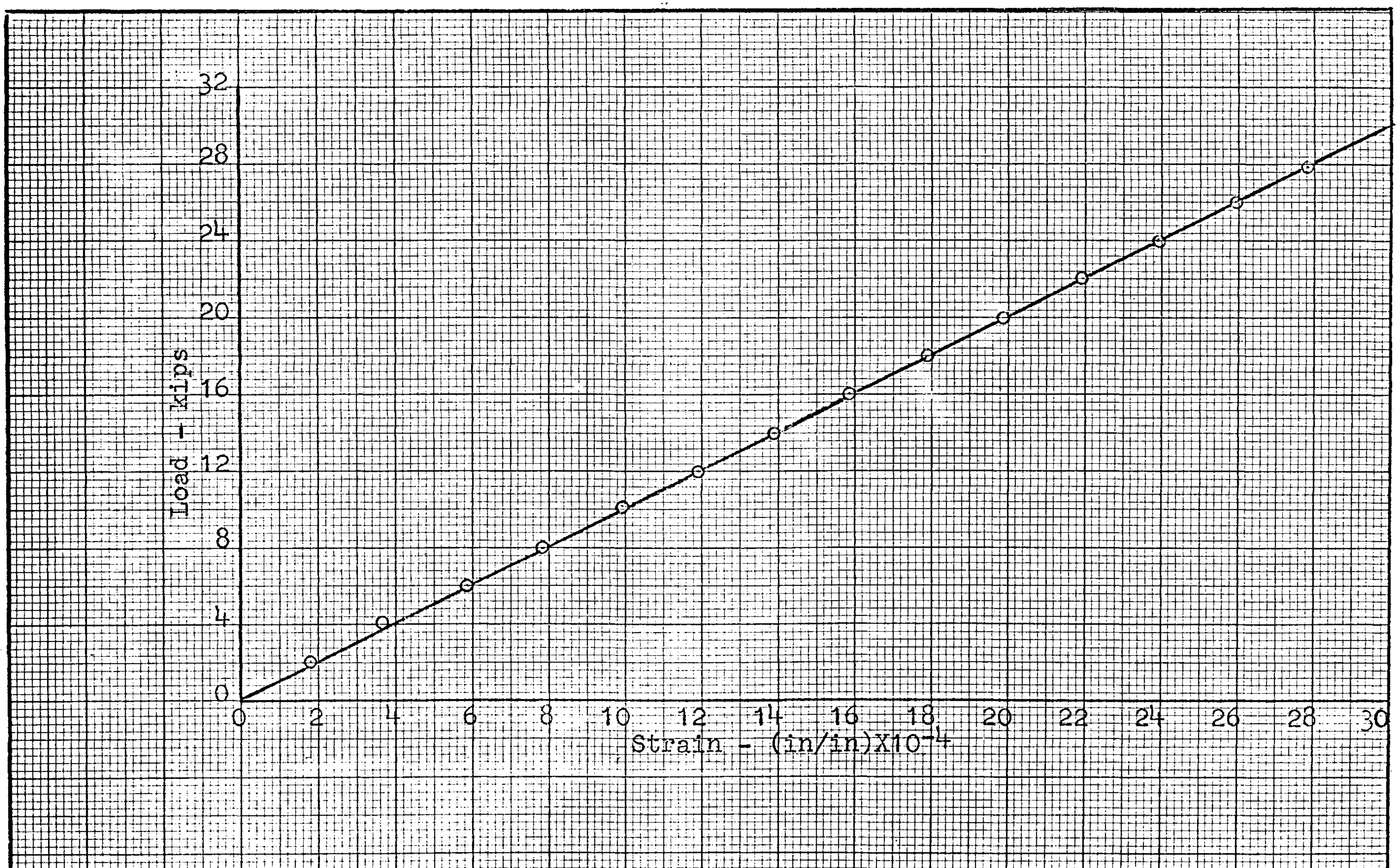

FIG. 23 LOAD CELL CALIBRATION CURVE SENSITIVE TO 32 KIPS

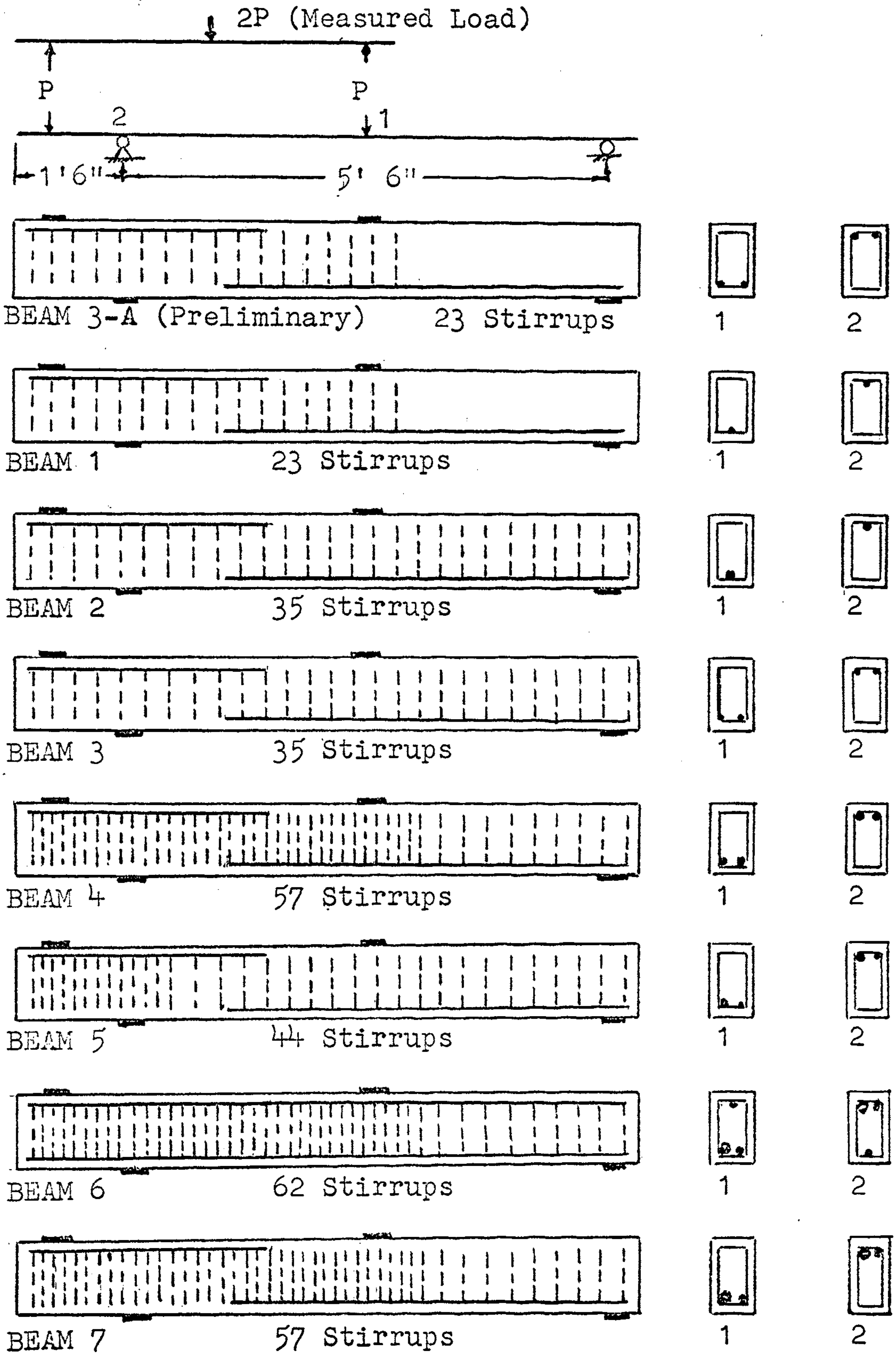

FIG. 24 BEAM SECTIONAL PROPERTIES

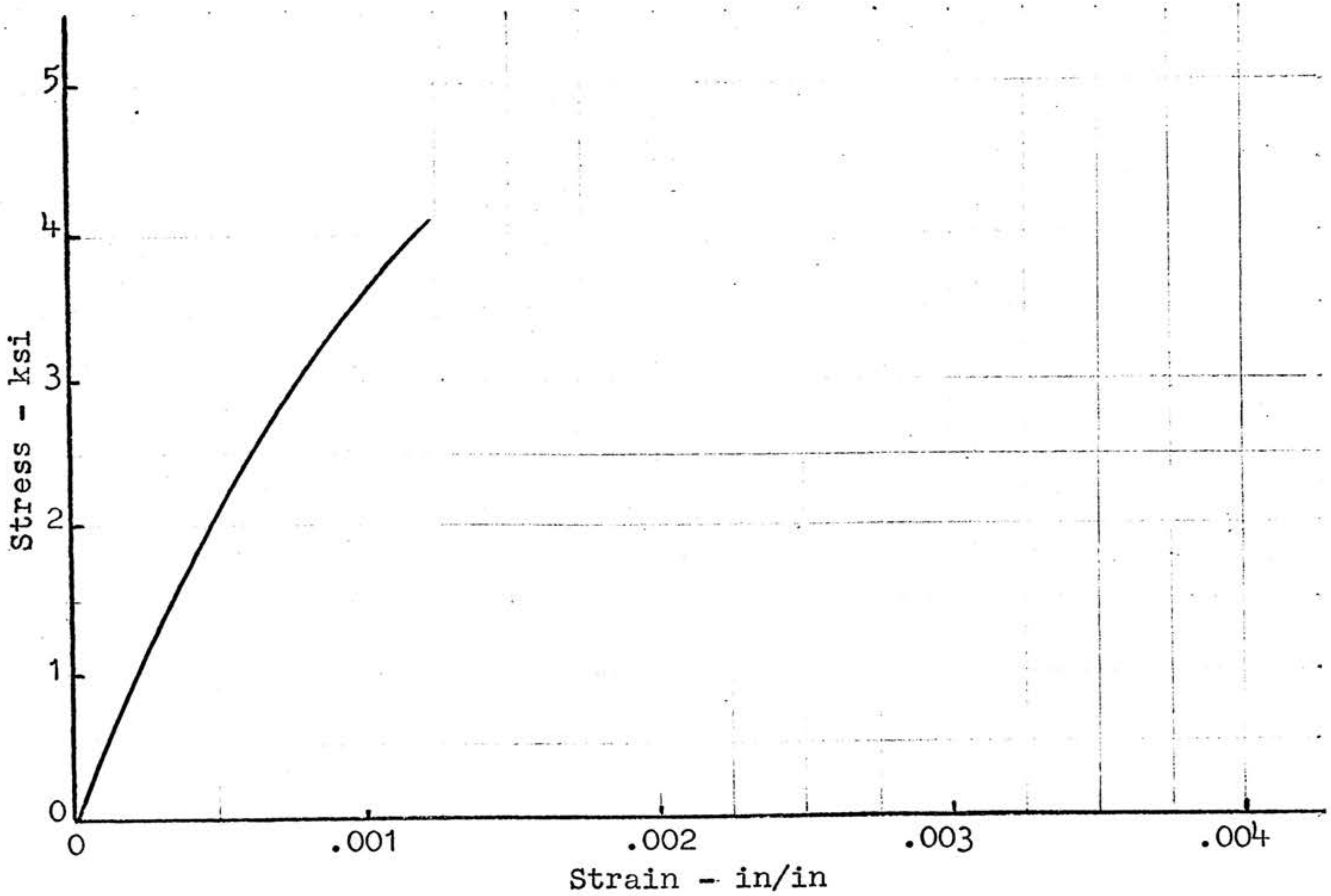

FIG. 25 CONCRETE CYLINDER STRESS VS STRAIN FOR BEAM 3-A

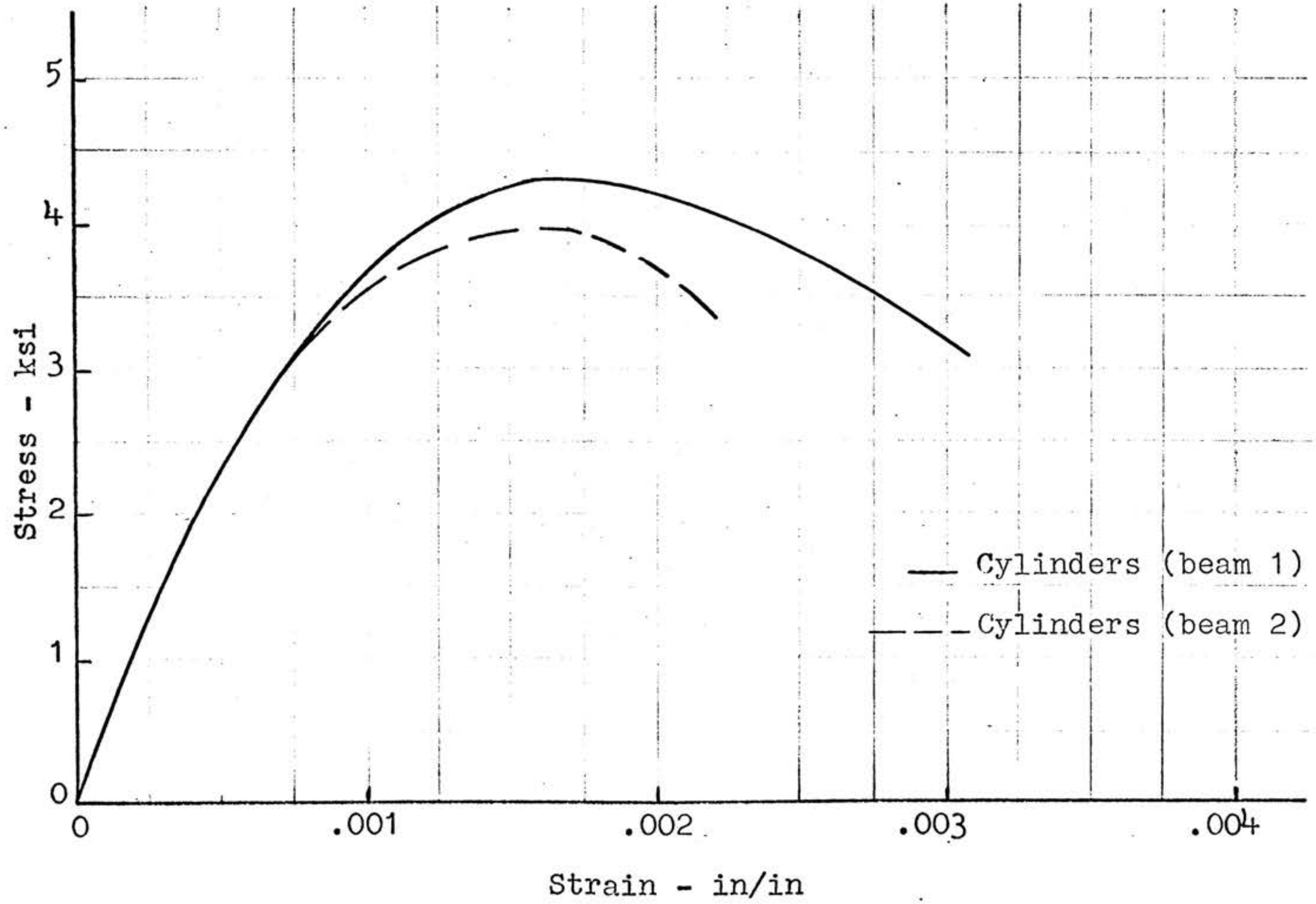

FIG. 26 CONCRETE CYLINDER STRESS VS STRAIN FOR BEAMS 1&2

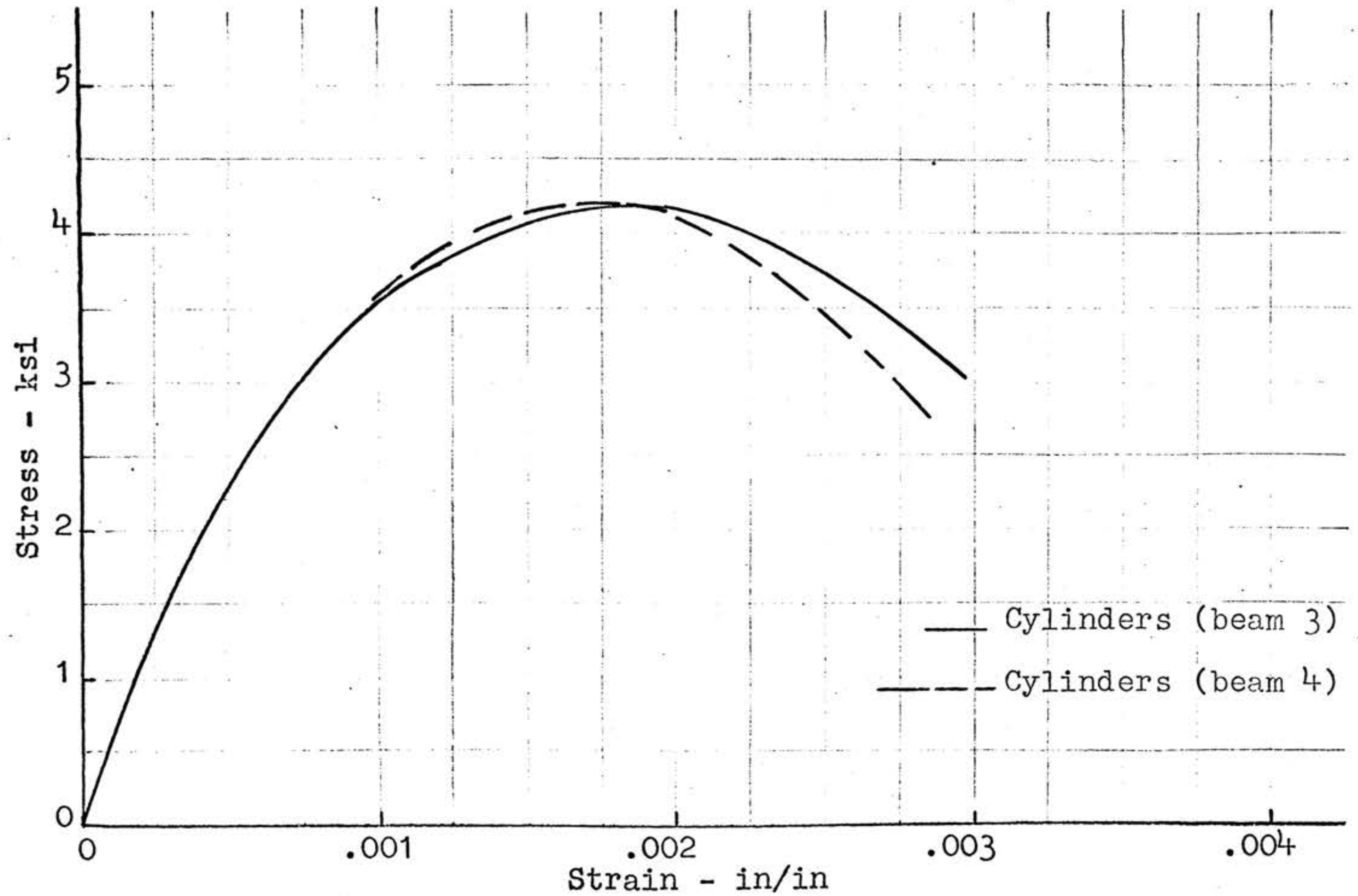

FIG. 27 CONCRETE CYLINDER STRESS VS STRAIN FOR BEAMS 3&4

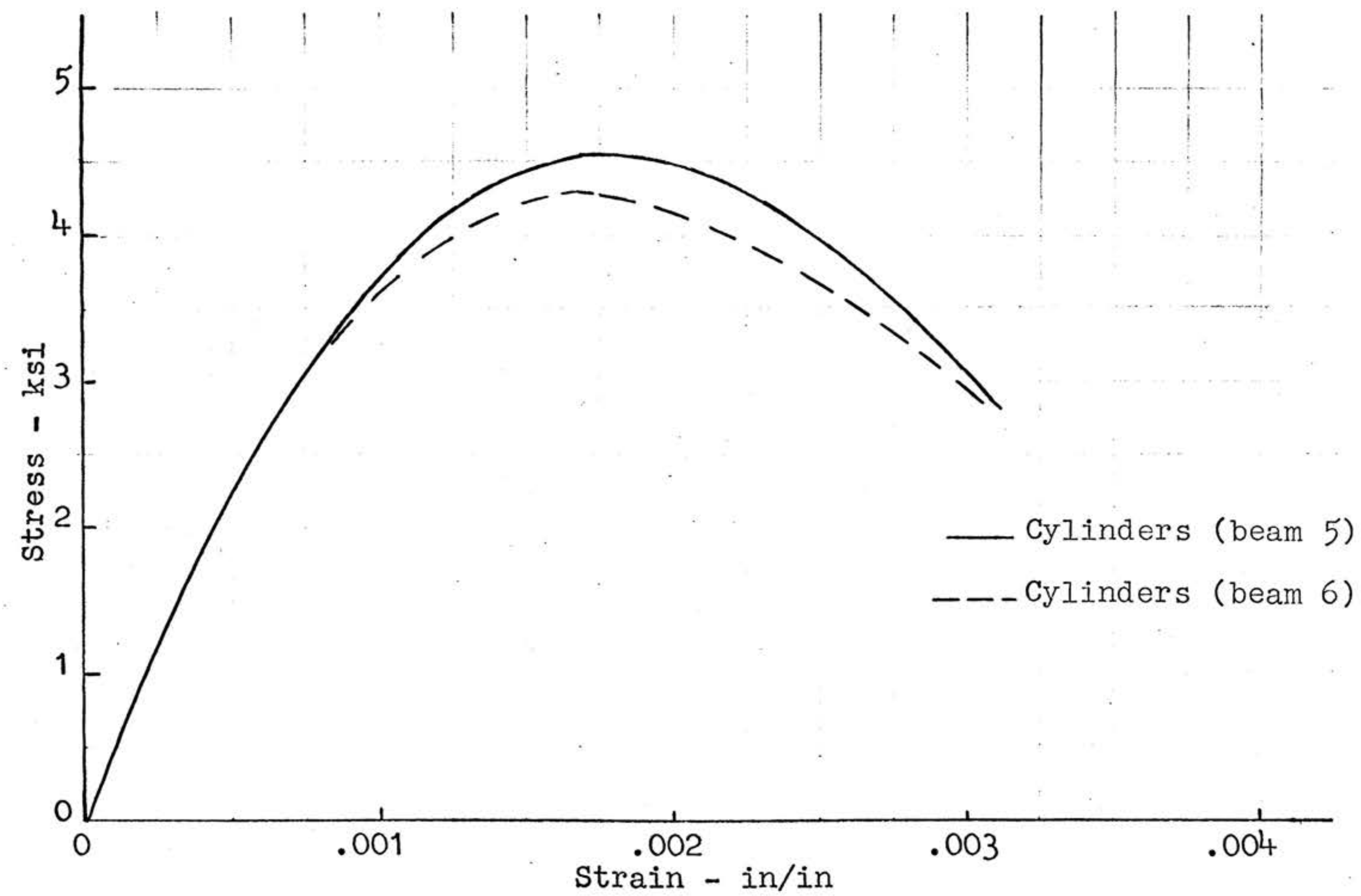

FIG. 28 CONCRETE CYLINDER STRESS VS STRAIN FOR BEAMS 5&6

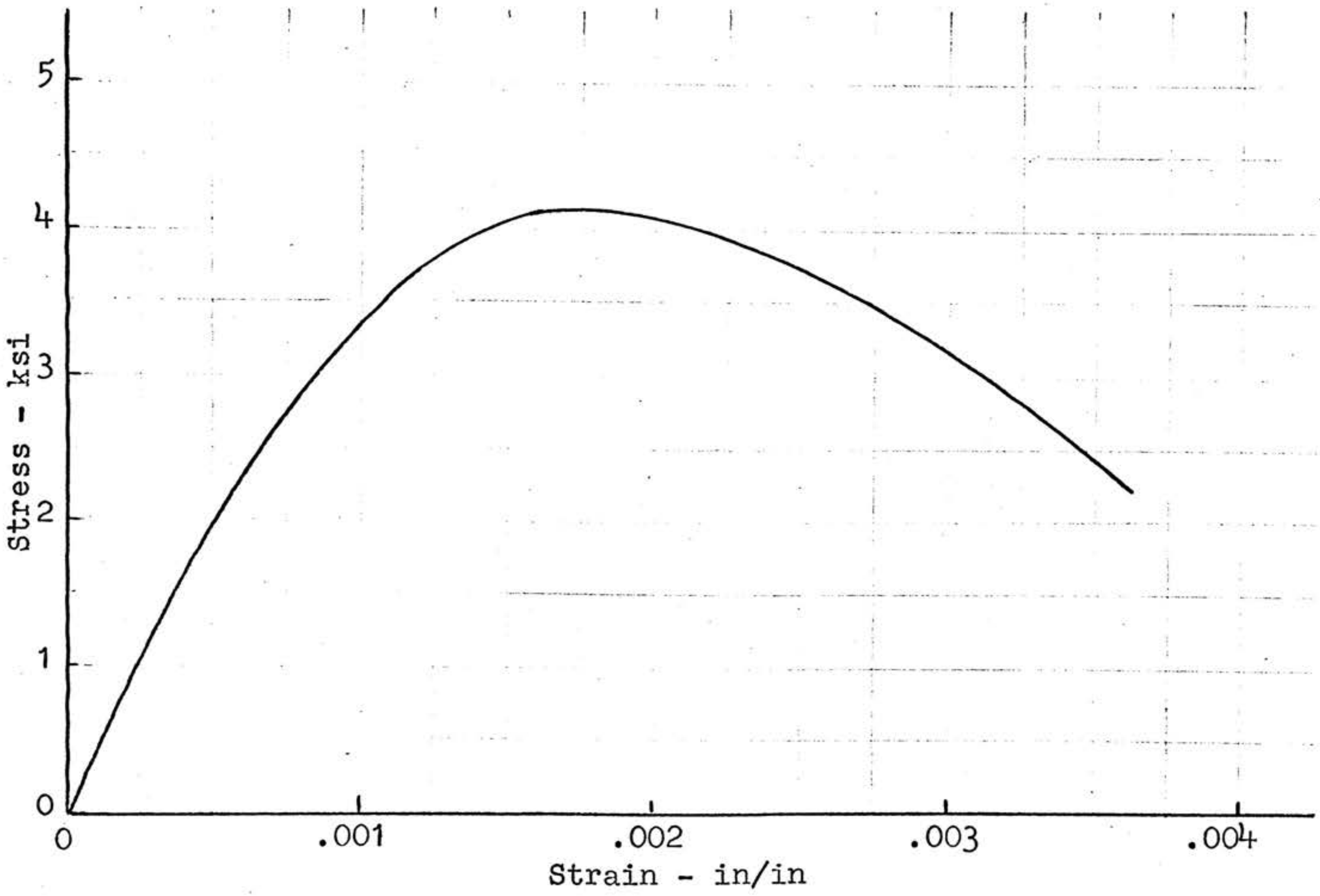

FIG. 29 CONCRETE CYLINDER STRESS VS STRAIN FOR BEAM 7

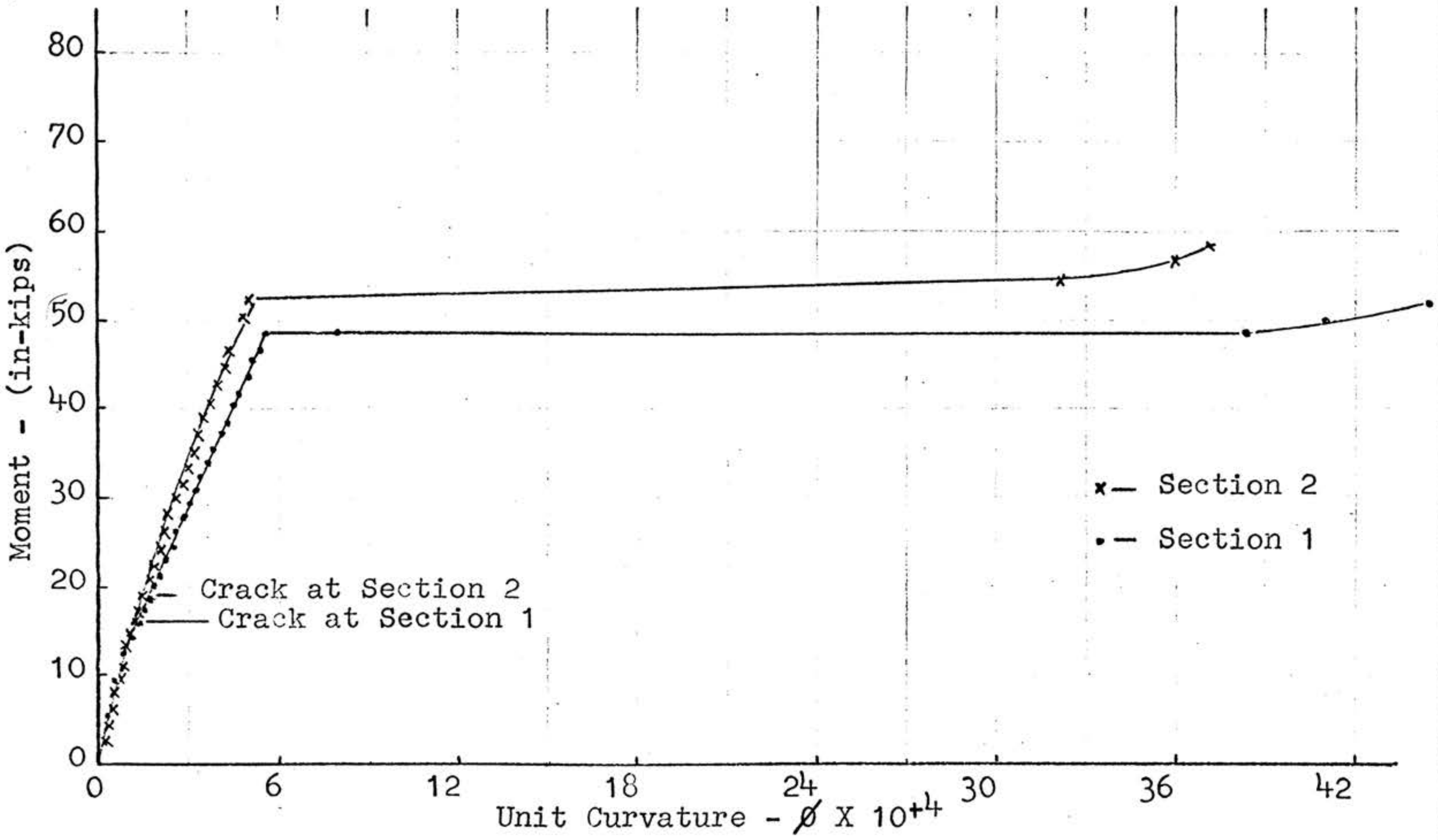

FIG. 30 MOMENT-CURVATURE (M-Ø) DIAGRAM FOR BEAM 3-A

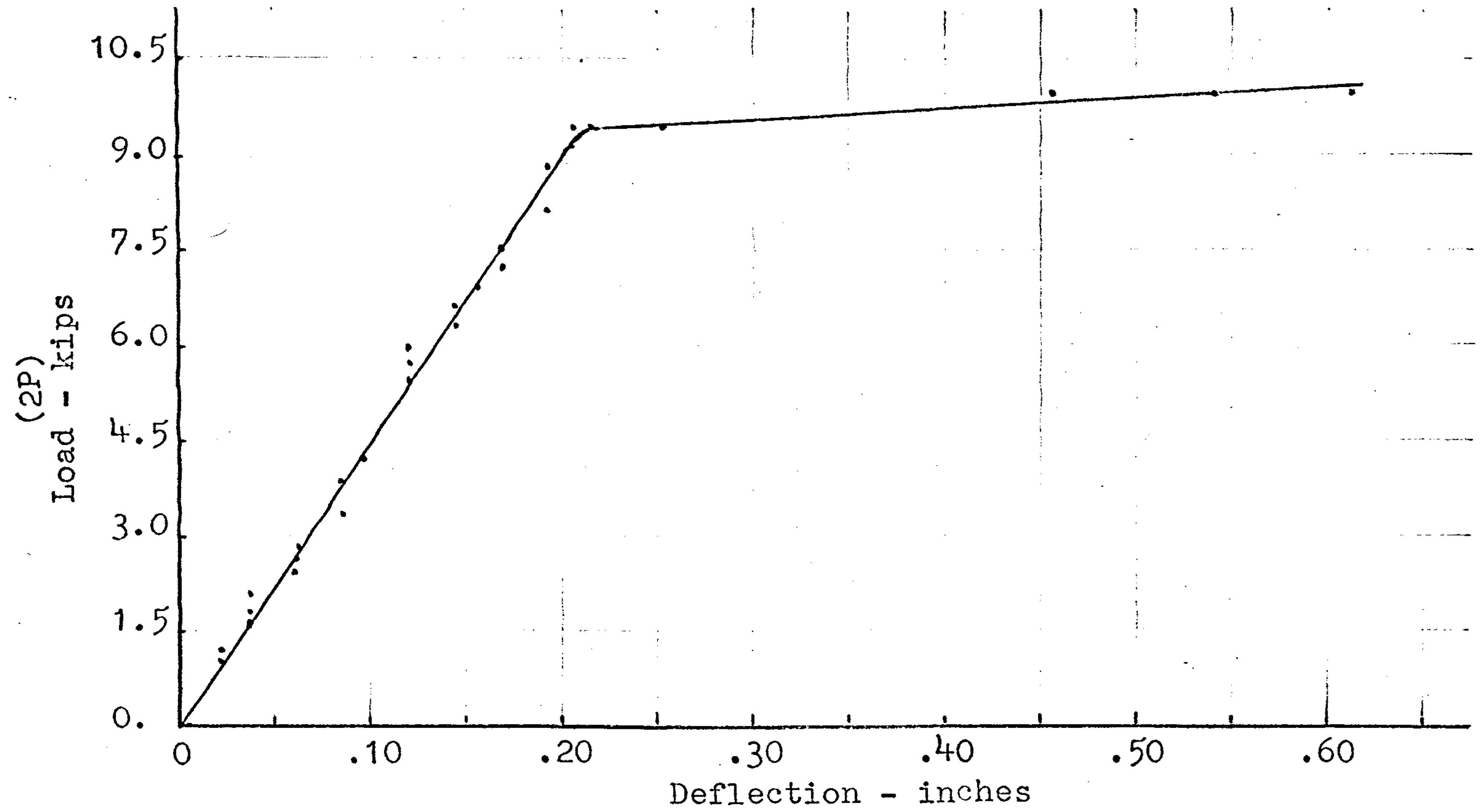

FIG. 31 LOAD-DEFLECTION DIAGRAM FOR BEAM 3-A

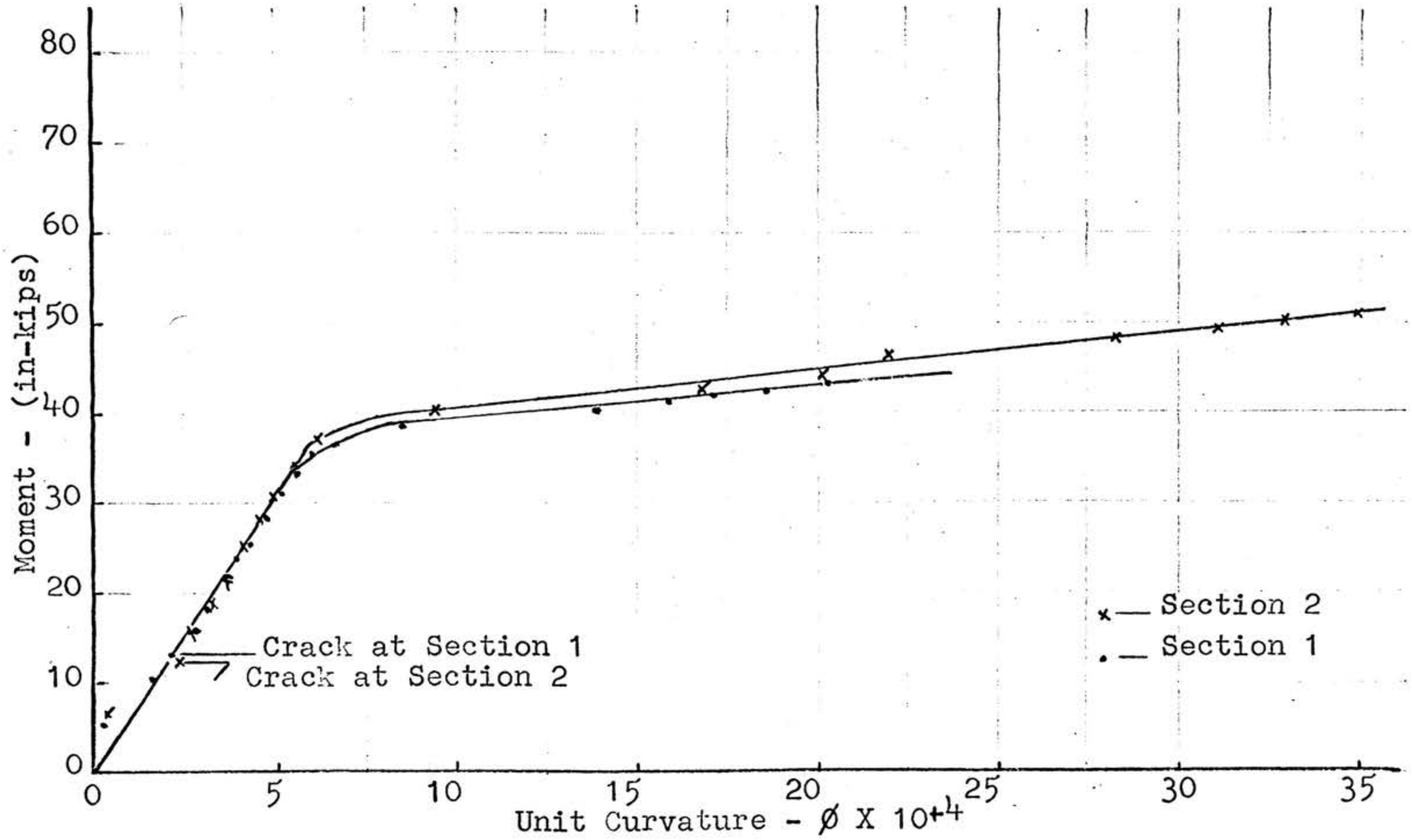

FIG. 32 MOMENT-CURVATURE (M-Ø) DIAGRAM FOR BEAM 1

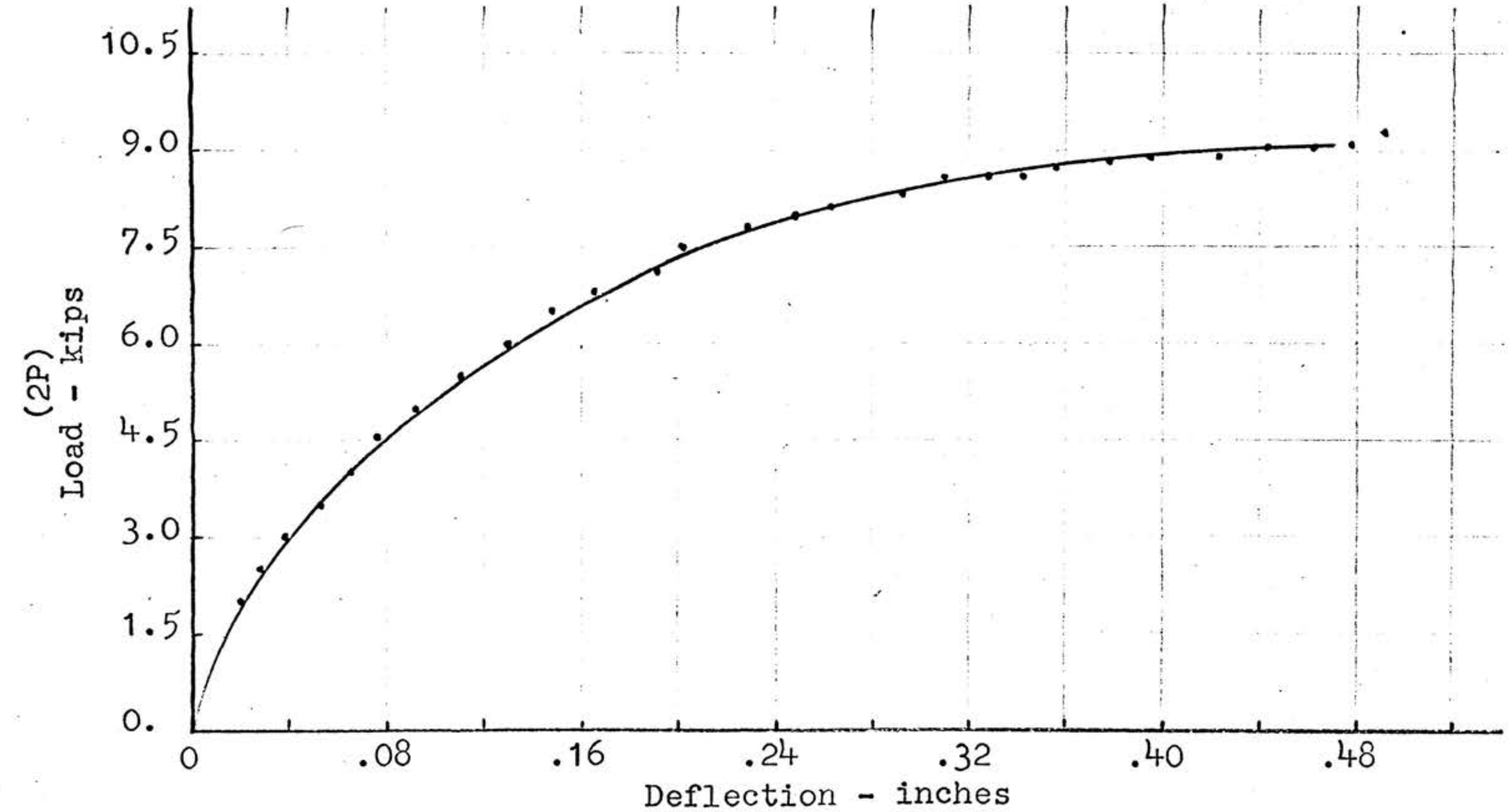

FIG. 33 LOAD-DEFLECTION DIAGRAM FOR BEAM 1

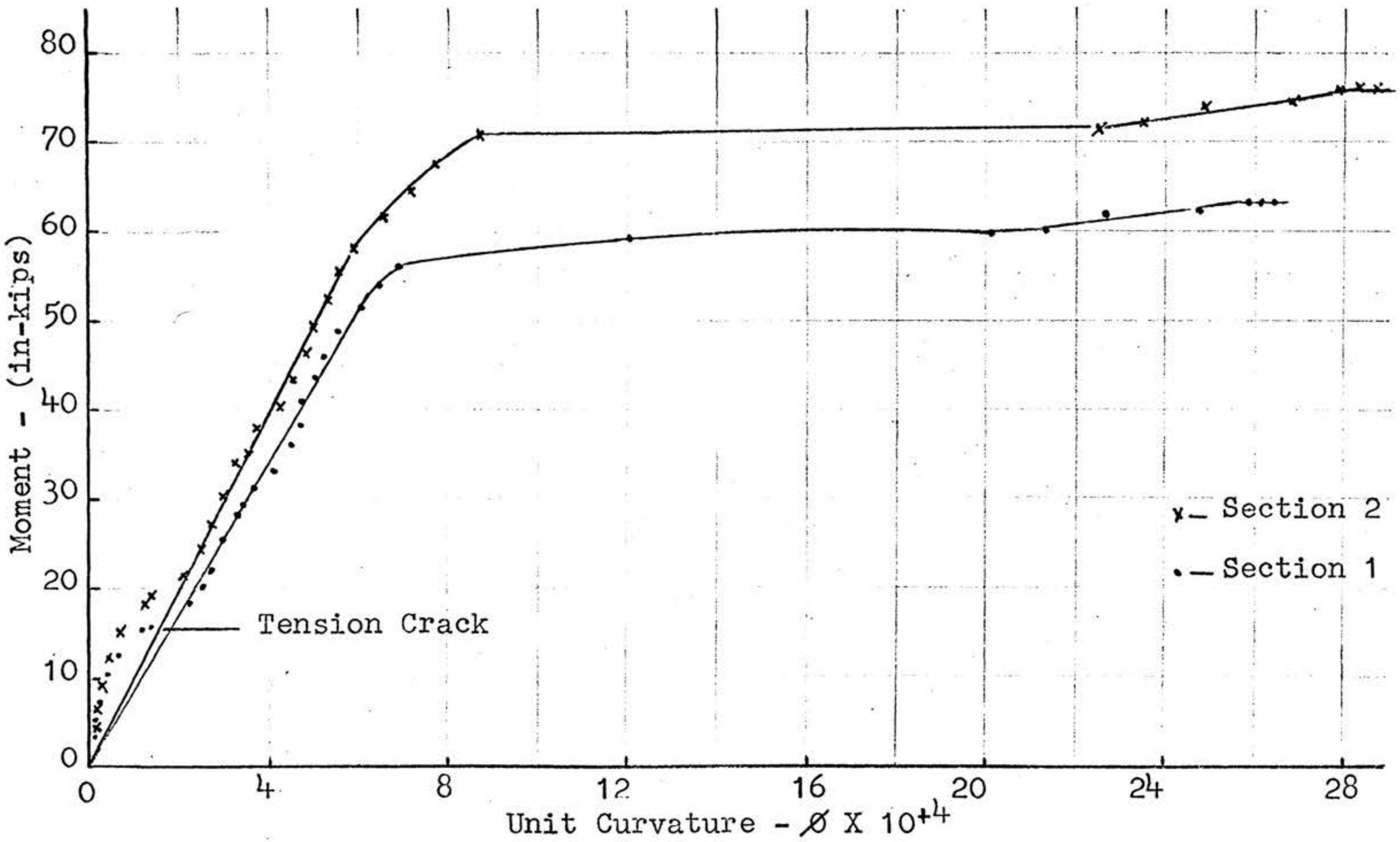

FIG. 34 . MOMENT-CURVATURE (M-Ø) DIAGRAM FOR BEAM 2

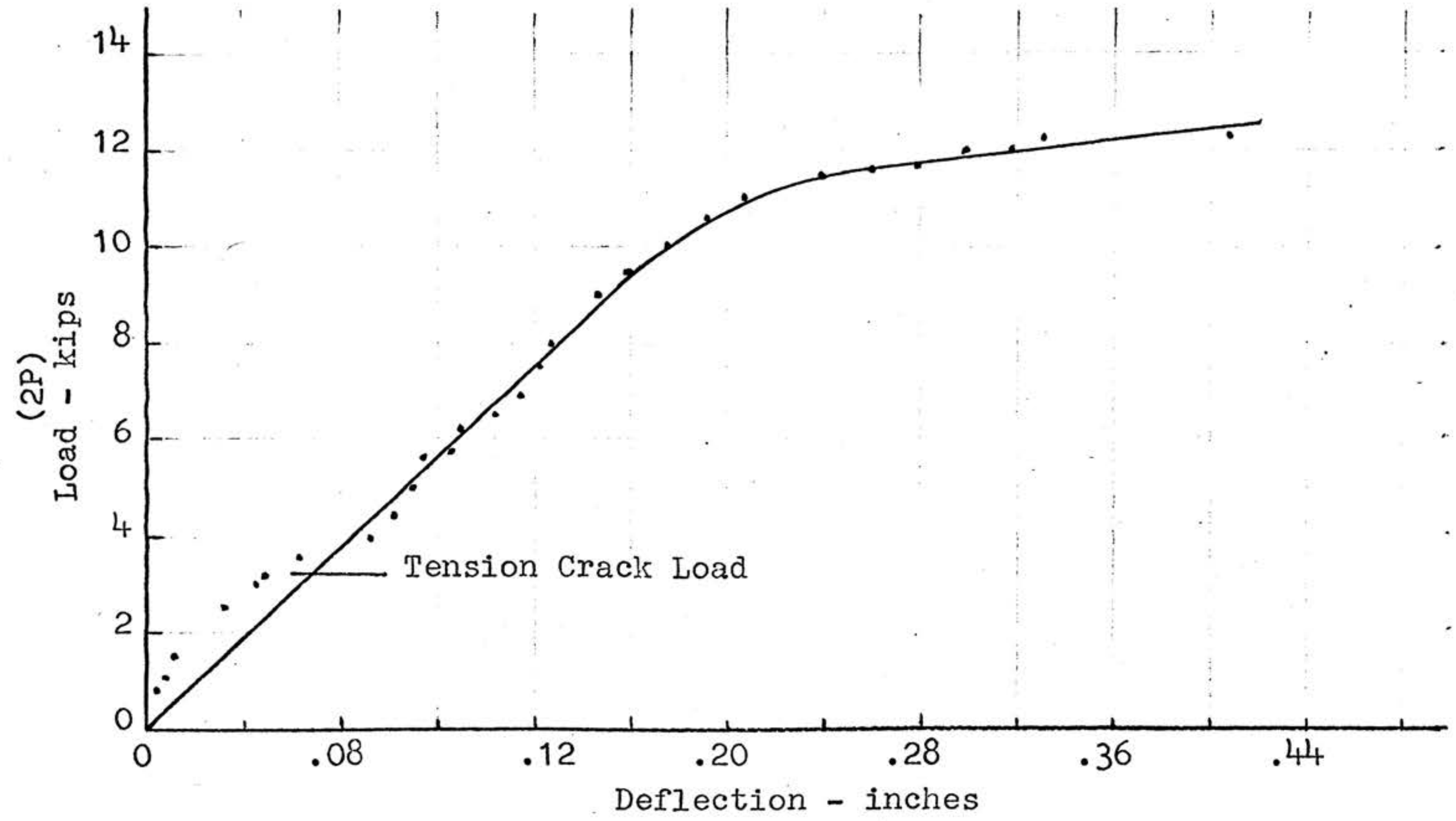

FIG. 35 LOAD-DEFLECTION DIAGRAM FOR BEAM 2

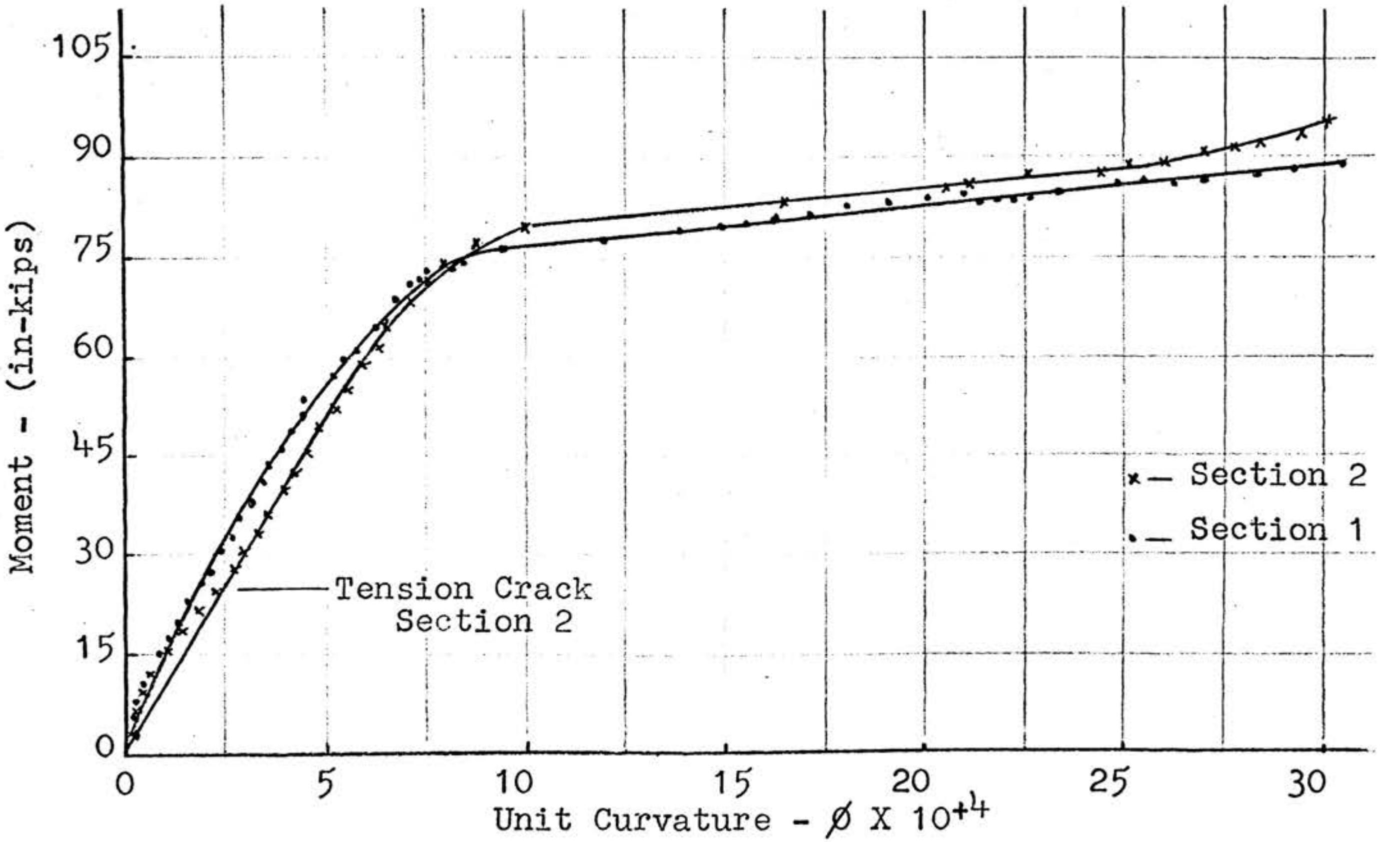

FIG. 36 MOMENT-CURVATURE (M-Ø) DIAGRAM FOR BEAM 3

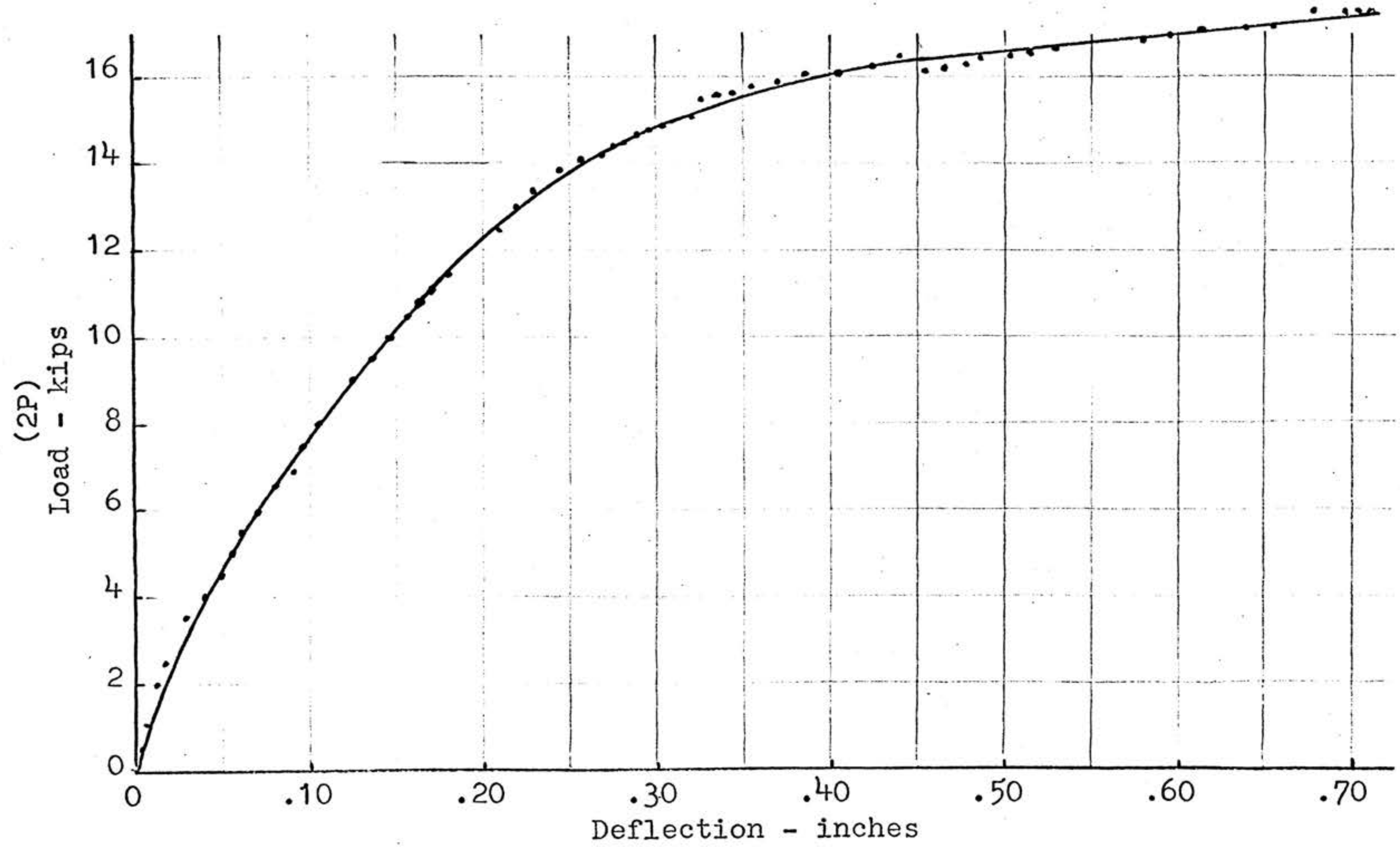

FIG. 37 LOAD-DEFLECTION DIAGRAM FOR BEAM 3

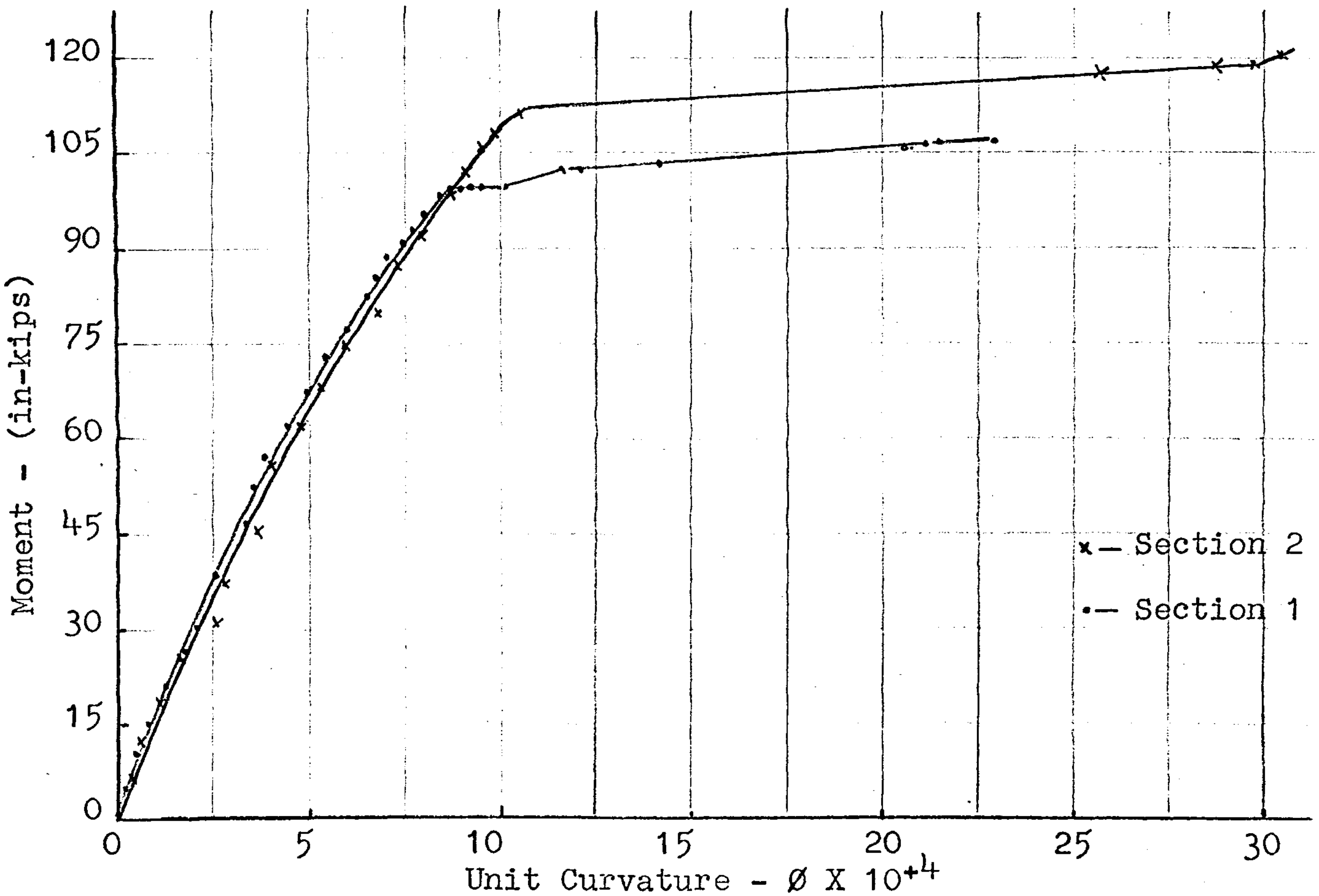

FIG. 38 MOMENT-CURVATURE (M-Ø) DIAGRAM FOR BEAM 4

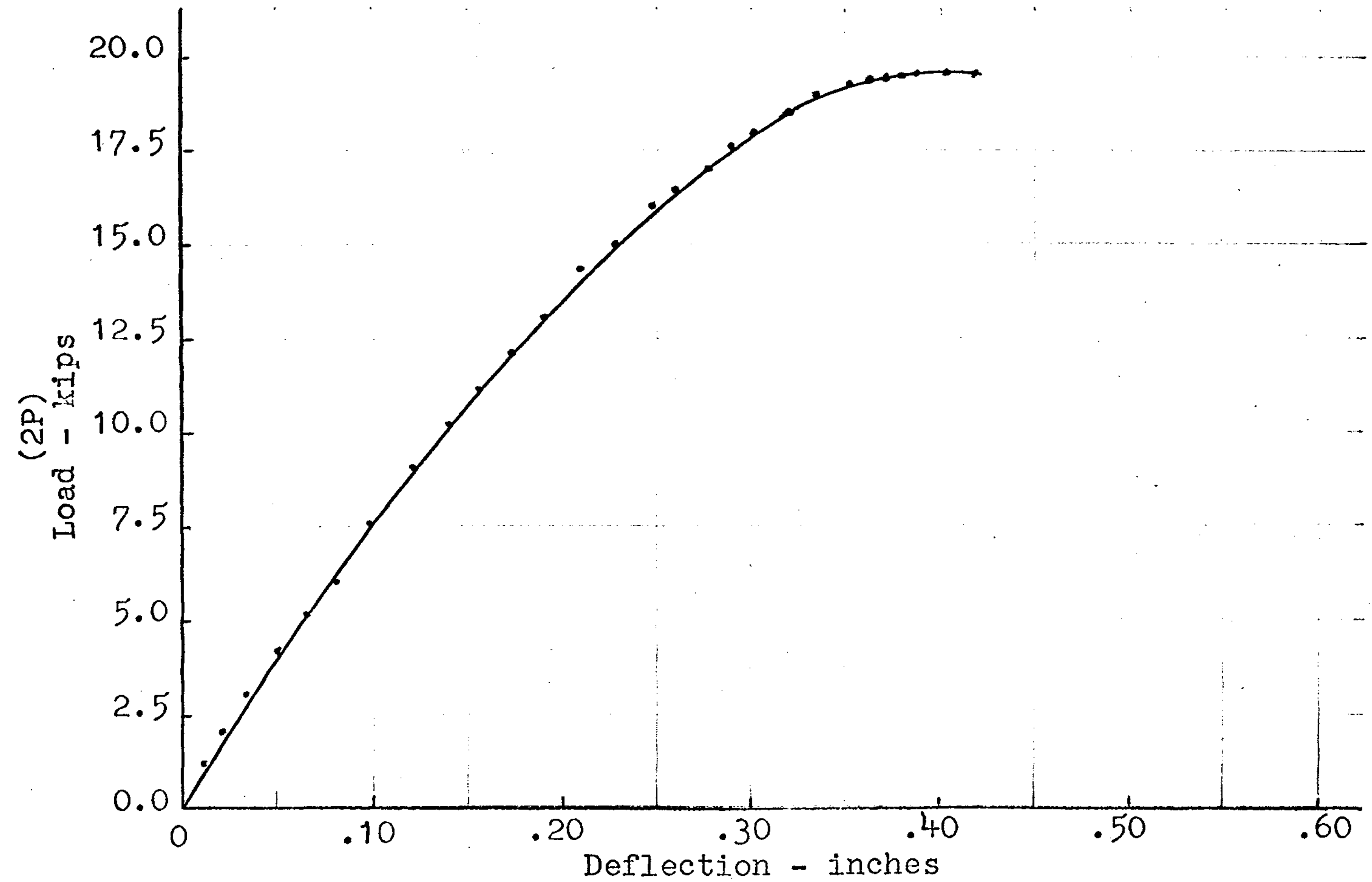

FIG. 39 LOAD-DEFLECTION DIAGRAM FOR BEAM 4

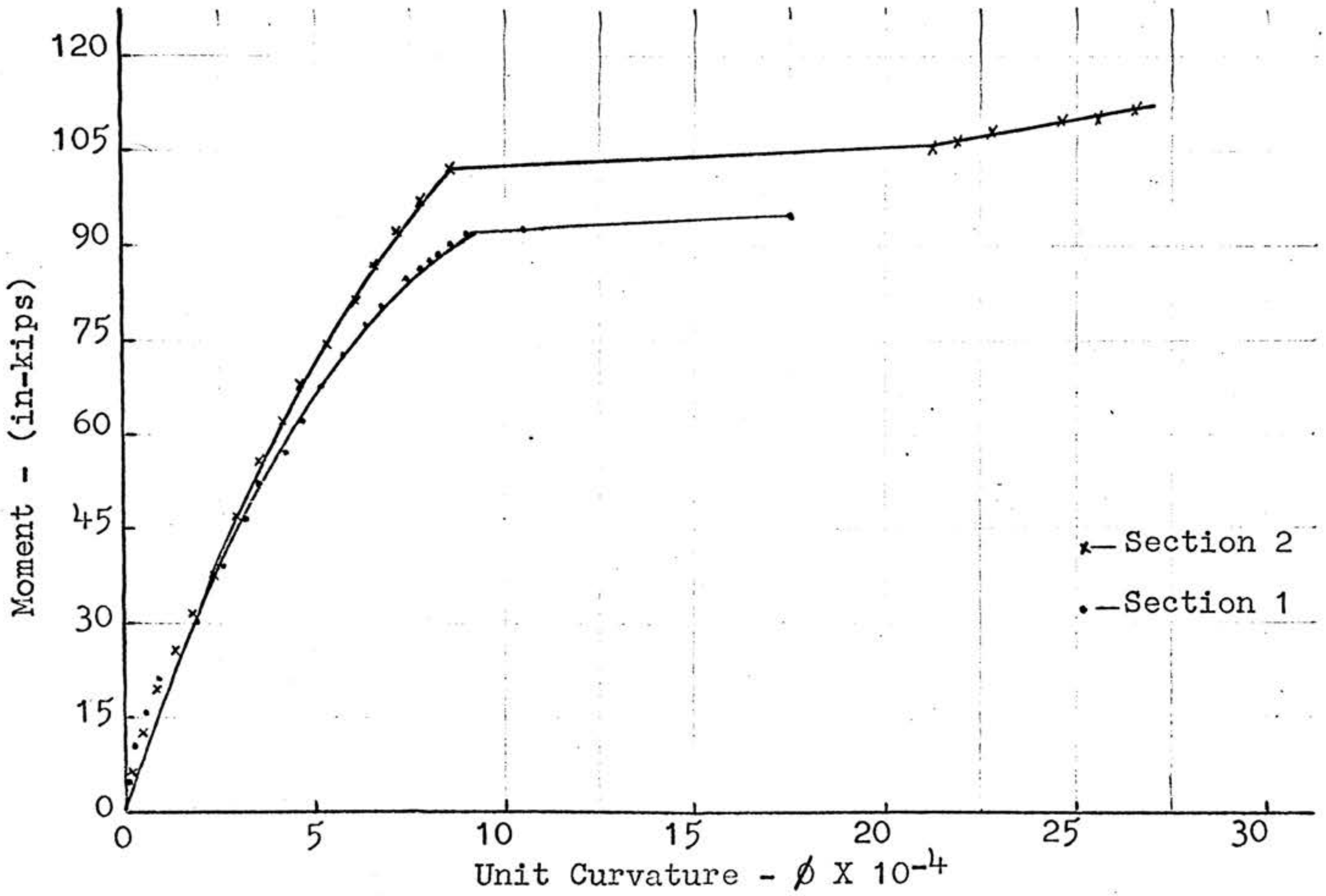

FIG. 40 MOMENT-CURVATURE (M-ϕ) DIAGRAM FOR BEAM 5

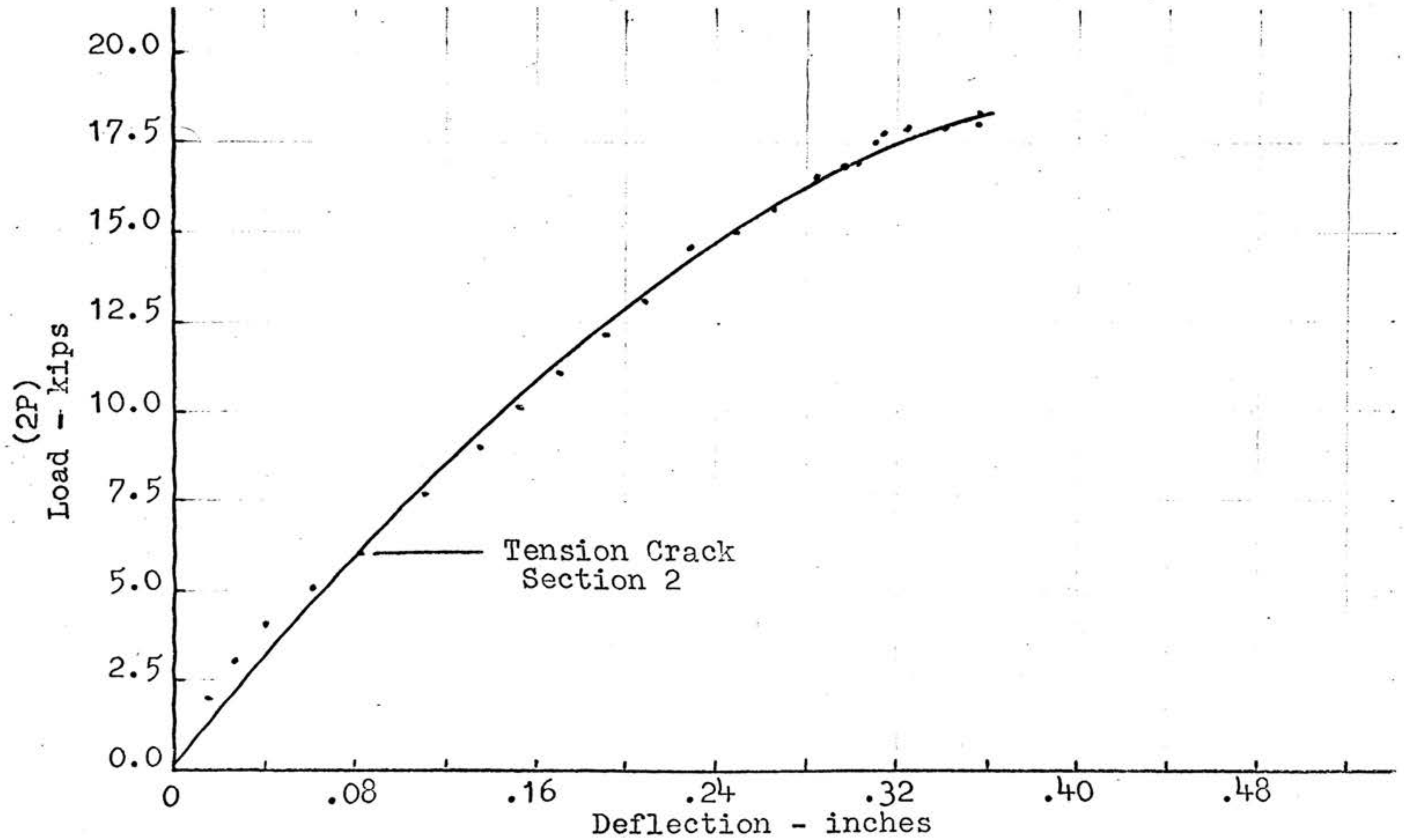

FIG. 41 LOAD-DEFLECTION DIAGRAM FOR BEAM 5

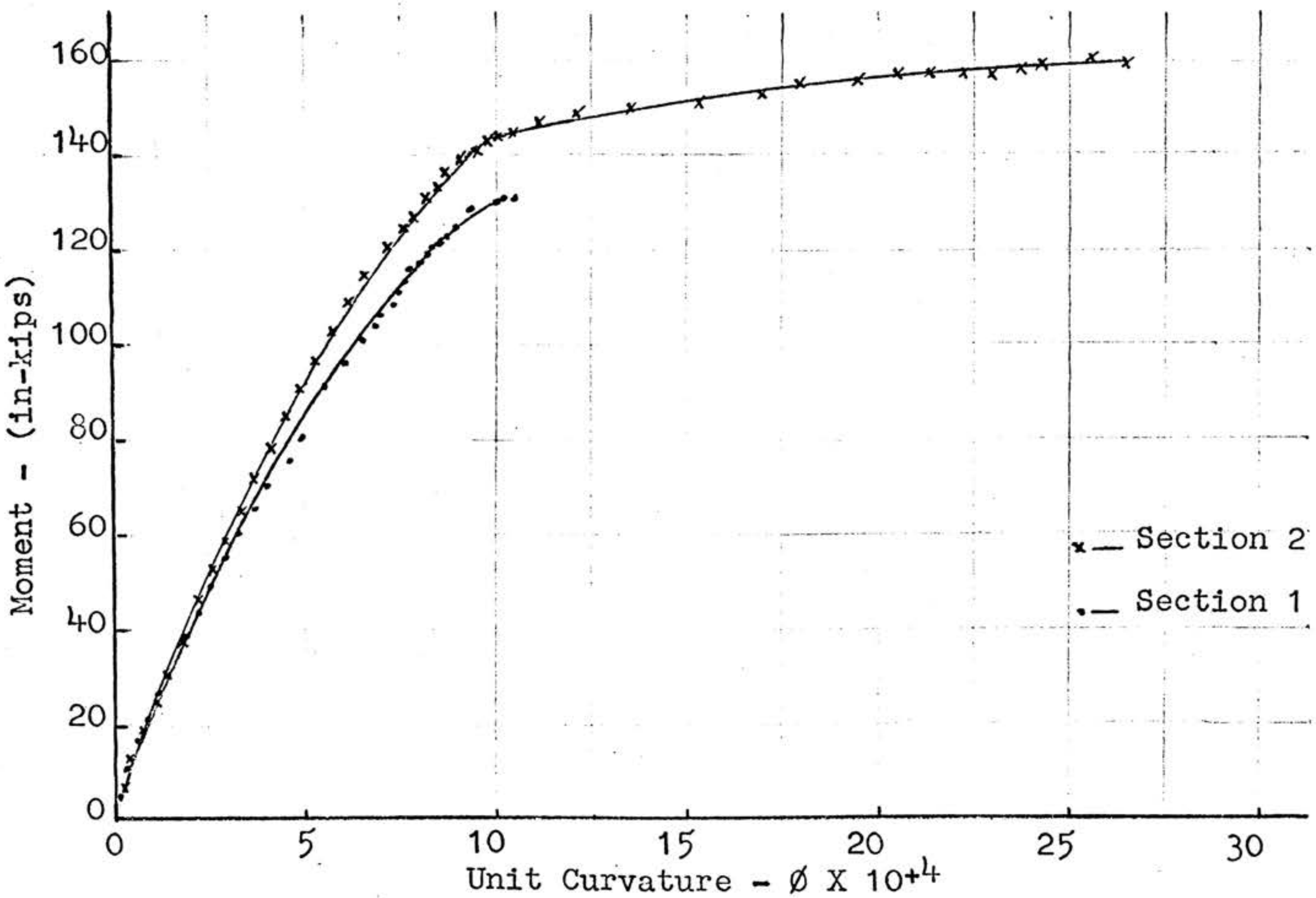

FIG. 42 MOMENT-CURVATURE (M-Ø) DIAGRAM FOR BEAM 6

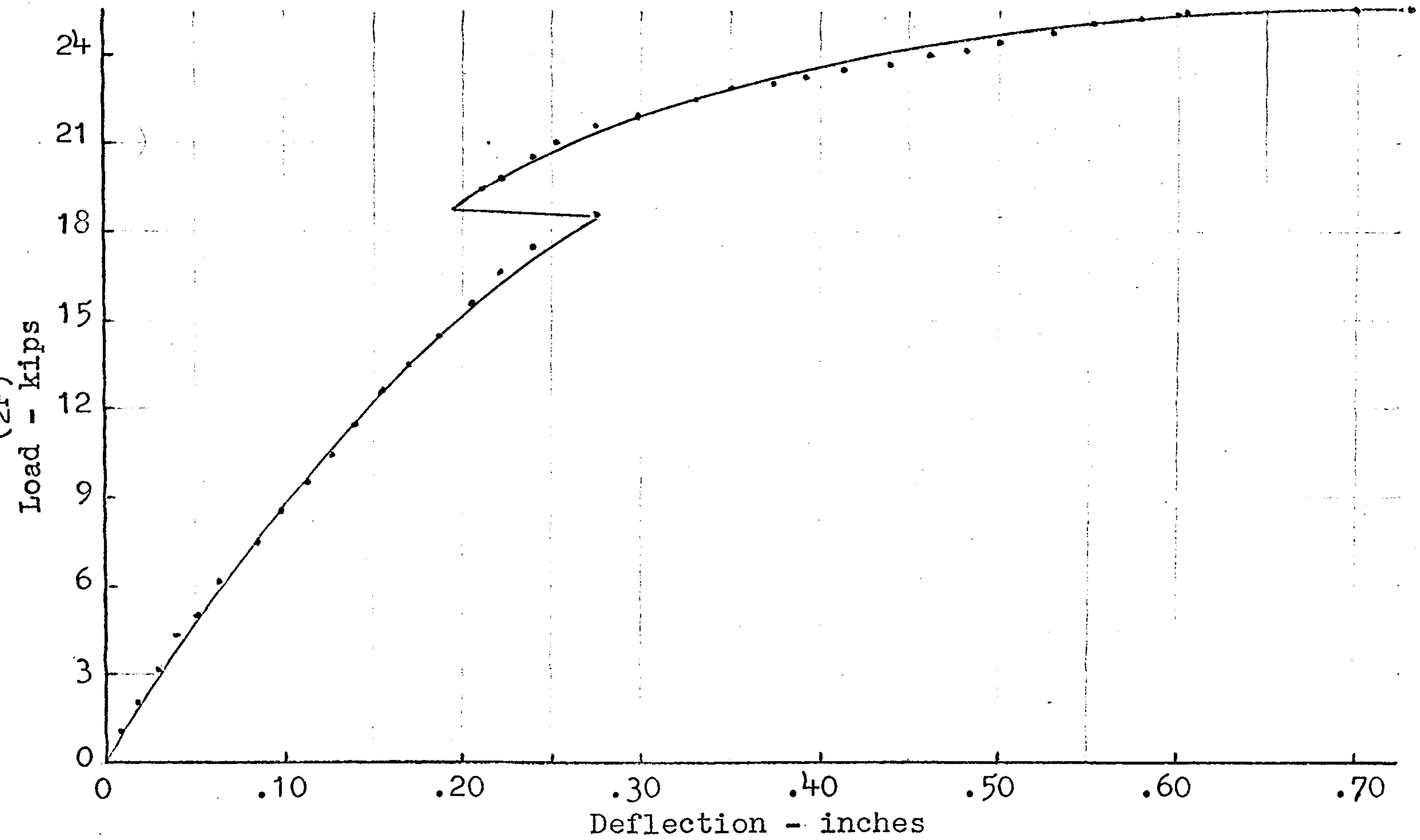

FIG. 43 LOAD-DEFLECTION DIAGRAM FOR BEAM 6

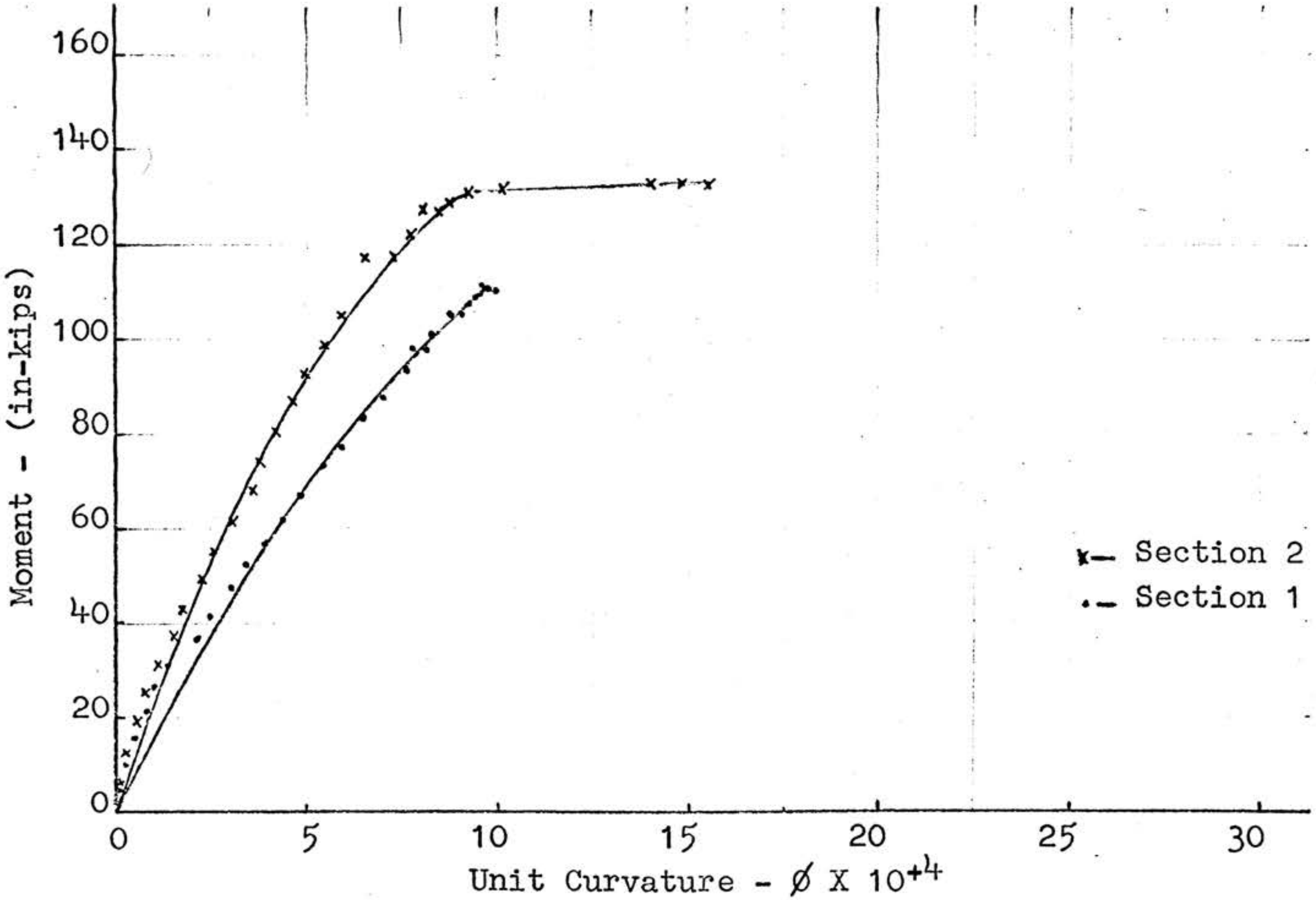

FIG. 44 MOMENT-CURVATURE (M-Ø) DIAGRAM FOR BEAM 7

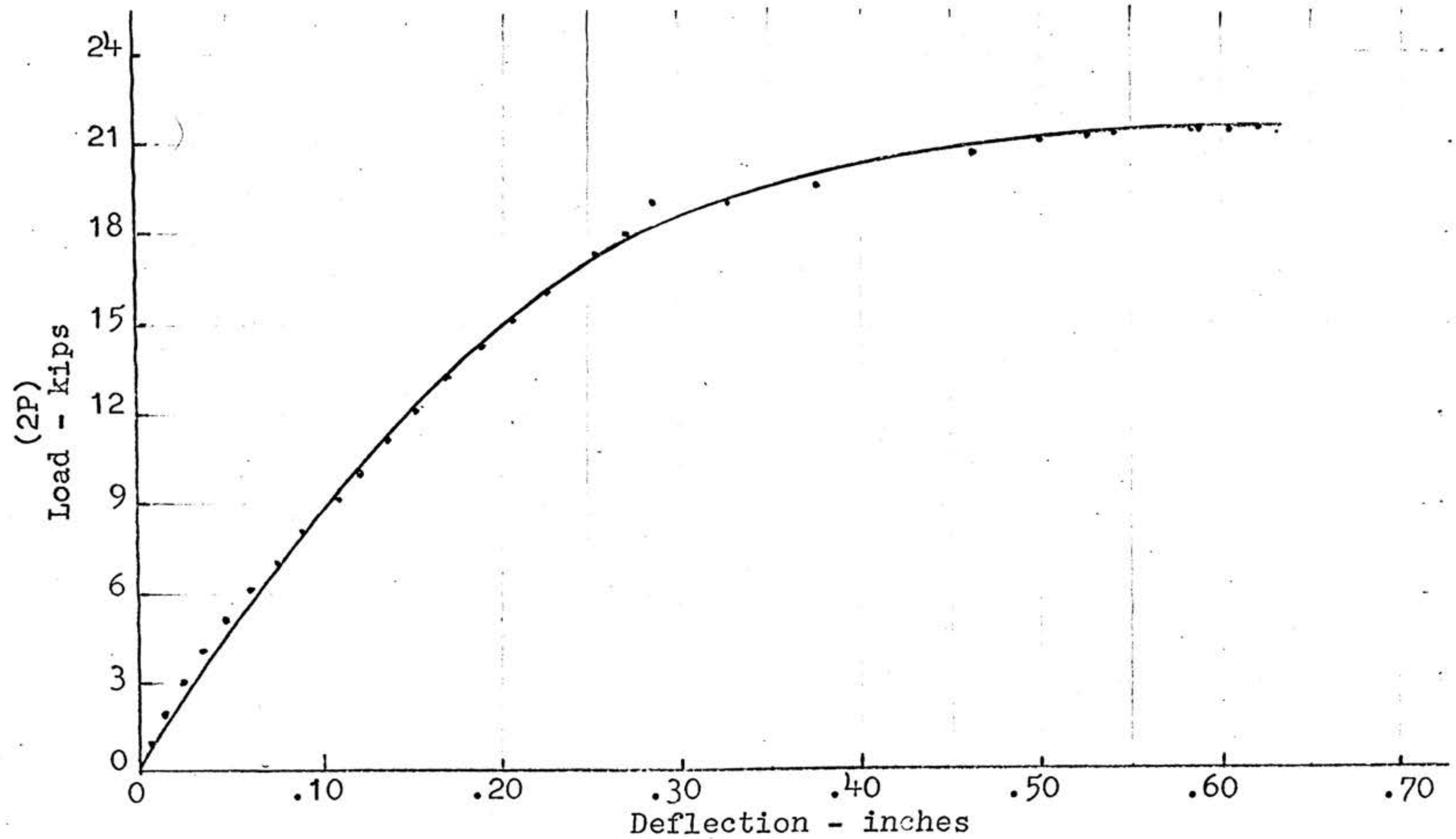

FIG. 45 LOAD-DEFLECTION DIAGRAM FOR BEAM 7

TABLE I - BEAM PROPERTIES

Beam Cross Section	b (in)	d (in)	k	Steel Tens. Bars	Steel Comp. Bars	(p) Steel ratio	(p') Steel ratio
#3-A - 1*	3.00	5.32	.282	2- #3	-----	.0139	-----
#3-A - 2	3.00	5.25	.284	2- #3	-----	.0141	-----
#1 - 1	3.00	5.38	.239	1- #3	-----	.0066	-----
#1 - 2	3.00	5.25	.247	1- #3	-----	.0068	-----
#2 - 1	3.00	5.38	.304	1- #4	-----	.0116	-----
#2 - 2	3.00	5.25	.296	1- #4	-----	.0119	-----
#3 - 1	3.00	5.31	.305	2- #3	-----	.0134	-----
#3 - 2	3.00	5.25	.307	2- #3	-----	.0135	-----
#4 - 1	3.00	5.25	.373	2- #4	-----	.0238	-----
#4 - 2	3.00	5.25	.373	2- #4	-----	.0238	-----
#5 - 1	3.00	5.29	.369	1- #3 & 1- #4	-----	.0185	-----
#5 - 2	3.00	5.25	.368	1- #3 & 1- #4	-----	.0186	-----
#6 - 1	3.00	5.31	.471	1- #4 & 1- #5	1- #3	.0310	.0067
#6 - 2	3.00	5.25	.473	1- #4 & 1- #5	1- #3	.0314	.0067
#7 - 1	3.00	5.25	.492	1- #4 & 1- #5	-----	.0314	-----
#7 - 2	3.00	5.25	.492	1- #4 & 1- #5	-----	.0314	-----

* Nos. indicate section of beam studied.

TABLE II - STRESS-STRAIN PROPERTIES

Beam Cross Section	fy ksi	f'c ksi	Es ksi $x10^3$	Ec ksi $x10^3$	Ec* ksi $x10^3$	Esp ksi $x10^3$	n = Es/Ec
3-A	45.8	4.60	18.0	4.50	4.38	----	4.00
1	70.0	4.28	23.3	4.50	4.20	1.68	5.18
2	65.8	3.96	28.0	4.90	4.05	----	5.72
3	70.0	4.20	23.5	4.70	4.17	1.36	5.00
4	65.9	4.20	28.0	4.65	4.17	----	6.03
5	65.9- #4 66.8- #3	4.55	27.0 27.0	4.65	4.34	.95	5.80
6	62.5- #5 65.9- #4 66.8- #3	4.30	27.0 27.0 27.0	4.35	4.23	.95	6.21
7	62.5- #5 63.8- #4	4.18	27.5	3.90	4.16	.95	7.05

*ACI code modulus of elasticity.

TABLE III- MOMENT-LOAD RELATIONSHIPS AT YIELD

Beam Cross Section	Py Load (kips)		My Moment (in-kips)	
	(theo.)	(exp.)	(theo.)	(exp.)
#3-A - 1*	4.46	4.70	49.0	48.9
#3-A - 2	3.90	4.25	48.3	52.6
#1 - 1	3.52	3.50	39.1	37.5
#1 - 2	3.06	3.00	37.9	36.5
#2 - 1	5.32	5.50	59.0	56.5
#2 - 2	4.62	4.75	57.3	58.2
#3 - 1	6.45	7.20	70.6	73.5
#3 - 2	5.50	6.00	68.2	75.0
#4 - 1	9.00	9.85	98.9	99.0
#4 - 2	8.00	9.25	98.9	112.5
#5 - 1	8.00	8.75	88.0	91.5
#5 - 2	6.95	8.25	86.0	102.0
#6 - 1	14.30	----	158.0	-----
#6 - 2	12.80	11.64	156.8	144.0
#7 - 1	10.70	-----	-----	-----
#7 - 2	9.52	10.67	118.0	133.0

* Nos. indicate sections of beams studied.

TABLE IV-BEAM CURVATURE-DEFLECTION RELATIONSHIPS						
Beam Cross Section	Yield Curvature		Yield Defl. (2)		Yield Defl. (1)	
	$\phi_y x\ 10^{+4}$ (theo.)	$\phi_y x\ 10^{+4}$ (exp.)	Δ_{y2} (inches) (theo.)	Δ_{y2} (inches) (exp.)	Δ_{y1} (inches) (theo.)	Δ_{y1} (inches) (exp.)
#3-A -1*	6.66	5.10	0.111	0.190	0.155	0.214
#3-A -2	6.78	5.60	-----	-----	-----	-----
#1 - 1	7.35	7.00	0.150	0.132	0.188	0.188
#1 - 2	7.50	6.00	-----	-----	-----	-----
#2 - 1	6.16	7.00	0.133	0.200	0.177	0.246
#2 - 2	6.35	6.00	-----	-----	-----	-----
#3 - 1	8.40	8.00	0.171	0.190	0.220	0.280
#3 - 2	7.60	8.50	-----	-----	-----	-----
#4 - 1	6.69	8.75	0.141	0.320	0.181	0.384
#4 - 2	6.69	10.75	-----	-----	-----	-----
#5 - 1	7.16	9.00	0.148	0.280	0.170	0.316
#5 - 2	7.16	8.50	-----	-----	-----	-----
#6 - 1	6.86	----	0.146	0.392	0.194	-----
#6 - 2	7.45	10.00	-----	-----	-----	-----
#7 - 1	6.60	8.50	0.140	0.525	0.180	0.547
#7 - 2	6.60	9.00	-----	-----	-----	-----

*Nos. indicate section of beam studied.

TABLE V - CYLINDER LOAD-DEFLECTION DATA

Beam No. 3-A

Date July 27, 1965

Test - 8 days
Gage Length = 10 inches
1 Division = .001 inches

Cylinder 1		Cylinder 2		Cylinder 3	
Load (lbs.)	Div.	Load (lbs.)	Div.	Load (lbs.)	Div.
10,000	0.25	10,000	0.4	10,000	0.5
15,000	0.5	15,000	0.7	15,000	1.0
20,000	0.8	20,000	1.1	20,000	1.4
25,000	1.3	25,000	1.5	25,000	1.8
30,000	1.6	30,000	2.0	30,000	2.3
35,000	1.9	35,000	2.3	35,000	2.8
40,000	2.2	40,000	2.8	40,000	3.2
45,000	2.7	45,000	3.3	45,000	3.7
50,000	3.0	50,000	3.8	50,000	4.2
55,000	3.6	55,000	4.2	55,500	4.7
60,000	4.0	60,000	4.6	60,000	5.2
65,000	4.4	65,000	5.0	65,000	5.6
70,000	4.8	70,000	5.5	70,000	6.2
75,000	5.4	75,000	6.0	75,000	6.8
80,000	5.9	80,000	6.7	80,000	7.4
85,000	6.4	85,000	7.4	85,000	8.0
90,000	6.9	90,000	8.0	90,000	8.7
		95,000	8.7	95,000	9.5
		100,000	9.4	100,000	10.2
		105,000	10.2	105,000	11.0
				110,000	12.0
				115,000	13.0
				120,000	14.2

TABLE VI - CYLINDER LOAD-DEFLECTION DATA

Beam No. 1

Date August 18, 1965

Test - 8 days
Gage Length = 10 inches
1 Division = .001 inches

Cylinder 1		Cylinder 2		Cylinder 3	
Load (lbs.)	Div.	Load (lbs.)	Div.	Load (lbs.)	Div.
5,000		5,000		5,000	
10,000	0.1	10,000	0.3	10,000	0.3
15,000	0.7	15,000	0.7	15,000	0.7
20,000	1.0	20,000	1.1	20,000	1.1
25,000	1.4	25,000	1.4	25,000	1.6
30,000	1.8	30,000	1.7	30,000	2.0
35,000	2.1	35,000	2.0	35,000	2.4
40,000	2.5	40,000	2.4	40,000	2.8
45,000	2.9	45,000	2.8	45,000	3.2
50,000	3.4	50,000	3.2	50,000	3.6
55,000	3.8	55,000	3.6	55,000	4.0
60,000	4.2	60,000	4.0	60,000	4.4
65,000	4.6	65,000	4.5	65,000	5.0
70,000	5.1	70,000	5.1	70,000	5.5
75,000	5.6	75,000	5.7	75,000	6.0
80,000	6.2	80,000	6.8	80,000	6.6
85,000	6.6	85,000	7.2	85,000	7.2
90,000	7.4	90,000	7.8	90,000	7.9
95,000	8.0	95,000	8.8	95,000	8.6
100,000	8.6	100,000	9.9	100,000	9.4
105,000	9.3	104,500	11.0	105,000	10.3
110,000	10.2	108,000	12.0	110,000	11.4
115,000	11.2	110,000	13.0	113,000	12.0
118,000	12.0	112,500	14.0	117,000	13.0
122,000	13.0	113,500	15.0	120,000	14.0
124,500	14.0	115,000	17.0	121,500	15.0
127,000	15.0	115,000	18.0	122,500	16.0
129,500	16.0	95,000	29.0	123,000	19.0
129,500	17.0	90,000	30.0	95,000	29.0
129,500	18.0			92,500	30.0
129,500	19.0			90,000	31.0
127,000	20.0				
125,000	21.0				
122,500	22.0				
120,000	23.0				
117,500	24.0				
110,000	25.0				
107,500	26.0				

TABLE VII - CYLINDER LOAD-DEFLECTION DATA

Beam No. 2

Date August 16, 1965

Test - 7 days
Gage Length = 10 inches
1 Division = .001 inches

Cylinder 1		Cylinder 2		Cylinder 3	
Load (lbs.)	Div.	Load (lbs.)	Div.	Load (lbs.)	Div.
5,000	0.1	5,000	0.1	5,000	0.1
10,000	0.4	10,000	0.3	10,000	0.4
15,000	0.8	15,000	0.6	15,000	0.7
20,000	1.2	20,000	1.0	20,000	1.0
25,000	1.5	25,000	1.4	25,000	1.4
30,000	1.9	30,000	1.7	30,000	1.8
35,000	2.4	35,000	2.0	35,000	2.1
40,000	2.8	40,000	2.4	40,000	2.5
45,000	3.2	45,000	2.7	45,000	2.8
50,000	3.8	50,000	3.3	50,000	3.4
55,000	4.4	55,000	3.8	55,000	3.9
60,000	4.7	60,000	4.3	60,000	4.3
65,000	5.3	65,000	4.6	65,000	4.8
70,000	5.8	70,000	5.2	70,000	5.4
75,000	6.4	75,000	5.7	75,000	6.0
80,000	7.2	80,000	6.2	80,000	6.6
85,000	8.0	85,000	6.9	85,000	7.4
90,000	8.9	90,000	7.8	90,000	8.1
95,000	9.8	95,000	8.4	95,000	8.9
100,000	10.9	100,000	9.3	101,000	11.5
105,000	12.4	105,000	10.5	95,000	12.5
110,000	14.7	110,000	12.0	85,000	13.5
111,500	17.9	115,000	15.0	80,000	14.5
90,000	20.1	114,000	16.5	77,500	16.5
		113,000	17.0		
		112,500	18.0		
		110,000	19.0		

TABLE VIII - CYLINDER LOAD-DEFLECTION DATA

Beam No. 3

Date August 16, 1965

Test - 7 days
Gage Length = 10 inches
1 Division = .001 inches

Cylinder 1		Cylinder 2		Cylinder 3	
Load (lbs.)	Div.	Load (lbs.)	Div.	Load (lbs.)	Div.
5,000		5,000		5,000	
10,000	0.4	10,000	0.2	10,000	0.3
15,000	0.8	15,000	0.6	15,000	0.6
20,000	1.1	20,000	1.0	20,000	1.0
25,000	1.6	25,000	1.4	25,000	1.3
30,000	2.0	30,000	1.8	30,000	1.6
35,000	2.5	35,000	2.3	35,000	2.0
40,000	2.8	40,000	2.7	40,000	2.4
45,000	3.4	45,000	3.1	45,000	2.8
50,000	3.8	50,000	3.6	50,000	3.2
55,000	4.3	55,000	4.0	55,000	3.6
60,000	4.7	60,000	4.5	60,000	4.2
65,000	5.1	65,000	4.9	65,000	4.6
70,000	5.4	70,000	5.5	70,000	5.4
75,000	5.7	75,000	6.0	75,000	6.0
80,000	6.3	80,000	6.7	80,000	6.6
85,000	7.0	85,000	7.3	85,000	7.5
90,000	8.4	90,000	8.0	90,000	8.2
95,000	9.0	95,000	8.8	95,000	9.2
100,000	10.0	100,000	9.6	100,000	10.6
105,000	11.0	105,000	10.5	105,000	12.5
110,000	12.1	110,000	11.7	110,000	14.8
115,000	14.0	115,000	13.2	114,000	18.5
120,000	16.4	118,000	15.0	114,000	20.0
122,500	19.5	115,000	16.0	113,500	21.0
122,000	20.0	90,000	17.0	113,000	22.0
120,000	21.0			109,500	23.0
117,500	22.0			100,000	24.0
113,000	23.0			96,000	25.0
110,500	24.0			93,500	26.0
108,000	25.0			90,000	27.0
105,000	26.0			87,500	28.0
102,500	27.0			85,500	29.0
99,000	28.0				
95,000	29.0				
90,200	30.0				

TABLE IX - CYLINDER LOAD-DEFLECTION DATA

Beam No. 4

Date August 18, 1965

Test - 8 days
Gage Length = 10 inches
1 Division = .001 inches

Cylinder 1		Cylinder 2		Cylinder 3	
Load (lbs.)	Div.	Load (lbs.)	Div.	Load (lbs.)	Div.
5,000	0.1	5,000		5,000	
10,000	0.5	10,000	0.3	10,000	0.4
15,000	0.8	15,000	0.8	15,000	0.9
20,000	1.2	20,000	1.1	20,000	1.3
25,000	1.6	25,000	1.5	25,000	1.6
30,000	2.0	30,000	1.9	30,000	2.1
35,000	2.4	35,000	2.3	35,000	2.5
40,000	2.8	40,000	2.7	40,000	3.0
45,000	3.1	45,000	3.1	45,000	3.4
50,000	3.6	50,000	3.6	50,000	4.0
55,000	4.0	55,000	4.0	55,000	4.5
60,000	4.5	60,000	4.4	60,000	4.9
65,000	4.9	65,000	5.0	65,000	5.4
70,000	5.4	70,000	5.5	70,000	5.9
75,000	6.0	75,000	6.1	75,000	6.5
80,000	6.5	80,000	6.7	80,000	7.0
85,000	7.1	85,000	7.4	85,000	7.7
90,000	7.9	90,000	8.1	90,000	8.2
95,000	8.5	95,000	9.0	95,000	9.0
100,000	9.3	100,000	9.8	100,000	9.8
105,000	10.4	105,000	10.7	105,000	10.8
110,000	11.8	110,000	12.0	110,000	12.0
115,000	13.4	113,000	13.0	114,000	13.0
117,800	16.0	116,000	14.0	117,000	14.0
117,000	17.0	117,500	15.0	118,500	15.0
115,000	18.0	118,000	16.0	121,000	16.0
112,500	19.0	117,500	17.0	122,000	17.0
114,500	20.0	117,000	18.0	122,500	18.0
106,000	21.0	114,500	19.0	122,000	19.0
103,000	22.0	110,500	20.0	121,200	20.0
96,500	23.0	106,000	21.0	120,000	21.0
90,500	24.0	95,000	22.0	117,500	22.0
				112,500	23.0
				110,000	24.0

TABLE X - CYLINDER LOAD-DEFLECTION DATA

Beam No. 5

Date August 20, 1965

Test - 8 days
Gage Length = 10 inches
1 Division = .001 inches

Cylinder 1		Cylinder 2		Cylinder 3	
Load (lbs.)	Div.	Load (lbs.)	Div.	Load (lbs.)	Div.
10,000	0.1	10,000		10,000	
15,000	0.5	15,000	0.2	15,000	0.5
20,000	0.9	20,000	0.5	20,000	0.9
25,000	1.3	25,000	1.0	25,000	1.3
30,000	1.6	30,000	1.5	30,000	1.7
35,000	2.0	35,000	1.9	35,000	2.2
40,000	2.4	40,000	2.3	40,000	2.6
45,000	2.7	45,000	2.7	45,000	3.0
50,000	3.1	50,000	3.2	50,000	3.4
55,000	3.6	55,000	3.7	55,000	3.9
60,000	4.0	60,000	4.1	60,000	4.4
65,000	4.4	65,000	4.5	65,000	4.7
70,000	4.9	70,000	5.0	70,000	5.2
80,000	5.9	75,000	5.6	75,000	5.7
85,000	6.4	80,000	6.2	80,000	6.2
90,000	6.9	85,000	6.8	85,000	6.8
95,000	7.5	90,000	7.4	90,000	7.4
100,000	8.1	95,000	8.1	100,000	8.6
105,000	8.8	100,000	9.0	105,000	9.4
110,000	9.5	105,000	9.7	110,000	10.4
115,000	10.5	110,000	10.6	115,000	11.4
120,000	11.6	115,000	11.5	120,000	12.8
125,000	13.0	120,000	12.9	123,500	14.0
128,000	14.0	124,500	14.0	125,500	15.0
130,000	14.9	127,000	15.0	127,500	16.0
132,500	16.0	129,000	16.0	128,500	17.0
132,000	17.0	131,000	17.0	129,000	18.0
130,000	18.0	131,500	18.0	127,500	19.0
130,000	19.0	131,500	19.0	125,000	20.0
127,500	20.0	131,500	20.0	120,000	22.0
125,500	21.0	127,500	21.0	90,000	28.0
122,500	22.0	120,000	22.0		
120,000	23.0				
115,000	24.0				
112,000	25.0				
107,500	26.0				
105,000	27.0				
95,000	30.0				

TABLE XI - CYLINDER LOAD-DEFLECTION DATA					
Beam No. 6 Date August 20, 1965			Test - 8 days Gage Length = 10 inches 1 Division = .001 inches		
Cylinder 1		Cylinder 2		Cylinder 3	
Load (lbs.)	Div.	Load (lbs.)	Div.	Load (lbs.)	Div.
10,000		10,000		10,000	
15,000	0.6	15,000	0.3	15,000	0.3
20,000	1.0	20,000	0.6	20,000	0.8
25,000	1.5	25,000	1.0	25,000	1.1
30,000	2.0	30,000	1.3	30,000	1.5
35,000	2.4	35,000	1.7	35,000	1.9
40,000	2.8	40,000	2.0	40,000	2.3
45,000	3.3	45,000	2.4	45,000	2.6
50,000	3.8	50,000	2.9	50,000	3.0
55,000	4.3	55,000	3.4	55,000	3.5
60,000	4.6	60,000	3.6	60,000	4.0
65,000	5.2	65,000	4.0	65,000	4.5
70,000	5.7	70,000	4.5	70,000	5.0
75,000	6.3	75,000	5.0	75,000	5.5
80,000	7.0	80,000	5.6	80,000	6.0
85,000	7.6	85,000	6.2	85,000	6.6
90,000	8.4	90,000	6.9	90,000	7.4
95,000	9.1	95,000	7.5	95,000	8.2
100,000	10.0	100,000	8.1	100,000	9.0
104,500	11.0	105,000	8.9	104,500	10.0
107,500	12.0	110,000	9.9	108,500	11.0
112,500	13.0	115,000	10.9	112,000	12.0
114,500	14.0	119,500	12.0	115,000	13.0
115,500	15.0	122,500	13.0	117,000	14.0
117,500	16.0	125,000	14.0	119,000	15.0
119,500	17.0	126,500	15.0	120,000	16.0
120,000	18.0	127,000	16.0	120,100	17.0
120,000	19.0	123,000	17.0	118,500	18.0
119,500	20.0	122,500	18.0	117,000	19.0
117,500	21.0	120,000	19.0	115,000	20.0
115,000	22.0	119,000	20.0	112,500	21.0
113,500	23.0	115,000	21.0	107,500	22.0
111,000	24.0	112,500	22.0		
105,000	25.0	108,000	23.0		
100,000	26.0	105,000	24.0		
95,000	27.0	102,000	25.0		
		101,500	26.0		
		87,500	30.0		

TABLE XII - CYLINDER LOAD-DEFLECTION DATA

Beam No. 7

Date August 21,1965

Test - 8 days
Gage Length = 10 inches
1 Division = .001 inches

Cylinder 1		Cylinder 2		Cylinder 3	
Load (lbs.)	Div.	Load (lbs.)	Div.	Load (lbs.)	Div.
10,000	0.2	10,000		10,000	
15,000	0.6	15,000	0.5	15,000	0.2
20,000	1.15	20,000	1.1	20,000	0.95
25,000	1.55	25,000	1.5	25,000	1.35
30,000	2.0	30,000	2.0	30,000	1.85
35,000	2.4	35,000	2.35	35,000	2.4
40,000	2.9	40,000	2.75	40,000	2.9
45,000	3.4	45,000	3.25	45,000	3.4
50,000	3.8	50,000	3.7	50,000	4.0
55,000	4.25	55,000	4.1	55,000	4.5
60,000	4.6	60,000	4.45	60,000	5.0
65,000	5.1	65,000	4.95	65,000	5.4
70,000	5.9	70,000	5.5	70,000	6.1
75,000	6.4	75,000	6.15	75,000	6.75
80,000	7.0	80,000	6.7	80,000	7.4
85,000	7.85	85,000	7.35	85,000	8.25
90,000	8.5	90,000	8.0	90,000	9.0
95,000	9.3	95,000	8.8	95,000	10.0
100,000	10.0	100,000	9.6	100,000	11.1
105,000	11.0	105,000	10.5	105,000	12.2
110,000	12.25	110,000	12.0	110,000	13.75
115,000	13.8	115,000	13.9	113,500	15.0
119,500	16.0	115,500	15.0	115,500	16.0
120,000	17.0	118,000	16.0	117,000	17.0
120,000	18.0	117,500	18.0	118,000	18.0
107,500	23.0	115,000	19.0	118,500	19.0
102,500	24.0			117,500	20.0
95,000	26.0			112,500	21.0
90,000	28.0			107,500	24.0
85,000	29.0			90,000	30.0
67,500	35.0			72,500	35.0

TABLE XIII - BEAM LOAD-STRAIN DATA

Beam No. 3-A
Date July 27, 1965

Test - 8 days
Strain- Micro-inches/inch

Load (lbs.)	Section 1			Section 2		
	Tens. Strain	Comp. Strain	Comp.* Strain	Tens. Strain	Comp. Strain	Comp.* Strain
400	26	18	22	30	25	26
670	55	36	46	72	50	54
1040	86	42	53	122	66	67
1300	110	56	70	156	84	85
1600	138	70	84	194	101	102
1800	157	88	103	217	118	120
2100	190	107	121	262	138	137
2400	240	126	131	320	157	151
2600	283	145	149	362	175	169
2800	334	160	156	419	182	178
3100	424	182	177	504	209	200
3400	492	214	216	578	242	232
3620	556	232	231	646	267	246
3900	608	258	254	697	292	268
4200	678	279	270	772	312	282
4500	762	302	293	852	336	302
4800	827	340	329	912	367	332
5100	911	362	350	968	386	348
5400	988	388	369	1034	402	366
5700	1061	410	388	1115	416	382
6000	1122	443	424	1176	424	412
6300	1188	470	450	1250	430	430
6600	1247	486	465	1319	434	437
6900	1323	520	498	1395	446	458
7200	1399	563	540	1480	449	483
7500	1462	580	552	1560	451	490
7800	1523	620	584	----	463	518
8100	1610	656	607	1768	462	539
8500	1677	698	643	1894	454	564
8800	1717	742	680	14735	---	596
9100	1807	788	710	16484	---	617
9400	1873	822	748	17104	---	633
9400	2710	1162	790	17650	---	648
9400	17162	1326	832	18578	---	668
9600	18340	1393	852	19428	---	688
9960	20101	1398	877	19428+	---	693
9960	21164	1322	890	-----	---	592
9960	24991	1470	936	-----	---	361

*Strain gage at d/2 distance from section

TABLE XIV - BEAM LOAD-STRAIN DATA

Beam No. 1
Date August 18, 1965

Test - 8 days
Strain - Micro-inches/inch

Load (lbs.)	Section 1			Section 2		
	Tens. Strain	Comp. Strain	Comp. Strain	Tens. Strain	Comp. Strain	Comp. Strain
1000	61	44	Faulty Gage	92	74	Faulty Gage
2000	650	159		900	180	
2500	866	207		1104	193	
3060	1072	254		1313	220	
3500	1225	286		1479	247	
4080	1406	326		1697	267	
4530	1543	356		1866	296	
5000	1692	386		2039	328	
5500	1870	422		2248	374	
6000	2039	455		2488	431	
6500	2209	491		3975	497	
6840	2441	528		7448	529	
7100	2710	558		8987	584	
7500	3633	585		9780	643	
7800	6217	606		12646	772	
7980	7090	608		13895	849	
8120	7722	620		14740	922	
8220	8386	618		15614	997	
8340	9135	610		16508	1067	
8600	9710	605		17292	1149	
8580	10365	593		18510	1214	
8660	10920	582		18788	1386	
8800	11429	600		19450	1420	
8840	12108	566			1480	
8930	11505	548			1559	
8960	12186	518			1680	
9100	12588	510			1792	
9100	13022	486			1952	
9100	13330	475			2144	
9300	13551	448		Bar Broke	2372	

TABLE XV - BEAM LOAD-STRAIN DATA

Beam No. 2 — Test - 7 days
Date August 16, 1965 — Strain - Micro-inches/inch

Load (lbs.)	Section 1			Section 2		
	Tens. Strain	Comp. Strain	Comp. Strain	Tens. Strain	Comp. Strain	Comp. Strain
700	30	5	Faulty	34	Faulty	
1000	52	22	Gage	59	Gage	18
1500	88	40		100		34
2000	113	74		150		84
2500	176	126		213		105
3000	413	210		408		188
3100	453	227		445		205
3500	810	275		760		263
3900	842	401		812		387
4400	920	440		881		427
5000	1029	428		990		430
5500	1084	482		1048		487
5700	1244	414		1210		440
6200	1248	532		1215		556
6500	1400	595		1376		650
7000	1496	655		1463		714
7500	1566	687		1536		760
8000	1573	742		1546		824
8500	1652	808		1625		902
9000	1703	857		1682		967
9500	1810	919		1787		1060
10000	1932	1000		1909		1185
10500	2087	1084		2054		1354
11000	2232	1167		2200		1512
11500	4540	1358		2332		1808
11620	8246	1524		8568		2127
11700	8798	1610		8920		2245
12000	9340	1722		9476		2365
12100	10210	1840		10220		2533
12300	10677	1920		10584		2652
12300	10809	1914		10728		2740
12300	10940	1940		10874		2802

TABLE XVI - BEAM LOAD-STRAIN DATA

Beam No. 3
Date August 16, 1965

Test - 7 days
Strain - Micro-inches/inch

Load (lbs.)	Section 1			Section 2		
	Tens. Strain	Comp. Strain	Comp. Strain	Tens. Strain	Comp. Strain	Comp. Strain
530	15	14	16	25	25	18
1120	30	52	54	64	48	64
1500	50	69	68	102	56	89
2000	76	86	83	164	83	120
2540	138	124	120	344	130	199
3000	224	173	152	470	166	265
3500	330	202	180	606	197	328
4000	417	241	210	747	234	390
4560	541	284	227	916	264	450
5000	586	352	282	979	326	528
5420	670	382	294	1088	352	567
5900	751	418	316	1206	382	617
6500	843	473	354	1326	426	683
6870	926	511	389	1410	464	742
7420	996	558	428	1500	510	812
8000	1072	594	457	1606	548	860
8500	1150	648	494	1708	604	920
9000	1226	702	536	1808	675	980
9520	1345	756	572	1944	724	1050
10000	1418	800	613	2032	779	1110
10500	1511	855	618	2158	825	1182
11040	1618	964	619	2287	950	1280
11560	1694	1018	756	2388	1024	1366
12000	1783	1071	800	2503	1102	1455
12500	1930	1164	856	2760	1233	1578
13000	1977	1221	901	3239	1342	1706
13400	2084	1283	939	6182	1520	1924
13840	2182	1382	1016	7787	1778	2196
13900	2220	1427	1046	7920	1900	2331
14120	2296	1484	1080	8480	2050	2480
14210	2430	1586	1128	9091	2280	2729
14400	2480	1625	1152	9328	2370	2823
14500	2546	1700	1196	9662	2490	2938
14680	2554	1770	1242	10040	2604	3046
14800	2620	1836	1282	10312	2698	3135
14920	2870	1912	1338	10550	2784	3225
15100	4055	2100	1476	10860	2949	3380
15500	4862	2180	1528	11040	3030	3457
15600	5268	2274	1593	11373	3108	3532
15650	5515	2366	1652	11611	3191	3612

TABLE XVI cont. - BEAM LOAD-STRAIN DATA

Beam No. 3 continued
Date August 16, 1965

Test - 7 days
Strain - Micro-inches/inch

Load (lbs.)	Section 1			Section 2		
	Tens. Strain	Comp. Strain	Comp. Strain	Tens. Strain	Comp. Strain	Comp. Strain
15800	5755	2465	1718	11847	3273	3692
15900	6057	2592	1798	12163	3365	3768
16100	6385	2727	1888	12523	3461	3856
16100	6766	2903	2014	12930	3586	3874
16300	7054	3038	2111	13280	3697	4090
16500	7379	3194	2229	13593	3845	4239
16150	7475	3268	2290	13676	3930	4330
16200	7597	3330	2341	13800	3995	4390
16240	7744	3430	2424	13945	4130	4530
16340	7974	3505	2485	14204	4200	4600
16400	8155	3584	2550	14422	4274	4669
16500	8438	3688	2633	14756	4366	4755
16540	8712	3782	2710	15086	4460	4848
16600	8946	3878	2793	15354	4550	4946
16700	9168	3970	2882	15616	4646	5057
16800	9460	4097	2983	15980	4758	5168
16940	9931	4272	3143	16630	4930	5353
17100	10248	4411	3280	16968	5106	5568
17100	10656	4559	3431	17425	5291	5786
17200	10960	4670	3552	17751	5471	6016
17500	11433	4794	3693	18315	5658	6390
17500	11743	4902	3817	18760	5816	7170
17500	11912	4964	3900	19207	5942	
17500	11967	5002	3950	19700	6070	
17500	12068	5040	4016	20676	6067	

TABLE XVII - BEAM LOAD-STRAIN DATA

Beam No. 4
Date August 18, 1965

Test - 8 days
Strain - Micro-inches/inch

Load (lbs.)	Section 1			Section 2		
	Tens. Strain	Comp. Strain	Comp. Strain	Tens. Strain	Comp. Strain	Comp. Strain
1100	48	18	72	82	33	62
2070	132	44	159	207	78	137
3000	248	70	245	367	137	210
4100	398	119	343	556	207	305
5080	520	174	414	767	273	396
6060	630	226	493	934	350	483
7500	786	302	604	1077	455	626
9000	950	396	719	1251	593	789
10120	1076	478	821	1416	709	945
11100	1183	547	926	1575	816	1102
12120	1299	626	1046	1731	938	1278
13010	1427	714	1167	1906	1066	1458
14120	1568	844	1341	2020	1251	1715
15000	1657	963	1430	2159	1399	1866
16030	1777	1112	1602	2284	1601	2118
16520	1831	1200	1711	2328	1727	2268
17120	1894	1305	1824	2390	1854	2430
17570	1942	1393	1920	2444	1963	2563
18090	2002	1401	2033	2581	2102	2730
18500	2048	1593	2125	----	2338	2936
19000	2108	1689	2230	9344	2709	3262
19230	2168	1798	2350	10327	3048	3640
19300	2195	1879	2430	10558	3278	3872
19460	2247	1948	2502	10718	3462	4068
19460	2278	2001	2579	10773	3649	4258
19500	2306	2044	2626	10832	3801	4407
19700	----	2082	2806	10931	4000	4594
19700	----	2196	2990	11059	4131	4729
19910	2910	2304	3111	11224	4290	4825
19900	3086	2368	3187	11500	4411	4946
19980	3358	2422	3257	11753	4546	5074
20000	3951	2472	3344	12027	4662	5190
20200	----	2524	3431	12338	4769	5302
20400	----	2581	3536	12650	4876	5424
20500	6670	2648	3647	13007	4991	5567
20500	6956	2711	3735	13218	5090	5689
20600	7036	2774	3817	13496	5149	5792
20600	7210	2838	3905	13715	5200	5888
20600	----	----	3978	-----	----	5989
20600	----	2896	----	13940	5265	----

TABLE XVIII - BEAM LOAD-STRAIN DATA

Beam No. 5
Date August 20, 1965

Test - 8 days
Strain - Micro-inches/inch

Load (lbs.)	Section 1			Section 2		
	Tens. Strain	Comp. Strain	Comp. Strain	Tens. Strain	Comp. Strain	Comp. Strain
1080	19	26	16	24	7	23
2000	58	77	47	106	41	82
3090	144	149	97	272	97	173
4080	252	232	140	413	140	260
5080	444	342	209	555	182	356
6020	581	439	255	702	231	448
7600	785	593	336	923	297	614
9000	964	746	416	1125	375	780
10100	1100	871	483	1281	436	920
11060	1224	1008	550	1424	486	1104
12100	1359	1145	628	1572	531	1319
13100	1490	1305	710	1716	580	1573
14060	1625	1482	800	1860	638	1835
15000	1751	1675	901	1996	699	2128
15610	1842	1822	976	2114	754	2350
16500	1971	2016	1065	2337	800	2682
16780	2062	2193	1117	----	892	3173
16990	2106	2313	1158	7740	966	3495
17180	2163	2418	1190	7992	1016	3742
17500	2220	2530	1225	8274	1068	3998
17780	2224	2708	1298	8982	1099	4339
17900	2893	2929	1390	9246	1171	4622
18100	----	3202	1515	9533	1234	4878
18340	6343	2904	1314	9132	1114	4740

TABLE XIX - BEAM LOAD-STRAIN DATA

Beam No. 6
August 20, 1965

Test - 8 days
Strain - Micro-inches/inch

Load (lbs.)	Section 1			Section 2		
	Tens. Strain	Comp.* Strain	Comp. Strain	Tens. Strain	Comp.* Strain	Comp. Strain
1120	35	34	39	45	44	55
2130	79	68	75	100	88	110
3180	149	119	125	191	142	174
4060	225	153	175	284	189	244
5000	313	196	231	374	241	316
6130	316	247	306	488	307	408
7500	544	308	393	619	388	534
8580	641	360	466	720	450	638
9580	735	407	542	818	512	748
10670	835	463	635	921	587	875
11650	933	509	720	1025	641	1002
12680	1033	563	814	1128	722	1139
13600	1120	625	921	1216	800	1292
14690	1309	697	1035	1304	886	1450
15680	1310	767	1171	1403	988	1636
16720	1404	828	1494	1495	1086	1812
17580	1492	890	1472	1577	1197	1965
18610	1595	942	1584	1688	1294	2078
19570	1685	946	1775	1800	1446	2283
20230	1746	980	1902	1865	1554	2420
20600	1774	1014	2006	1891	1652	2525
21120	1815	1042	2100	1931	1746	2626
21580	1858	1057	2189	1983	1824	2724
21980	1898	1066	2270	2033	1896	2812
22530	1950	1057	2372	2108	1988	2930
22860	1986	1075	2489	2174	2107	3059
23100	2022	1085	2541	2227	2158	3121
23290	2042	1088	2585	2300	2210	3192
23500	2066	1090	2635	2415	2267	3271
23760	2101	1096	2716	2653	2366	3394
24020	2130	1100	2768	3014	2438	3482
24260	2162	1195	2817	3630	2514	3557
24520	2224	1108	2896	4283	2603	3658
24750	2300	1110	2990	4880	2728	3782
25000	2361	1115	3079	5270	2880	3895
25200	2454	1128	3200	5674	3111	4042
25400	2534	1134	3286	5908	3313	4149
25500	2633	1195	3351	6153	3476	4242
25500	2656	1050	3385	6282	3630	4300
25500	2709	1031	3437	6485	3827	4392

*Indicates compression steel strain

TABLE XIX cont. - BEAM LOAD-STRAIN DATA

Beam No. 6 continued Test - 8 days
Date August 20, 1965 Strain - Micro-inches/inch

Load (lbs.)	Section 1			Section 2		
	Tens. Strain	Comp.* Strain	Comp. Strain	Tens. Strain	Comp.* Strain	Comp. Strain
25600	2798	1023	3486	6682	3989	4479
25700	2896	1024	3520	6844	4114	4546
25900	3233	992	3565	7235	4292	4650
25820	3353	977	3594	7422	4484	4710
25820	3458	953	3617	7623	4704	4767

* Indicates compression steel strain

TABLE XX - BEAM LOAD-STRAIN DATA

Beam No. 7 Test - 8 days
Date August 21, 1965 Strain - Micro-inches/inch

Load (lbs.)	Section 1			Section 2		
	Tens. Strain	Comp. Strain	Comp. Strain	Tens. Strain	Comp. Strain	Comp. Strain
1000	20	Faulty Gage	14	21	14	18
2000	54		60	64	43	65
3000	113		119	136	86	107
4000	188		180	222	122	146
5000	308		278	349	184	204
6000	420		375	464	238	277
7000	536		480	590	296	358
8000	628		578	684	339	435
9000	742		702	796	407	534
10000	843		815	889	465	627
11000	931		930	974	536	724
12000	1030		1056	1065	607	834
13000	1125		1186	1152	692	950
14080	1238		1350	1247	787	1114
15060	1332		1500	1334	874	1267
16030	1425		1670	1418	972	1436
17000	1520		1821	1502	1070	1601
18000	1653		1996	1596	1166	1794
19000	1655		2038	1651	1185	1911
19000	1726		2135	1730	1370	2047
19760	1804		2234	1820	1458	2229
20500	1840		2308	1871	1555	2369
20500	1895		2387	1996	1568	2422
21000	1939		2453	2158	1572	2466
21200	1966		2496	2358	1566	2500
21340	1993		2547	2751	1570	2546
21500	2010		2584	----	1584	2560
21500	2026		2612	4578	1600	2575
21500	2039		2638	4963	1615	2585
21500	2047		2660	5268	1622	2585

TABLE XXI - BEAM LOAD-DEFLECTION DATA

Beam No. 3 Date August 16		Beam No. 3 continued		Beam No. 4 Date August 18	
Load (lbs.)	Dial Gage (inches)	Load (lbs.)	Dial Gage (inches)	Load (lbs.)	Dial Gage (inches)
530	.002	15900	.369	1100	.010
1120	.006	16100	.3855	2070	.021
1500	----	16100	.407	3000	.034
2000	.0105	16300	.424	4100	.050
2540	.015	16500	.440	5080	.065
3000	----	16150	----	6060	.080
3500	.028	16200	.455	7500	.100
4000	.039	16240	.465	9000	.122
4560	.049	16340	.478	10120	.141
5000	.055	16400	.487	11100	.157
5420	.062	16500	.503	12120	.174
5900	.070	16540	.517	13010	.190
6500	.080	16600	.530	14120	.210
6870	.090	16700	----	15000	.228
7420	.097	16800	.581	16030	.249
8000	.1065	16940	.594	16520	.262
8500	----	17100	.615	17120	.278
9000	.124	17100	.639	17570	.290
9520	.1362	17200	.655	18090	.308
10000	.145	17500	.678	18500	.321
10500	.156	17500	.697	19000	.334
11040	.170	17500	.705	19230	.352
11560	.180	17500	----	19300	.363
12000	----	17500	.711	19460	.372
12500	.210			19460	.380
13000	.218			19500	.388
13400	.2295			19700	.401
13840	.243			19700	.419
13900	----			19910	----
14120	.257			19900	----
14210	.2695			19980	----
14400	.275			20000	----
14500	.2815			20200	----
14680	.289			20400	----
14800	.296			20500	----
14920	.304			20500	----
15100	.318			20600	----
15500	.326			20600	----
15600	.336			20600	----
15650	.345			20600	----
15800	.355				

TABLE XXII - BEAM LOAD-DEFLECTION DATA

Beam No. 3-A Date July 27		Beam No. 1 Date August 18		Beam No. 2 Date August 16	
Load (lbs.)	Def. (inches)	Load (lbs.)	Dial Gage (inches)	Load (lbs.)	Dial Gage (inches)
400	.000	1000	----	700	.003
670	----	2000	.020	1000	.006
1040	.024	2500	.028	1500	.011
1300	.024	3060	.037	2000	----
1600	.036	3500	.050	2500	.031
1800	.036	4080	.065	3000	.044
2100	.072	4530	.076	3100	.047
2400	.072	5000	.092	3500	.063
2600	.072	5500	.111	3900	.092
2800	----	6000	.1295	4400	.100
3100	.084	6500	.147	5000	.108
3400	----	6840	.165	5500	.114
3620	.084	7100	.191	5700	.124
3900	.096	7500	.202	6200	.129
4200	----	7800	.228	6500	.143
4500	----	7980	.248	7000	.154
4800	----	8120	.262	7500	.161
5100	.120	8220	.276	8000	.166
5400	.120	8340	.2925	8500	----
5700	.120	8600	.310	9000	.185
6000	.144	8580	.3286	9500	.197
6300	.144	8660	.342	10000	.213
6900	.156	8800	.357	10500	.231
7200	.168	8840	.377	11000	.247
7500	.168	8930	.3982	11500	.279
7800	----	8960	.424	11620	.303
8100	.192	9100	.444	11700	.3195
8500	----	9100	.462	12000	.339
8800	.192	9100	.478	12100	.3585
9100	.204	9300	.492	12300	.372
9400	.204			12300	.448
9400	.216			12300	----
9400	.252				
9600	----				
9960	.456				
9960	.540				
9960	.612				

TABLE XXIII - BEAM LOAD-DEFLECTION DATA

Beam No. 5 Date August 20		Beam No. 6 Date August 20		Beam No. 7 Date August 21	
Load (lbs.)	Dial Gage (inches)	Load (lbs.)	Dial Gage (inches)	Load (lbs.)	Dial Gage (inches)
1080	----	1120	.009	1000	.005
2000	.014	2130	.0175	2000	.013
3090	.026	3180	.029	3000	.023
4080	.040	4060	.040	4000	.034
5080	.060	5000	.052	5000	.047
6020	.082	6130	.067	6000	.061
7600	.112	7500	.085	7000	.076
9000	.135	8580	.099	8000	.090
10100	.153	9580	.112	9000	.108
11060	.170	10670	.128	10000	.122
12100	.190	11650	.141	11000	.138
13100	.209	12680	.156	12000	.154
14060	.229	13600	.171	13000	.170
15000	.251	14690	.187	14080	.191
15610	.266	15680	.205	15060	.209
16500	.285	16720	.221	16030	.229
16780	.296	17580	.238	17000	.248
16990	.303	18610	.278	18000	.270
17180	.310	19570	.209	19000	.284
17500	.317	20230	.2262	19000	.324
17780	.329	20600	.239	19760	.378
17900	.341	21120	.2545	20500	.418
18100	.357	21580	.275	20500	.462
18340	.356	21980	.294	21000	.500
		22530	.332	21200	.525
		22860	.356	21340	.547
		23100	.375	21500	.566
		23290	.392	21500	.589
		23500	.414	21500	.605
		23760	.440	21500	.622
		24020	.462		
		24260	.482		
		24520	.503		
		24750	.531		
		25000	.552		
		25200	.580		
		25400	.6025		
		25500	.6485		
		25500	.701		
		25500	.733		
		25600	.758		
		25700	.772		

VITA

Johnny Leroy Hulsey was born October 6, 1941, in Sullivan, Missouri, the son of John and Eva Hulsey. He received his primary education in the public school system of Bourbon, Missouri and graduated from Bourbon High School in 1959. The following fall, he entered the Missouri School of Mines and Metallurgy, and graduated in 1964. The author was employed by his father, who was a building contractor, in the spring of 1962 and during all vacations throughout undergraduate study. In the summer following graduation the author was employed by the Soil Conservation Service as a Civil Engineer. In the fall of 1964, the author entered graduate school at the University of Missouri at Rolla, and served as a Graduate Assistant in the Department of Civil Engineering.

In September 1964, Mr. Hulsey married Velma Faye Reynolds, formerly of Rolla, Missouri.